# Guide for the Design and Construction of Structural Concrete Reinforced with FRP Bars

Reported by ACI Committee 440


John P. Busel
Chair

Carol K. Shield*
Secretary

| | | | |
|---|---|---|---|
| Tarek Alkhrdaji | Edward R. Fyfe | James Korff | Morris Schupack |
| Charles E. Bakis* | T. Russell Gentry | Michael W. Lee | David W. Scott |
| P. N. Balaguru | Janos Gergely | John Levar | Rajan Sen |
| Lawrence C. Bank | William J. Gold | Ibrahim M. Mahfouz | Khaled A. Soudki |
| Abdeldjelil Belarbi | Nabil F. Grace | Orange S. Marshall | Samuel A. Steere |
| Brahim Benmokrane | Mark F. Green | Amir Mirmiran | Robert Steffen |
| Gregg J. Blaszak | Zareh B. Gregorian | Ayman S. Mosallam | Gamil S. Tadros |
| Timothy E. Bradberry* | Doug. D. Gremel | Antonio Nanni*† | Jay Thomas |
| Gordon L. Brown | H.R. Trey Hamilton | Kenneth Neale | Houssam A. Toutanji |
| Vicki L. Brown | Issam E. Harik | John P. Newhook | J. Gustavo Tumialan |
| T. Ivan Campbell | Kent A. Harries | Max L. Porter | Milan Vatovec |
| Raafat El-Hacha | Mark P. Henderson | Mark Postma | Stephanie L. Walkup |
| Garth J. Fallis | Bohdan N. Horeczko | Hayder A. Rasheed | David White |
| Amir Z. Fam | Vistasp M. Karbhari | Sami H. Rizkalla | |

*Contributing authors. The committee also thanks Robert J. Frosch, Shawn Gross, Renato Parretti, and Carlos E. Ospina for their contributions.
†Subcommittee Chair.



*Fiber-reinforced polymer (FRP) materials have emerged as an alternative material for producing reinforcing bars for concrete structures. FRP reinforcing bars offer advantages over steel reinforcement in that FRP bars are noncorrosive, and some FRP bars are nonconductive. Due to other differences in the physical and mechanical behavior of FRP materials versus steel, unique guidance on the engineering and construction of concrete structures reinforced with FRP bars is needed. Other countries, such as Japan and Canada, have established design and construction guidelines specifically for the use of FRP bars as concrete reinforcement. This guide offers general information on the history and use of FRP reinforcement, a description of the unique material properties of FRP, and guidelines for the construction and design of structural concrete members reinforced with FRP bars. This guide is based on the knowledge gained from worldwide experimental research, analytical work, and field applications of FRP reinforcement.*



**keywords:** aramid fibers; carbon fibers; development length; fiber-reinforced polymers; flexure; glass fibers; moment; reinforcement; shear; slab; strength.




## CONTENTS




ACI 440.1R-06 supersedes ACI 440.1R-03 and became effective February 10, 2006.

## CHAPTER 1—INTRODUCTION

This is the third revision of the design and construction guide on fiber-reinforced polymer (FRP) reinforcement for concrete structures. Many successful applications worldwide using FRP composite reinforcing bars during the past decade have demonstrated that it can be used successfully and practically. The professional using this technology should exercise judgment as to the appropriate application of FRP reinforcement and be aware of its limitations as discussed in this guide. Currently, areas where there is limited knowledge of the performance of FRP reinforcement include fire resistance, durability in outdoor or severe exposure conditions, bond fatigue, and bond lengths for lap splices. Further research is needed to provide additional information in these areas.

Conventional concrete structures are reinforced with nonprestressed and prestressed steel. The steel is initially protected against corrosion by the alkalinity of the concrete, usually resulting in durable and serviceable construction. For many structures subjected to aggressive environments, such as marine structures, bridges, and parking garages exposed to deicing salts, combinations of moisture, temperature, and chlorides reduce the alkalinity of the concrete and result in the corrosion of reinforcing steel. The corrosion process ultimately causes concrete deterioration and loss of serviceability. To address corrosion problems, professionals have started using alternatives to bare steel bars, such as epoxy-coated steel bars and specialty concrete admixtures. While effective in some situations, such remedies may not be able to completely eliminate the problems of steel corrosion in reinforced concrete structures (Keesler and Powers 1988).

Recently, composite materials made of fibers embedded in a polymeric resin, also known as FRPs, have become an alternative to steel reinforcement for concrete structures. Because FRP materials are nonmagnetic and noncorrosive, the problems of electromagnetic interference and steel corrosion can be avoided with FRP reinforcement. Additionally, FRP materials exhibit several properties, such as high tensile strength, that make them suitable for use as structural reinforcement (ACI 440R; Benmokrane and Rahman 1998; Burgoyne 2001; Cosenza et al. 2001; Dolan et al. 1999; El-Badry 1996; Figueiras et al. 2001; Humar and Razaqpur 2000; Iyer and Sen 1991; Japan Society of Civil Engineers [JSCE] 1992; JSCE 1997a; Nanni 1993a; Nanni and Dolan 1993; Neale and Labossiere 1992; Saadatmanesh and Ehsani 1998; Taerwe 1995; Teng 2001; White 1992).

The mechanical behavior of FRP reinforcement differs from the behavior of conventional steel reinforcement. Accordingly, a change in the traditional design philosophy of concrete structures is needed for FRP reinforcement. FRP materials are anisotropic and are characterized by high tensile strength only in the direction of the reinforcing fibers. This anisotropic behavior affects the shear strength and dowel action of FRP bars as well as the bond performance. Furthermore, FRP materials do not yield; rather, they are elastic until failure. Design procedures must account for a lack of ductility in structural concrete members reinforced with FRP bars.

Other countries, such as Japan (JSCE 1997b) and Canada (Canadian Standards Association [CSA] 2000 and 2002), have established design procedures specifically for the use of FRP reinforcement for concrete structures. The analytical and experimental phases for FRP construction are sufficiently complete; therefore this document establishes recommendations for the design of structural concrete reinforced with FRP bars.

## 1.1—Scope

This document provides recommendations for the design and construction of FRP-reinforced concrete structures. The document only addresses nonprestressed FRP reinforcement (concrete structures prestressed with FRP tendons are covered in ACI 440.4R). The basis for this document is the knowledge gained from worldwide experimental research, analytical research work, and field applications of FRP reinforcement. The recommendations in this document are intended to be conservative.

Design recommendations are based on the current knowledge and intended to supplement existing codes and guidelines for conventionally reinforced concrete structures and to provide engineers and building officials with assistance in the specification, design, and construction of structural concrete reinforced with FRP bars.

ACI 440.3R provides a comprehensive list of test methods and material specifications to support design and construction guidelines.

The use of FRP reinforcement in combination with steel reinforcement for structural concrete is not addressed in this document.

## 1.2—Definitions

The following definitions clarify terms pertaining to FRP that are not commonly used in concrete practice.

### A

**AFRP**—aramid fiber-reinforced polymer.

**aging**—the effects of time on the properties of material exposed to different environments.

**alkalinity**—the condition of having or containing hydroxyl (OH–) ions; containing alkaline substances. In concrete, the alkaline environment has a pH above 12.

### B

**balanced FRP reinforcement ratio**—an amount and distribution of reinforcement in a flexural member such that in strength design, the tensile FRP reinforcement reaches its ultimate design strain simultaneously with the concrete in compression reaching its assumed ultimate strain of 0.003.

**bar, FRP**—a composite material formed into a long, slender structural shape suitable for the internal reinforcement of concrete and consisting of primarily longitudinal unidirectional fibers bound and shaped by a rigid polymer resin material. The bar may have a cross section of variable shape (commonly circular or rectangular) and may have a deformed or roughened surface to enhance bonding with concrete.

**braiding**—a process whereby two or more systems of yarns are intertwined in the bias direction to form an integrated structure. Braided material differs from woven and knitted fabrics in the method of yarn introduction into the fabric and the manner by which the yarns are interlaced.

### C

**CFRP**—carbon fiber-reinforced polymer.

**composite**—a combination of one or more materials differing in form or composition on a macroscale. Note: The constituents retain their identities; that is, they do not dissolve or merge completely into one another, although they act in concert. Normally, the components can be physically identified and exhibit an interface between one another.

**cross-link**—a chemical bond between polymer molecules. Note: An increased number of cross-links per polymer molecule increases strength and modulus at the expense of ductility.

**curing of FRP bars**—a process that irreversibly changes the properties of a thermosetting resin by chemical reaction, such as condensation, ring closure, or addition. Note: Curing can be accomplished by the addition of cross-linking (curing) agents with or without heat and pressure.

### D

**deformability factor**—the ratio of energy absorption (area under the moment-curvature curve) at ultimate strength of the section to the energy absorption at service level.

**degradation**—a deleterious change in the chemical structure, physical properties, or appearance of an FRP composite.

**design modulus of elasticity**—the modulus of elasticity of FRP ($E_f$) to be used in any design calculation and defined as the mean modulus of a sample of test specimens ($E_f = E_{f,ave}$).

**design rupture strain**—the ultimate tensile strain of FRP ($\varepsilon_{fu}$) to be used in any design calculation and defined as the guaranteed tensile rupture strain multiplied by the environmental reduction factor ($C_E\, \varepsilon_{fu}^*$).

**design tensile strength**—the tensile strength of FRP ($f_{fu}$) to be used in any design calculation and defined as the guaranteed tensile strength multiplied by the environmental reduction factor ($C_E\, f_{fu}^*$).

### E

**E-glass**—a family of glass with a calcium alumina borosilicate composition and a maximum alkali content of 2.0%. A general-purpose fiber that is used in reinforced polymers.

**endurance limit**—the number of cycles of deformation or load that causes a material, test specimen, or structural member to fail.

### F

**fatigue strength**—the greatest stress that can be sustained for a given number of load cycles without failure.

**fiber**—any fine thread-like natural or synthetic object of mineral or organic origin. Note: This term is generally used for materials whose length is at least 100 times its diameter.

**fiber, aramid**—highly oriented organic fiber derived from polyamide incorporating into an aromatic ring structure.

**fiber, carbon**—fiber produced by heating organic precursor materials containing a substantial amount of carbon, such as rayon, polyacrylonitrile (PAN), or pitch in an inert environment.

**fiber, glass**—fiber drawn from an inorganic product of fusion that has cooled without crystallizing.

**fiber content**—the amount of fiber present in a composite. Note: This usually is expressed as a percentage volume fraction or weight fraction of the composite.

**fiber-reinforced polymer (FRP)**—composite material consisting of continuous fibers impregnated with a fiber-binding polymer then molded and hardened in the intended shape.

**fiber volume fraction**—the ratio of the volume of fibers to the volume of the composite.

**fiber weight fraction**—the ratio of the weight of fibers to the weight of the composite.

### G

**GFRP**—glass fiber-reinforced polymer.

**grid**—a two-dimensional (planar) or three-dimensional (spatial) rigid array of interconnected FRP bars that form a contiguous lattice that can be used to reinforce concrete. The lattice can be manufactured with integrally connected bars or made of mechanically connected individual bars.

### H

**hybrid**—a combination of two or more different fibers, such as carbon and glass or carbon and aramid, into a structure.

### I

**impregnate**—in fiber-reinforced polymers, to saturate the fibers with resin.

### M

**matrix**—in the case of fiber-reinforced polymers, the materials that serve to bind the fibers together, transfer load to the fibers, and protect them against environmental attack and damage due to handling.

### P

**pitch**—a black residue from the distillation of petroleum.

**polymer**—a high-molecular-weight organic compound, natural or synthetic, containing repeating units.

**precursor**—for carbon or graphite fiber, the rayon, PAN or pitch fibers from which carbon and graphite fibers are derived.

**pultrusion**—a continuous process for manufacturing composites that have a uniform cross-sectional shape. The process consists of pulling a fiber-reinforcing material through a resin impregnation bath then through a shaping die where the resin is subsequently cured.

### R

**resin**—polymeric material that is rigid or semirigid at room temperature, usually with a melting point or glass transition temperature above room temperature.

### S

**stress concentration**—the magnification of the local stresses in the region of a bend, notch, void, hole, or inclusion, in comparison to the stresses predicted by the ordinary formulas of mechanics without consideration of such irregularities.

**sustained stress**—stress caused by unfactored sustained loads, including dead loads and the sustained portion of the live load.

### T

**thermoplastic**—class of resin capable of being repeatedly softened by an increase of temperature and hardened by a decrease in temperature.

**thermoset**—class of resin that, when cured by application of heat or chemical means, changes into a substantially infusible and insoluble material.

### V

**vinyl esters**—a class of thermosetting resins containing ester of acrylic, methacrylic acids, or both, many of which have been made from epoxy resin.

### W

**weaving**—a multidirectional arrangement of fibers. For example, polar weaves have reinforcement yarns in the circumferential, radial, and axial (longitudinal) directions; orthogonal weaves have reinforcement yarns arranged in the orthogonal (Cartesian) geometry, with all yarns intersecting at 90 degrees.

## 1.3—Notation

| | | |
|---|---|---|
| $A_f$ | = | area of FRP reinforcement, in.$^2$ (mm$^2$) |
| $A_{f,bar}$ | = | area of one FRP bar, in.$^2$ (mm$^2$) |
| $A_{f,min}$ | = | minimum area of FRP reinforcement needed to prevent failure of flexural members upon cracking, in.$^2$ (mm$^2$) |
| $A_{f,sh}$ | = | area of shrinkage and temperature FRP reinforcement per linear foot, in.$^2$ (mm$^2$) |
| $A_{fv}$ | = | amount of FRP shear reinforcement within spacing $s$, in.$^2$ (mm$^2$) |
| $A_{fv,min}$ | = | minimum amount of FRP shear reinforcement within spacing $s$, in.$^2$ (mm$^2$) |
| $A_s$ | = | area of tension steel reinforcement, in.$^2$ (mm$^2$) |
| $a$ | = | depth of equivalent rectangular stress block, in. (mm) |
| $b$ | = | width of rectangular cross section, in. (mm) |
| $b_o$ | = | perimeter of critical section for slabs and footings, in. (mm) |
| $b_w$ | = | width of the web, in. (mm) |
| $C$ | = | spacing or cover dimension, in. (mm) |
| $C_E$ | = | environmental reduction factor for various fiber type and exposure conditions, given in Table 7.1 |
| $c$ | = | distance from extreme compression fiber to the neutral axis, in. (mm) |
| $c_b$ | = | distance from extreme compression fiber to neutral axis at balanced strain condition, in. (mm) |
| $d$ | = | distance from extreme compression fiber to centroid of tension reinforcement, in. (mm) |
| $d_b$ | = | diameter of reinforcing bar, in. (mm) |

$d_c$ = thickness of concrete cover measured from extreme tension fiber to center of bar or wire location closest thereto, in. (mm)
$E_c$ = modulus of elasticity of concrete, psi (MPa)
$E_f$ = design or guaranteed modulus of elasticity of FRP defined as mean modulus of sample of test specimens ($E_f = E_{f,ave}$), psi (MPa)
$E_{f,ave}$ = average modulus of elasticity of FRP, psi (MPa)
$E_s$ = modulus of elasticity of steel, psi (MPa)
$f'_c$ = specified compressive strength of concrete, psi (MPa)
$\sqrt{f'_c}$ = square root of specified compressive strength of concrete, psi (MPa)
$f_f$ = stress in FRP reinforcement in tension, psi (MPa)
$f_{fb}$ = strength of bent portion of FRP bar, psi (MPa)
$f_{fe}$ = bar stress that can be developed for embedment length $\ell_e$, psi (MPa)
$f_{fr}$ = required bar stress, psi (MPa)
$f_{f,s}$ = stress level induced in FRP by sustained loads, psi (MPa)
$f_{fu}$ = design tensile strength of FRP, considering reductions for service environment, psi (MPa)
$f^*_{fu}$ = guaranteed tensile strength of FRP bar, defined as mean tensile strength of sample of test specimens minus three times standard deviation ($f^*_{fu} = f_{fu,ave} - 3\sigma$), psi (MPa)
$f_{fv}$ = tensile strength of FRP for shear design, taken as smallest of design tensile strength $f_{fu}$, strength of bent portion of FRP stirrups $f_{fb}$, or stress corresponding to $0.004E_f$, psi (MPa)
$f_s$ = allowable stress in steel reinforcement, psi (MPa)
$f_{u,ave}$ = mean tensile strength of sample of test specimens, psi (MPa)
$f_y$ = specified yield stress of nonprestressed steel reinforcement, psi (MPa)
$h$ = overall height of flexural member, in. (mm)
$I$ = moment of inertia, in.$^4$ (mm$^4$)
$I_{cr}$ = moment of inertia of transformed cracked section, in.$^4$ (mm$^4$)
$I_e$ = effective moment of inertia, in.$^4$ (mm$^4$)
$I_g$ = gross moment of inertia, in.$^4$ (mm$^4$)
$K_1$ = parameter accounting for boundary conditions (Eq. (8-10))
$k$ = ratio of depth of neutral axis to reinforcement depth
$k_b$ = bond-dependent coefficient
$L$ = distance between joints in a slab on grade, ft (m)
$\ell$ = span length of member, ft (m)
$\ell_a$ = additional embedment length at support or at point of inflection, in. (mm)
$\ell_{bhf}$ = basic development length of FRP standard hook in tension, in. (mm)
$\ell_d$ = development length, in. (mm)
$\ell_e$ = embedded length of reinforcing bar, in. (mm)
$\ell_{thf}$ = length of tail beyond hook in FRP bar, in. (mm)
$M_a$ = maximum moment in member at stage deflection is computed, lb-in. (N-mm)
$M_{cr}$ = cracking moment, lb-in. (N-mm)
$M_n$ = nominal moment capacity, lb-in. (N-mm)
$M_s$ = moment due to sustained load, lb-in. (N-mm)
$M_u$ = factored moment at section, lb-in. (N-mm)
$n_f$ = ratio of modulus of elasticity of FRP bars to modulus of elasticity of concrete
$r_b$ = internal radius of bend in FRP reinforcement, in. (mm)
$s$ = stirrup spacing or pitch of continuous spirals, and longitudinal FRP bar spacing, in. (mm)
$T_g$ = glass transition temperature, °F (°C)
$u$ = average bond stress acting on the surface of FRP bar, psi (MPa)
$V_c$ = nominal shear strength provided by concrete, lb (N)
$V_f$ = shear resistance provided by FRP stirrups, lb (N)
$V_n$ = nominal shear strength at section, lb (N)
$V_s$ = shear resistance provided by steel stirrups, lb (N)
$V_u$ = factored shear force at section, lb (N)
$w$ = maximum crack width, in. (mm)
$\alpha$ = angle of inclination of stirrups or spirals (Chapter 9), top bar modification factor (Chapter 11)
$\alpha_1$ = ratio of average stress of equivalent rectangular stress block to $f'_c$
$\alpha_L$ = longitudinal coefficient of thermal expansion, 1/°F (1/°C)
$\alpha_T$ = transverse coefficient of thermal expansion, 1/°F (1/°C)
$\beta$ = ratio of distance from neutral axis to extreme tension fiber to distance from neutral axis to center of tensile reinforcement (Section 8.3.1)
$\beta_1$ = factor taken as 0.85 for concrete strength $f'_c$ up to and including 4000 psi (28 MPa). For strength above 4000 psi (28 MPa), this factor is reduced continuously at a rate of 0.05 per each 1000 psi (7 MPa) of strength in excess of 4000 psi (28 MPa), but is not taken less than 0.65
$\beta_d$ = reduction coefficient used in calculating deflection (Section 8.3.2)
$\Delta_{(cp+sh)}$ = additional deflection due to creep and shrinkage under sustained loads, in. (mm)
$(\Delta_i)_{sus}$ = immediate deflection due to sustained loads, in. (mm)
$(\Delta/\ell)_{max}$ = limiting deflection-span ratio (Chapter 8)
$\varepsilon_c$ = strain in concrete
$\varepsilon_{cu}$ = ultimate strain in concrete
$\varepsilon_f$ = strain in FRP reinforcement
$\varepsilon_{fu}$ = design rupture strain of FRP reinforcement
$\varepsilon^*_{fu}$ = guaranteed rupture strain of FRP reinforcement defined as the mean tensile strain at failure of sample of test specimens minus three times standard deviation ($\varepsilon^*_{fu} = \varepsilon_{u,ave} - 3\sigma$), in./in. (mm/mm)
$\varepsilon_{u,ave}$ = mean tensile strain at rupture of sample of test specimens

**Table 1.1—Advantages and disadvantages of FRP reinforcement**

| Advantages of FRP reinforcement | Disadvantages of FRP reinforcement |
|---|---|
| High longitudinal tensile strength (varies with sign and direction of loading relative to fibers) | No yielding before brittle rupture |
| Corrosion resistance (not dependent on a coating) | Low transverse strength (varies with sign and direction of loading relative to fibers) |
| Nonmagnetic | Low modulus of elasticity (varies with type of reinforcing fiber) |
| High fatigue endurance (varies with type of reinforcing fiber) | Susceptibility of damage to polymeric resins and fibers under ultraviolet radiation exposure |
| Lightweight (about 1/5 to 1/4 the density of steel) | Low durability of glass fibers in a moist environment |
| Low thermal and electric conductivity (for glass and aramid fibers) | Low durability of some glass and aramid fibers in an alkaline environment |
| | High coefficient of thermal expansion perpendicular to the fibers, relative to concrete |
| | May be susceptible to fire depending on matrix type and concrete cover thickness |

$\eta$ = ratio of distance from extreme compression fiber to centroid of tension reinforcement ($d$) to overall height of flexural member ($h$) (Chapter 8)
$\lambda$ = multiplier for additional long-term deflection
$\mu$ = coefficient of subgrade friction for calculation of shrinkage and temperature reinforcement
$\xi$ = time-dependent factor for sustained load
$\rho'$ = ratio of steel compression reinforcement, $\rho' = A'_s/bd$
$\rho_b$ = steel reinforcement ratio producing balanced strain conditions
$\rho_f$ = FRP reinforcement ratio
$\rho'_f$ = ratio of FRP compression reinforcement
$\rho_{fb}$ = FRP reinforcement ratio producing balanced strain conditions
$\rho_{fv}$ = ratio of FRP shear reinforcement
$\rho_{f,ts}$ = reinforcement ratio for temperature and shrinkage FRP reinforcement
$\rho_{min}$ = minimum reinforcement ratio for steel
$\sigma$ = standard deviation
$\phi$ = strength reduction factor

### 1.4—Applications and use

The material characteristics of FRP reinforcement need to be considered when determining whether FRP reinforcement is suitable or necessary in a particular structure. The material characteristics are described in detail in Chapter 3. Table 1.1 lists some of the advantages and disadvantages of FRP reinforcement for concrete structures when compared with conventional, steel reinforcement.

The corrosion resistance of FRP reinforcement is a significant benefit for structures in highly corrosive environments such as seawalls and other marine structures, bridge decks and superstructures exposed to deicing salts, and pavements treated with deicing salts. In structures supporting magnetic resonance imaging (MRI) units or other equipment sensitive to electromagnetic fields, the nonmagnetic properties of FRP reinforcement are unrivaled. FRP reinforcement has a nonductile behavior that is partially compensated by its high tensile strength. The use of FRP reinforcement should be limited to structures that will significantly benefit from other properties such as the noncorrosive or nonconductive behavior of its materials. Due to lack of experience in its use, FRP reinforcement is not recommended for moment frames or zones where moment redistribution is required.

FRP reinforcement should not be relied on to resist compression. Available data indicate that the compressive modulus of FRP bars is lower than its tensile modulus (refer to discussion in Section 3.2.2). Due to the combined effect of this behavior and the relatively lower modulus of FRP compared with steel, the maximum contribution of compression FRP reinforcement calculated at crushing of concrete (typically at $\varepsilon_{cu} = 0.003$) is small. Therefore, FRP reinforcement should neither be used as reinforcement in columns nor other in compression members, nor as compression reinforcement in flexural members. It is acceptable for FRP tension reinforcement to experience compression due to moment reversals or changes in load pattern. The compressive strength of the FRP reinforcement should not, however, be neglected. Further research is needed in this area.

## CHAPTER 2—BACKGROUND INFORMATION

### 2.1—Historical development

The development of FRP reinforcement can be traced to the expanded use of composites after World War II. The aerospace industry had long recognized the advantages of the high strength and light weight of composite materials, and during the Cold War, the advancements in the aerospace and defense industry increased the use of composites. Furthermore, the rapidly expanding economy of the U.S. demanded inexpensive materials to meet consumer demands. Pultrusion offered a fast and economical method of forming constant profile parts, and pultruded composites were being used to make golf clubs and fishing poles. It was not until the 1960s, however, that these materials were seriously considered for use as reinforcement in concrete.

The expansion of the national highway systems in the 1950s increased the need to provide year-round maintenance. It became common to apply deicing salts on highway bridges. As a result, reinforcing steel in these structures and those subject to marine salt experienced extensive corrosion, and thus became a major concern. Various solutions were investigated, including galvanized coatings, electro-static-spray fusion-bonded (powder resin) coatings, polymer-impregnated concrete, epoxy coatings, and glass FRP (GFRP) reinforcing bars (ACI 440R). Of these options, epoxy-coated steel reinforcement appeared to be the best solution, and was implemented in aggressive corrosion environments. The FRP reinforcing bar was not considered a viable solution and was not commercially available until the late 1970s. In 1983, the first project funded by the U.S. Department of Transportation (USDOT) was on "Transfer of Composite Technology to Design and Construction of Bridges" (Plecnik and Ahmad 1988).

Marshall-Vega Inc. led the initial development of GFRP reinforcing bars in the U.S. Initially, GFRP bars were

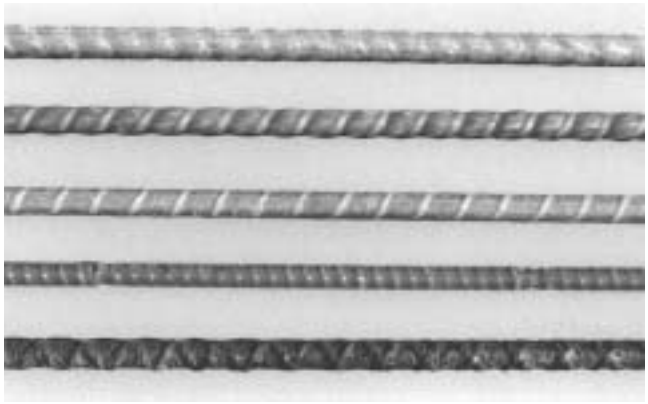

*Fig. 2.1—Commercially available GFRP reinforcing bars.*

*Fig. 2.2—GFRP bars installed during the construction of the Crowchild Bridge deck in Calgary, Alberta, Canada, in 1997.*

considered a viable alternative to steel as reinforcement for polymer concrete due to the incompatibility of thermal expansion characteristics between polymer concrete and steel. In the late 1970s, International Grating Inc. entered the North American FRP reinforcement market. Marshall-Vega and International Grating led the research and development of FRP reinforcing bars into the 1980s.

The 1980s market demanded nonmetallic reinforcement for specific advanced technology. The largest demand for electrically nonconductive reinforcement was in facilities for MRI medical equipment. FRP reinforcement became the standard in this type of construction. Other uses developed as the advantages of FRP reinforcement became better known and desired, specifically in seawall construction, substation reactor bases, airport runways, and electronics laboratories (Brown and Bartholomew 1996).

The concern for the deterioration of bridges due to chloride-ion-induced corrosion dates back to the 1970s, and its effects on aging bridges in the U.S. has become apparent (Boyle and Karbhari 1994). Additionally, detection of corrosion in the commonly used epoxy-coated reinforcing bars increased interest in alternative methods of avoiding corrosion. Once again, FRP reinforcement began to be considered as a general solution to address problems of corrosion in bridge decks and other structures (Benmokrane et al. 1996).

## 2.2—Commercially available FRP reinforcing bars

Commercially available FRP reinforcing materials are made of continuous aramid FRP (AFRP), carbon FRP (CFRP), or GFRP fibers embedded in a resin matrix (ACI 440R). Typical FRP reinforcement products are grids, bars, fabrics, and ropes. The bars have various types of cross-sectional shapes (square, round, solid, and hollow) and deformation systems (exterior wound fibers, sand coatings, and separately formed deformations). A sample of five distinctly different GFRP reinforcing bars is shown in Fig. 2.1.

## 2.3—History of use

Up to the mid-1990s, the Japanese had the most FRP reinforcement applications, with more than 100 demonstration or commercial projects. FRP design provisions were included in the design and construction recommendations of the JSCE (1997b). In Asia, China has recently become the largest user of composite reinforcement for new construction in applications that span from bridge decks to underground works (Ye et al. 2003).

The use of FRP reinforcement in Europe began in Germany with the construction of a prestressed FRP highway bridge in 1986 (Meier 1992). Since the construction of this bridge, programs have been implemented to increase the research and use of FRP reinforcement in Europe. The European BRITE/EURAM Project, "Fibre Composite Elements and Techniques as Nonmetallic Reinforcement," conducted extensive testing and analysis of the FRP materials from 1991 to 1996 (Taerwe 1997). More recently, EUROCRETE has headed the European effort with research and demonstration projects.

Canadian civil engineers have developed provisions for FRP reinforcement in the Canadian Highway Bridge Design Code and have constructed a number of demonstration projects. The Headingley Bridge in Manitoba included both CFRP and GFRP reinforcement (Rizkalla 1997). Additionally, the Kent County Road No. 10 Bridge used CFRP grids to reinforce the negative moment regions (Tadros et al. 1998). The Joffre Bridge, located over the St.-François River in Sherbrooke, Quebec, included CFRP grids in its deck slab and GFRP reinforcing bars in the traffic barrier and sidewalk. The bridge, which was opened to traffic in December 1997, included fiber-optic sensors that were structurally integrated into the FRP reinforcement for remotely monitoring strains (Benmokrane et al. 2004). Photographs of two applications (bridge and building) are shown in Fig. 2.2 and 2.3. Canada continues to remain a leader in the application of FRP reinforcement in bridge deck construction (Benmokrane et al. 2004).

In the U.S., typical uses of FRP reinforcement have been previously reported (ACI 440R). Figure 2.4 through 2.6 show applications in bridge deck construction. The use of GFRP bars in MRI hospital room additions is becoming commonplace. Other applications, such as waterfront construction, top mat reinforcing for bridge decks, various precast applications, and ornamental and architectural concrete are also becoming more frequent. Some of the largest projects include the Gonda Building at the Mayo

*Fig. 2.3—GFRP bars used in a winery in British Columbia in 1998.*

*Fig. 2.4—FRP-reinforced deck constructed in Lima, Ohio (Pierce Street Bridge), in 1999.*

*Fig. 2.5—GFRP bars used in the redecking of Dayton, Ohio's Salem Avenue Bridge in 1999.*

Clinic in Rochester, Minn. and the National Institute of Health in Bethesda, Md. for MRI applications, and the bridge on RM 1061 at Sierrita de la Cruz Creek in Potter County, Tex. and the bridge at 53rd Ave. in Bettendorf, Iowa for deck reinforcement applications (Nanni 2001).

Tunnel works where GFRP reinforcement is used in the portion of the concrete wall to be excavated by the tunnel-

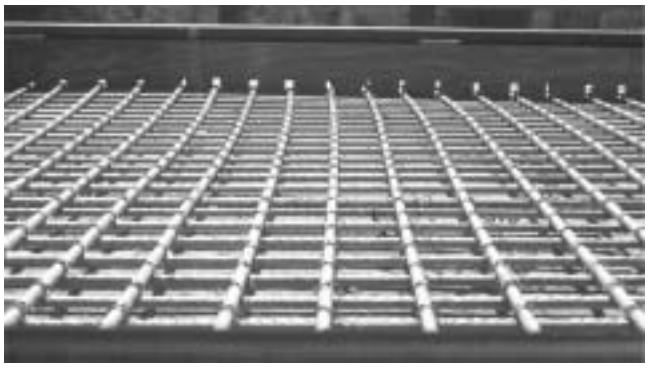

*Fig. 2.6—Transverse view of GFRP bars in Sierrita de la Cruz Creek Bridge deck near Amarillo, Tex., in 2000.*

boring machine (TBM) called soft-eye have become common in many major metropolitan areas of the world, including Asia (for example, Bangkok, Hong Kong, and New Delhi) and Europe (for example, London and Berlin).

## CHAPTER 3—MATERIAL CHARACTERISTICS

This chapter presents physical and mechanical properties of FRP reinforcing bars to provide a fundamental understanding of the behavior of these bars and the properties that affect their use in concrete structures. Furthermore, the effects of factors, such as loading history and duration, temperature, and moisture, on the properties of FRP bars are discussed.

FRP bars are anisotropic in nature and can be manufactured using a variety of techniques such as pultrusion, braiding, and weaving (Bank 1993; Bakis 1993). Factors such as fiber volume, type of fiber, type of resin, fiber orientation, dimensional effects, and quality control during manufacturing all play a major role in defining the characteristics of an FRP bar. The material characteristics described in this chapter should be considered as generalizations, and may not apply to all products commercially available.

Several standards development organizations have developed consensus-based test methods for FRP reinforcement for use in structural concrete (ACI 440.3R; JSCE 1997b). In addition, International Standards Organization (ISO) Committee ISO/TC71, Subcommittee 6 (ISO/TC71/SC6) (Non Traditional Reinforcing Materials for Concrete) is developing two documents. The first draft document is "Test Methods for FRP Bars and Grids," and the second draft document is "Test Methods for FRP Sheets."

### 3.1—Physical properties

**3.1.1** *Density*—FRP bars have a density ranging from 77.8 to 131.3 lb/ft$^3$ (1.25 to 2.1 g/cm$^3$), one-sixth to one-fourth that of steel (Table 3.1). Reduced weight lowers transportation costs and may ease handling of the bars on the project site.

**3.1.2** *Coefficient of thermal expansion*—The coefficients of thermal expansion of FRP bars vary in the longitudinal and transverse directions depending on the types of fiber, resin, and volume fraction of fiber. The longitudinal coefficient of thermal expansion is dominated by the properties of the fibers, while the transverse coefficient is dominated by the resin (Bank 1993). Table 3.2 lists the longitudinal and transverse

coefficients of thermal expansion for typical FRP and steel bars. Note that a negative coefficient of thermal expansion indicates that the material contracts with increased temperature and expands with decreased temperature. For reference, concrete has a coefficient of thermal expansion that varies from $4 \times 10^{-6}$ to $6 \times 10^{-6}$/°F ($7.2 \times 10^{-6}$ to $10.8 \times 10^{-6}$/°C) and is usually assumed to be isotropic (Mindess et al. 2003).

### 3.2—Mechanical properties and behavior

**3.2.1** *Tensile behavior*—When loaded in tension, FRP bars do not exhibit any plastic behavior (yielding) before rupture. The tensile behavior of FRP bars consisting of one type of fiber material is characterized by a linearly elastic stress-strain relationship until failure. The tensile properties of some commonly used FRP bars are summarized in Table 3.3.

The tensile strength and stiffness of an FRP bar are dependent on several factors. Because the fibers in an FRP bar are the main load-carrying constituent, the ratio of the volume of fiber to the overall volume of the FRP (fiber-volume fraction) significantly affects the tensile properties of an FRP bar. Strength and stiffness variations will occur in bars with various fiber-volume fractions, even in bars with the same diameter, appearance, and constituents. The rate of curing, the manufacturing process, and the manufacturing quality control also affect the mechanical characteristics of the bar (Wu 1990).

Unlike steel, the unit tensile strength of an FRP bar can vary with diameter. For example, GFRP bars from three different manufacturers show tensile strength reductions of up to 40% as the diameter increases proportionally from 0.375 to 0.875 in. (9.5 to 22.2 mm) (Faza and GangaRao 1993b). On the other hand, similar cross section changes do not seem to affect the strength of twisted CFRP strands (Santoh 1993). The sensitivity of AFRP bars to cross section size has been shown to vary from one commercial product to another. For example, in braided AFRP bars, there is a less than 2% strength reduction as bars increase in diameter from 0.28 to 0.58 in. (7.3 to 14.7 mm) (Tamura 1993). The strength reduction in a unidirectionally pultruded AFRP bar with added aramid fiber surface wraps is approximately 7% for diameters increasing from 0.12 to 0.32 in. (3 to 8 mm) (Noritake et al. 1993). The FRP bar manufacturer should be contacted for particular strength values of differently sized FRP bars.

Determination of FRP bar strength by testing is complicated because stress concentrations in and around anchorage points on the test specimen can lead to premature failure. An adequate testing grip should allow failure to occur in the middle of the test specimen. Proposed test methods for determining the tensile strength and stiffness of FRP bars are available in ACI 440.3R.+

The tensile properties of a particular FRP bar should be obtained from the bar manufacturer. Usually, a normal (Gaussian) distribution is assumed to represent the strength of a population of bar specimens (Kocaoz et al. 2005). Manufacturers should report a guaranteed tensile strength $f_{fu}^*$, defined by this guide as the mean tensile strength of a sample of test specimens minus three times the standard deviation ($f_{fu}^* = f_{u,ave} - 3\sigma$), and similarly report a guaranteed rupture strain, $\varepsilon_{fu}^*$ ($\varepsilon_{fu}^* = \varepsilon_{u,ave} - 3\sigma$) and a specified tensile modulus, $E_f$ ($E_f = E_{f,ave}$). These guaranteed values of strength and strain provide a 99.87% probability that the indicated values are exceeded by similar FRP bars, provided that at least 25 specimens are tested (Dally and Riley 1991; Mutsuyoshi et al. 1990). If fewer specimens are tested or a different distribution is used, texts and manuals on statistical analysis should be consulted to determine the confidence level of the distribution parameters (MIL-17 1999). In any case, the manufacturer should provide a description of the method used to obtain the reported tensile properties.

An FRP bar cannot be bent once it has been manufactured (an exception to this would be an FRP bar with a thermoplastic resin that could be reshaped with the addition of heat and pressure). FRP bars, however, can be fabricated with bends. In FRP bars produced with bends, a strength reduction of 40 to 50% compared with the tensile strength of a straight bar can occur in the bend portion due to fiber bending and stress concentrations (Nanni et al. 1998).

**3.2.2** *Compressive behavior*—While it is not recommended to rely on FRP bars to resist compressive stresses, the following section is presented to fully characterize the behavior of FRP bars.

Tests on FRP bars with a length-diameter ratio from 1:1 to 2:1 have shown that the compressive strength is lower than

**Table 3.1—Typical densities of reinforcing bars, lb/ft$^3$ (g/cm$^3$)**

| Steel | GFRP | CFRP | AFRP |
|---|---|---|---|
| 493.00 (7.90) | 77.8 to 131.00 (1.25 to 2.10) | 93.3 to 100.00 (1.50 to 1.60) | 77.80 to 88.10 (1.25 to 1.40) |

**Table 3.2—Typical coefficients of thermal expansion for reinforcing bars***

| Direction | CTE, $\times 10^{-6}$/°F ($\times 10^{-6}$/°C) | | | |
|---|---|---|---|---|
| | Steel | GFRP | CFRP | AFRP |
| Longitudinal, $\alpha_L$ | 6.5 (11.7) | 3.3 to 5.6 (6.0 to 10.0) | –4.0 to 0.0 (–9.0 to 0.0) | –3.3 to –1.1 (–6 to –2) |
| Transverse, $\alpha_T$ | 6.5 (11.7) | 11.7 to 12.8 (21.0 to 23.0) | 41 to 58 (74.0 to 104.0) | 33.3 to 44.4 (60.0 to 80.0) |

*Typical values for fiber volume fraction ranging from 0.5 to 0.7.

**Table 3.3—Usual tensile properties of reinforcing bars***

| | Steel | GFRP | CFRP | AFRP |
|---|---|---|---|---|
| Nominal yield stress, ksi (MPa) | 40 to 75 (276 to 517) | N/A | N/A | N/A |
| Tensile strength, ksi (MPa) | 70 to 100 (483 to 690) | 70 to 230 (483 to 1600) | 87 to 535 (600 to 3690) | 250 to 368 (1720 to 2540) |
| Elastic modulus, $\times 10^3$ ksi (GPa) | 29.0 (200.0) | 5.1 to 7.4 (35.0 to 51.0) | 15.9 to 84.0 (120.0 to 580.0) | 6.0 to 18.2 (41.0 to 125.0) |
| Yield strain, % | 0.14 to 0.25 | N/A | N/A | N/A |
| Rupture strain, % | 6.0 to 12.0 | 1.2 to 3.1 | 0.5 to 1.7 | 1.9 to 4.4 |

*Typical values for fiber volume fractions ranging from 0.5 to 0.7.

the tensile strength (Wu 1990). The mode of failure for FRP bars subjected to longitudinal compression can include transverse tensile failure, fiber microbuckling, or shear failure. The mode of failure depends on the type of fiber, the fiber-volume fraction, and the type of resin. Compressive strengths of 55, 78, and 20% of the tensile strength have been reported for GFRP, CFRP, and AFRP, respectively (Mallick 1988; Wu 1990). In general, compressive strengths are higher for bars with higher tensile strengths, except in the case of AFRP, where the fibers exhibit nonlinear behavior in compression at a relatively low level of stress.

The compressive modulus of elasticity of FRP reinforcing bars appears to be smaller than its tensile modulus of elasticity. Test reports on samples containing 55 to 60% volume fraction of continuous E-glass fibers in a matrix of vinyl ester or isophthalic polyester resin indicate a compressive modulus of elasticity of 5000 to 7000 ksi (35 to 48 GPa) (Wu 1990). According to reports, the compressive modulus of elasticity is approximately 80% for GFRP, 85% for CFRP, and 100% for AFRP of the tensile modulus of elasticity for the same product (Mallick 1988; Ehsani 1993). The slightly lower values of modulus of elasticity in the reports may be attributed to the premature failure in the test resulting from end brooming and internal fiber microbuckling under compressive loading.

Standard test methods are not yet established to characterize the compressive behavior of FRP bars. If the compressive properties of a particular FRP bar are needed, these should be obtained from the bar manufacturer. The manufacturer should provide a description of the test method used to obtain the reported compression properties.

**3.2.3** *Shear behavior*—Most FRP bar composites are relatively weak in interlaminar shear where layers of unreinforced resin lie between layers of fibers. Because there is usually no reinforcement across layers, the interlaminar shear strength is governed by the relatively weak polymer matrix. Orientation of the fibers in an off-axis direction across the layers of fiber will increase the shear resistance, depending upon the degree of offset. For FRP bars, this can be accomplished by braiding or winding fibers transverse to the main fibers. Off-axis fibers can also be placed in the pultrusion process by introducing a continuous strand mat in the roving/mat creel. Standard test methods are not yet established to characterize the shear behavior of FRP bars. If the shear properties of a particular FRP bar are needed, these should be obtained from the bar manufacturer. The manufacturer should provide a description of the test method used to obtain the reported shear values.

**3.2.4** *Bond behavior*—Bond performance of an FRP bar is dependent on the design, manufacturing process, mechanical properties of the bar itself, and the environmental conditions (Al-Dulaijan et al. 1996; Nanni et al. 1997; Bakis et al. 1998b; Bank et al. 1998; Freimanis et al. 1998). When anchoring a reinforcing bar in concrete, the bond force can be transferred by:

- Adhesion resistance of the interface, also known as chemical bond;
- Frictional resistance of the interface against slip; and
- Mechanical interlock due to irregularity of the interface.

In FRP bars, it is postulated that bond force is transferred through the resin to the reinforcement fibers, and a bond-shear failure in the resin is also possible. When a bonded deformed bar is subjected to increasing tension, the adhesion between the bar and the surrounding concrete breaks down, and deformations on the surface of the bar cause inclined contact forces between the bar and the surrounding concrete. The stress at the surface of the bar resulting from the force component in the direction of the bar can be considered the bond stress between the bar and the concrete.

The bond properties of FRP bars have been extensively investigated by numerous researchers through different types of tests, such as pullout tests, splice tests, and cantilever beams, to determine an empirical equation for embedment length (Faza and GangaRao 1990; Ehsani et al. 1996a,b; Benmokrane 1997; Shield et al. 1999; Mosley 2002; Wambeke and Shield 2006; Tighiouart et al. 1999).

### 3.3—Time-dependent behavior

**3.3.1** *Creep rupture*—FRP reinforcing bars subjected to a constant load over time can suddenly fail after a time period called the endurance time. This phenomenon is known as creep rupture (or static fatigue). Creep rupture is not an issue with steel bars in reinforced concrete except in extremely high temperatures, such as those encountered in a fire. As the ratio of the sustained tensile stress to the short-term strength of the FRP bar increases, endurance time decreases. The creep rupture endurance time can also irreversibly decrease under sufficiently adverse environmental conditions such as high temperature, ultraviolet radiation exposure, high alkalinity, wet and dry cycles, or freezing-and-thawing cycles. Literature on the effects of such environments exists, although the extraction of generalized design criteria is hindered by a lack of standard creep test methods and reporting and the diversity of constituents and processes used to make proprietary FRP products. In addition, little data are currently available for endurance times beyond 100 hours. These factors have resulted in design criteria judged to be conservative until more research has been done on this subject. Several representative examples of endurance times for bar and bar-like materials follow. No creep strain data are available in these cases.

In general, carbon fibers are the least susceptible to creep rupture, whereas aramid fibers are moderately susceptible, and glass fibers are the most susceptible. A comprehensive series of creep rupture tests was conducted on 0.25 in. (6 mm) diameter smooth FRP bars reinforced with glass, aramid, and carbon fibers (Yamaguchi et al. 1997). The bars were tested at different load levels at room temperature in laboratory conditions using split conical anchors. Results indicated that a linear relationship exists between creep rupture strength and the logarithm of time for times up to nearly 100 hours. The ratios of stress level at creep rupture to the initial strength of the GFRP, AFRP, and CFRP bars after 500,000 hours (more than 50 years) were linearly extrapolated to be 0.29, 0.47, and 0.93, respectively.

In another extensive investigation, endurance times were determined for braided AFRP bars and twisted CFRP bars,

both using epoxy resin as the matrix material (Ando et al. 1997). These commercial bars were tested at room temperature in laboratory conditions and were anchored with an expansive cementitious grout inside of friction-type grips. Bar diameters ranged from 0.26 to 0.6 in. (5 to 15 mm), but were not found to affect the results. The percentage of stress at creep rupture versus the initial strength after 50 years calculated using a linear relationship extrapolated from data available to 100 hours was found to be 79% for CFRP, and 66% for AFRP.

An investigation of creep rupture in GFRP bars in room-temperature laboratory conditions was reported by Seki et al. (1997). The molded E-glass/vinyl ester bars had a small (0.0068 in.$^2$ [4.4 mm$^2$]) rectangular cross section and integral GFRP tabs. The percentage of initial tensile strength retained followed a linear relationship with logarithmic time, reaching a value of 55% at an extrapolated 50-year endurance time.

Creep rupture data characteristics of a 0.5 in. (12.5 mm) diameter commercial CFRP twisted strand in an indoor environment is available from the manufacturer (Tokyo Rope 2000). The rupture strength at a projected 100-year endurance time is reported to be 85% of the initial strength.

An extensive investigation of creep deformation (not rupture) in one commercial AFRP and two commercial CFRP bars tested to 3000 hours has been reported (Saadatmanesh and Tannous 1999a,b). The bars were tested in laboratory air and in room-temperature solutions with a pH equal to 3 and 12. The bars had diameters between 0.313 to 0.375 in. (8 to 10 mm), and the applied stress was fixed at 40% of initial strength. The results indicated a slight trend toward higher creep strain in the larger-diameter bars and in the bars immersed in the acidic solution. Bars tested in air had the lowest creep strains of the three environments. Considering all environments and materials, the range of strains recorded after 3000 hours was 0.002 to 0.037%. Creep strains were slightly higher in the AFRP bar than in the CFRP bars.

For experimental characterization of creep rupture, the designer can refer to the test method proposed by a committee of JSCE (1997b), the with the specific title of "Test Method on Tensile Creep-Rupture of Fiber Reinforced Materials, JSCE-E533-1995." Creep characteristics of FRP bars can also be determined from pullout test methods cited in ACI 440.3R. Recommendations on sustained stress limits imposed to avoid creep rupture are provided in the design section of this guide.

**3.3.2** *Fatigue*—A substantial amount of data for fatigue behavior and life prediction of stand-alone FRP materials has been generated in the last 30 years (National Research Council 1991). During most of this time period, the focus of research investigations was on materials suitable for aerospace applications. Some general observations on the fatigue behavior of FRP materials can be made, even though the bulk of the data is obtained from FRP specimens intended for aerospace applications rather than construction. Unless stated otherwise, the cases that follow are based on flat, unidirectional coupons with approximately 60% fiber-volume fraction and subjected to tension-tension sinusoidal cyclic loading at:

- A frequency low enough not to cause self-heating;
- Ambient laboratory environments;
- A stress ratio (ratio of minimum applied stress to maximum applied stress) of 0.1; and
- A direction parallel to the principal fiber alignment.

Test conditions that raise the temperature and moisture content of FRP materials generally degrade the ambient environment fatigue behavior.

Of all types of current FRP composites for infrastructure applications, CFRP is generally thought to be the least prone to fatigue failure. On a plot of stress versus the logarithm of the number of cycles at failure (S-N curve), the average downward slope of CFRP data is usually about 5 to 8% of initial static strength per decade of logarithmic life. At 1 million cycles, the fatigue strength is generally between 50 and 70% of initial static strength and is relatively unaffected by realistic moisture and temperature exposures of concrete structures unless the resin or fiber/resin interface is substantially degraded by the environment. Some specific reports of data to 10 million cycles indicated a continued downward trend of 5 to 8% decade in the S-N curve (Curtis 1989).

Individual glass fibers, such as E-glass and S-glass, are generally not prone to fatigue failure. Individual glass fibers, however, have demonstrated delayed rupture caused by the stress corrosion induced by the growth of surface flaws in the presence of even minute quantities of moisture in ambient laboratory environment tests (Mandell and Meier 1983). When many glass fibers are embedded into a matrix to form an FRP composite, a cyclic tensile fatigue effect of approximately 10% loss in the initial static capacity per decade of logarithmic lifetime has been observed (Mandell 1982). This fatigue effect is thought to be due to fiber-fiber interactions and not is dependent on the stress corrosion mechanism described for individual fibers. No clear fatigue limit can usually be defined. Environmental factors play an important role in the fatigue behavior of glass fibers due to their susceptibility to moisture, alkaline, and acidic solutions.

Aramid fibers, for which substantial durability data are available, appear to behave similarly to carbon and glass fibers in fatigue. The tension-tension fatigue behavior of an impregnated aramid fiber bar is excellent. Strength degradation per decade of logarithmic lifetime is approximately 5 to 6% (Roylance and Roylance 1981). While no distinct endurance limit is known for AFRP, 2-million-cycle fatigue strengths of commercial AFRP bars for concrete applications have been reported in the range of 54 to 73% of initial bar strengths (Odagiri et al. 1997). Based on these findings, Odagiri et al. suggested that the maximum stress be set at 54 to 73% of the initial tensile strength. Because the slope of the applied stress versus logarithmic creep-rupture time of AFRP is similar to the slope of the stress versus logarithmic cyclic lifetime data, the individual fibers appear to fail by a strain-limited creep-rupture process. This failure condition in commercial AFRP bars was noted to be accelerated by exposure to moisture and elevated temperature (Roylance and Roylance 1981; Rostasy 1997).

Although the influence of moisture on the fatigue behavior of unidirectional FRP materials is generally thought to be

detrimental if the resin or fiber/matrix interface is degraded, research findings are inconclusive because the performance depends on fiber and matrix types, preconditioning methods, solution content, and the environmental condition during fatigue (Hayes et al. 1998; Rahman et al. 1997). In addition, factors such as gripping and presence of concrete surrounding the bar during the fatigue test need to be considered.

Fatigue strength of CFRP bars encased in concrete has been observed to decrease when the environmental temperature increases from 68 to 104 °F (20 to 40 °C) (Adimi et al. 1998). In this same investigation, the endurance limit was found to be inversely proportional to the loading frequency. It was also found that higher cyclic loading frequencies in the 0.5 to 8 Hz range corresponded to higher bar temperatures due to sliding friction. Thus, an endurance limit at 1 Hz could be more than 10 times higher than that at 5 Hz. In the cited investigation, a stress ratio (minimum stress divided by maximum stress) of 0.1 and a maximum stress of 50% of initial strength resulted in runouts of greater than 400,000 cycles when the loading frequency was 0.5 Hz. These runout specimens had no loss of residual tensile strength.

It has been found with CFRP bars that the endurance limit also depends on the mean stress and the ratio of maximum-to-minimum cyclic stress. Higher mean stress or a lower stress ratio (minimum divided by maximum) will cause a reduction in the endurance limit (Rahman and Kingsley 1996; Saadatmanesh and Tannous 1999a).

Even though GFRP is weaker than steel in shear, fatigue tests on specimens with unbonded GFRP dowel bars have shown fatigue behavior similar to that of steel dowel bars for cyclic transverse shear loading of up to 10 million cycles. The test results and the stiffness calculations have shown that an equivalent performance can be achieved between FRP and steel bars subjected to transverse shear by changing some of the parameters, such as diameter, spacing, or both (Porter et al. 1993; Hughes and Porter 1996).

The addition of ribs, wraps, and other types of deformations improve the bond behavior of FRP bars. Such deformations, however, have been shown to induce local stress concentrations that significantly affect the performance of a GFRP bar under fatigue loading situations (Katz 1998). Local stress concentrations degrade fatigue performance by imposing multiaxial stresses that serve to increase matrix-dominated damage mechanisms normally suppressed in fiber-dominated composite materials. Additional fiber-dominated damage mechanisms can be also activated near deformations, depending on the construction of the bar.

The effect of fatigue on the bond of deformed GFRP bars embedded in concrete has been investigated in detail using specialized bond tests (Sippel and Mayer 1996; Bakis et al. 1998a; Katz 2000). Different GFRP materials, environments, and test methods were followed in each cited case, and the results indicated that bond strength can either increase, decrease, or remain the same following cyclic loading. Bond fatigue behavior has not been sufficiently investigated to date, and conservative design criteria based on specific materials and experimental conditions are recommended.

Design limitations on fatigue stress ranges for FRP bars ultimately depend on the manufacturing process of the FRP bar, environmental conditions, and the type of fatigue load being applied. Given the ongoing development in the manufacturing process of FRP bars, conservative design criteria should be used for all commercially available FRP bars. Design criteria are given in Section 8.4.2.

With regard to the fatigue characteristics of FRP bars, the designer is referred to the provisional standard test methods cited in ACI 440.3R. The designer should always consult with the bar manufacturer for fatigue response properties.

### 3.4—Effects of high temperatures and fire

The use of FRP reinforcement is not recommended for structures in which fire resistance is essential to maintain structural integrity. Because FRP reinforcement is embedded in concrete, the reinforcement cannot burn due to a lack of oxygen; however, the polymers will soften due to the excessive heat. The temperature at which a polymer will soften is known as the glass-transition temperature $T_g$. Beyond the $T_g$, the elastic modulus of a polymer is significantly reduced due to changes in its molecular structure. The value of $T_g$ depends on the type of resin, but is normally in the region of 150 to 250 °F (65 to 120 °C) (Bootle et al. 2001). In a composite material, the fibers, which exhibit better thermal properties than the resin, can continue to support some load in the longitudinal direction; however, the tensile properties of the overall composite are reduced due to a reduction in force transfer between fibers through bond to the resin. Test results have indicated that temperatures of 480 °F (250 °C), much higher than the $T_g$, will reduce the tensile strength of GFRP and CFRP bars in excess of 20% (Kumahara et al. 1993). Other properties more directly affected by the shear transfer through the resin, such as shear and bending strength, are reduced significantly at temperatures above the $T_g$ (Wang and Evans 1995). For purposes of design, some researchers recommended that materials have a $T_g$ at least 54 °F (30 °C) above the maximum expected temperature (Kollár and Springer et al. 2003).

For FRP-reinforced concrete, the properties of the polymer at the surface of the bar are essential in maintaining bond between FRP and concrete. At a temperature close to its $T_g$, however, the mechanical properties of the polymer are significantly reduced, and the polymer is not able to transfer stresses from the concrete to the fibers. One study carried out with bars having a $T_g$ of 140 to 255 °F (60 to 124 °C) reports a reduction in pullout (bond) strength of 20 to 40% at a temperature of approximately 210 °F (100 °C), and a reduction of 80 to 90% at a temperature of 390 °F (200 °C) (Katz et al. 1998, 1999). In a study on flexural behavior of beams with partial pretensioning with AFRP tendons and reinforcement with either AFRP or CFRP bars, beams were subjected to elevated temperatures under a sustained load. Failure of the beams occurred when the temperature of the reinforcement reached approximately 390 and 572 °F (200 and 300 °C) in the carbon and aramid bars, respectively (Okamoto et al. 1993). Another study involving FRP-reinforced beams reported reinforcement tensile failures when the reinforcement

reached temperatures of 480 to 660 °F (250 to 350 ºC) (Sakashita et al. 1997). Structural collapse can occur if anchorage is lost due to softening of the polymer and also when the temperature rises above the temperature threshold of fibers: 1600 °F (880 °C) for glass fibers, 360 °F (180 °C) for aramid fibers, and 2900 °F (1600 °C) for carbon fibers (Wallenberger et al. 2001; Chang 2001; Walsh 2001). For carbon fibers, elevated temperatures cause higher oxidizing rates when there is oxygen in the atmosphere. While there is no sharp threshold that can be called a safe temperature for infinite life, a recommended upper-use temperature in the presence of air would be roughly 900 °F (500 °C). To be conservative, this temperature should be used as the limiting temperature for carbon fibers even if they might be partially isolated from oxygen by uncracked concrete and charred polymer (Lamouroux et al. 1999).

Locally, such behavior can result in increased crack widths and deflections. Structural collapse can be avoided if high temperatures are not experienced at the end regions of FRP bars, allowing anchorage to be maintained. Structural collapse can occur if all anchorage is lost due to softening of the polymer or if the temperature rises above the temperature threshold of the fibers themselves. The latter can occur at temperatures near 1800 ºF (980 ºC) for glass fibers and 350 ºF (175 ºC) for aramid fibers. Carbon fibers are capable of resisting temperatures in excess of 3000 ºF (1600 ºC). The behavior and endurance of FRP-reinforced concrete structures under exposure to fire and high heat is still not well understood, and further research in this area is required. ACI 216R may be used for an estimation of temperatures at various depths of a concrete section.

## CHAPTER 4—DURABILITY

FRP bars are susceptible to varying amounts of strength and stiffness changes in the presence of environments before, during, and after construction. These environments can include water, ultraviolet exposure, elevated temperature, alkaline or acidic solutions, and saline solutions. Strength and stiffness may increase, decrease, or remain the same, depending on the particular material and exposure conditions. Tensile and bond properties of FRP bars are the primary parameters of interest for reinforced concrete construction.

The environmental condition that has attracted the most interest by investigators concerned with FRP bars is the highly alkaline pore water found in outdoor concrete structures (Gerritse 1992; Takewaka and Khin 1996; Rostasy 1997; and Yamaguchi et al. 1997). Methods for systematically accelerating the strength degradation of bare, unstressed, glass filaments in concrete using temperature have been successful (Litherland et al. 1981), and have also often been applied to GFRP materials to predict long-term performance in alkaline solutions. There is no substantiation to date, however, that accelerated methods for bare glass (where only one chemical reaction controls degradation) apply to GFRP composites (where multiple reactions and degradation mechanisms may be activated at once or sequentially). Furthermore, the effect of applied stress during exposure needs to be factored into the situation as well. Due to insufficient data on combined weathering and applied stress, the discussions of weathering, creep, and fatigue are kept separate in this document. Hence, while short-term experiments using aggressive environments certainly enable quick comparisons of materials, extrapolation of the results to field conditions and expected lifetimes are not possible in the absence of real-time data (Gentry et al. 1998; Clarke and Sheard 1998). In most cases available to date, bare bars were subjected to the aggressive environment under no load. The relationships between data on bare bars and data on bars embedded in concrete are affected by additional variables, such as the degree of protection offered to the bars by the concrete (Clarke and Sheard 1998; Scheibe and Rostasy 1998; Sen et al. 1998a,b). Test times included in this review are typically in the 10- to 30-month range. Due to the large amount of literature on the subject (Benmokrane and Rahman 1998) and the limited space herein, some generalizations must be made at the expense of presenting particular quantitative results. With these cautions in mind, representative experimental results for a range of FRP bar materials and test conditions are reviewed in the balance of this section. Conservatism is advised in applying these results in design until additional long-term durability data are available.

Aqueous solutions with high values of pH varying from 11.5 to 13.0 are known to degrade the tensile strength and stiffness of GFRP bars (Porter and Barnes 1998), although particular results vary significantly according to differences in test methods that, in addition to pH, include composition of the chemical solution, temperature, and presence of load. Higher temperatures and longer exposure times exacerbate the problem. Most data have been generated using temperatures as low as slightly subfreezing and as high as a few degrees below the $T_g$ of the resin. The degree to which the resin protects the glass fibers from the diffusion of deleterious hydroxyl ($OH^-$) ions figures prominently in the alkali resistance of GFRP bars (Bank and Puterman 1997; Coomarasamy and Goodman 1997; GangaRao and Vijay 1997b; Porter et al. 1997; Bakis et al. 1998b; Tannous and Saadatmanesh 1999; Uomoto 2000). Most researchers believe that vinyl ester resins have superior resistance to moisture ingress compared with other commodity resins. The type of glass fiber also appears to be an important factor in the alkali resistance of GFRP bars (Devalapura et al. 1996). Tensile strength reductions in GFRP bars ranging from 0 to 75% of initial values have been reported in the cited literature. Tensile stiffness reductions in stressed and unstressed GFRP bars range between 0 and 20% in many cases. Tensile strength and stiffness of AFRP rods in elevated-temperature alkaline solutions either with or without tensile stress applied have been reported to decrease between 10 and 50% and 0 and 20% of initial values, respectively (Takewaka and Khin 1996; Rostasy 1997; Sen at al. 1998b). In the case of unstressed CFRP, strength and stiffness have been reported to each decrease between 0 and 20% (Takewaka and Khin 1996).

Exposure of FRP bars to ultraviolet rays and moisture before their placement in concrete could adversely affect their tensile strength due to degradation of the polymer constituents, including aramid fibers and all resins. Proper

construction practices and resin additives can ameliorate this type of weathering problem significantly. It is highly recommended that, before placement in concrete, FRP bars are protected from direct exposure to sunlight and moisture. Some results from combined ultraviolet and moisture exposure tests with and without applied stress applied to the bars have shown tensile strength reductions of 0 to 20% of initial values in CFRP, 0 to 30% in AFRP, and 0 to 40% in GFRP (Sasaki et al. 1997; Uomoto 2000). An extensive study of GFRP, AFRP, and CFRP bars kept outdoors in a rack by the ocean showed no significant change of tensile strength or modulus of any of the bars (Tomosowa and Nakatsuji 1996, 1997).

It has been shown (Rahman et al. 1996) that the addition of various types of salts to the solution in which FRP bars are immersed does not necessarily make a significant difference in the strength and stiffness of many FRP bars when compared with those in a solution without salt. Most studies, however, do not separate the effects of water and salt added to water. One study found a 0 to 20% reduction of initial tensile strength in GFRP bars subjected to a saline solution at room temperature and cyclic freezing-and-thawing temperatures (Vijay and GangaRao 1999), and another found a 15% reduction in the strength of AFRP bars in a marine environment (Sen et al. 1998b).

Studies of the durability of bond between FRP and concrete have been mostly concerned with the moist, alkaline environment found in concrete. The bond of FRP reinforcement relies on the transfer of shear and transverse forces at the interface between bar and concrete, and between individual fibers within the bar. These resin-dominated mechanisms are in contrast to the fiber-dominated mechanisms that control properties such as longitudinal strength and stiffness of FRP bars. Environments that degrade the polymer resin or fiber/resin interface are thus also likely to degrade the bond strength of an FRP bar.

Numerous bond test methods (that is, pullout tests, tension tests, and beam-end tests) have been proposed for FRP bars, although the direct pullout test has been the most popular due to its simplicity and low cost despite its inability to represent the concrete stress state in most of the practical situations (Nanni et al. 1995; Tepfers 2002). Pullout specimens with CFRP and GFRP bars have been subjected to natural environmental exposures, and have not indicated significant decreases in bond strength over periods of time between 1 and 2 years (Clarke and Sheard 1998; Sen et al. 1998a). Positive and negative trends in pullout strength with respect to shorter periods of time have been obtained with GFRP bars subjected to wet elevated-temperature environments in concrete, with or without artificially added alkalinity (Al-Dulaijan et al. 1996; Bakis et al. 1998b; Bank et al. 1998; Porter and Barnes 1998). Similar observations on such pullout tests using specimens subjected to accelerated environmental exposure carry over to AFRP and CFRP bars (Conrad et al. 1998). Longitudinal cracking in the concrete cover can seriously degrade the bond capability of FRP bars, and sufficient measures must be taken to prevent such cracking in laboratory tests and field applications (Sen et al. 1998a). The ability of chemical agents to pass through the concrete to the FRP bar is another important factor thought to affect bond strength (Porter and Barnes 1998). Specific recommendations on bond-related parameters, such as development and splice lengths, are provided in Chapter 11.

With regard to the durability characterization of FRP bars, refer to the test method cited in ACI 440.3R. The designer should always consult with the bar manufacturer to obtain durability factors.

## CHAPTER 5—MATERIAL REQUIREMENTS AND TESTING

FRP bars made of continuous fibers (aramid, carbon, glass, or any combination) should conform to quality standards as described in Section 5.1. FRP bars are anisotropic, with the longitudinal axis being the major axis. Their mechanical properties vary significantly from one manufacturer to another. Factors, such as volume fraction and type of fiber, resin, fiber orientation, dimensional effects, quality control, and manufacturing process, have a significant effect on the physical and mechanical characteristics of the FRP bars.

FRP bars should be designated with different grades according to their engineering characteristics (such as tensile strength and modulus of elasticity). Bar designation should correspond to tensile properties, which should be uniquely marked so that the proper FRP bar is used.

### 5.1—Strength and modulus grades of FRP bars

FRP reinforcing bars are available in different grades of tensile strength and modulus of elasticity. The tensile strength grades are based on the tensile strength of the bar, with the lowest grade being 60,000 psi (414 MPa). Finite strength increments of 10,000 psi (69 MPa) are recognized according to the following strength-grade designation:

- Grade F60: corresponds to 60,000 psi (414 MPa) ≤ $f_{fu}^{*}$ < 70,000 psi (483 MPa);
- Grade F70: corresponds to 70,000 psi (483 MPa) ≤ $f_{fu}^{*}$ < 80,000 psi (552 MPa);
- Grade F290: corresponds to 290,000 psi (1999 MPa) ≤ $f_{fu}^{*}$ < 300,000 psi (2069 MPa).

For design purposes, the engineer should select any FRP strength grade between F60 and F290 without having to choose a specific commercial FRP bar type.

The modulus of elasticity grades for different types of FRP bars are summarized in Table 5.1. For all of these FRP bars, the rupture strain should not be less than 0.005 in./in.

A modulus of elasticity grade is established similar to the strength grade. For the modulus of elasticity grade, the minimum value is prescribed depending on the fiber type. For design purposes, the engineer should select the minimum modulus of elasticity grade that corresponds to the chosen fiber type for the member or project. For example, an FRP bar specified with a modulus grade of E5.7 indicates that the modulus of the bar should be at least 5700 ksi (39.3 GPa). Manufacturers producing FRP bars with a modulus of elasticity in excess of the minimum specified will have superior FRP bars that can result in savings on the amount of FRP reinforcement used for a particular application.


*Fig. 5.1—Surface deformation patterns for commercially available FRP bars: (a) ribbed; (b) sand-coated; and (c) wrapped and sand-coated.*

### 5.2—Surface geometry

FRP reinforcing bars are produced through a variety of manufacturing processes. Each manufacturing method produces a different surface condition. The physical characteristics of the surface of the FRP bar is an important property for mechanical bond with concrete. Three types of surface deformation patterns for FRP bars that are commercially available are shown in Fig. 5.1.

Presently, there is no standardized classification of surface deformation patterns. Research is in progress to produce a bond grade similar to the strength and modulus grades.

### 5.3—Bar sizes

FRP bar sizes are designated by a number corresponding to the approximate nominal diameter in eighths of an inch, similar to standard ASTM steel reinforcing bars. There are 10 standard sizes, as illustrated in Table 5.2, which also includes the corresponding metric conversion.

The nominal diameter of a deformed FRP bar is equivalent to that of a plain round bar having the same area as the deformed bar. When the FRP bar is not of the conventional solid round shape (that is, rectangular or hollow), the outside diameter of the bar or the maximum outside dimension of the bar will be provided in addition to the equivalent nominal diameter. The nominal diameter of these unconventional bars would be equivalent to that of a solid plain round bar having the same area.

### 5.4—Bar identification

With the various grades, sizes, and types of FRP bars available, it is necessary to provide some means of easy identification. Each bar producer should label the bars, container/packaging, or both, with the following information:

- A symbol to identify the producer;
- A letter to indicate the type of fiber (that is, “G” for glass, “C” for carbon, “A” for aramid, or “H” for a hybrid) followed by the number corresponding to the nominal bar size designation according to the ASTM standard;
- A marking to designate the strength grade;
- A marking to designate the modulus of elasticity of the bar in thousands of ksi; and

**Table 5.1—Minimum modulus of elasticity, by fiber type, for reinforcing bars**

| | Modulus grade, × $10^3$ ksi (GPa) |
|---|---|
| GFRP bars | E5.7 (39.3) |
| AFRP bars | E10.0 (68.9) |
| CFRP bars | E16.0 (110.3) |

**Table 5.2—ASTM standard reinforcing bars**

| Bar size designation | | Nominal diameter, in. (mm) | Area, in.$^2$ (mm$^2$) |
|---|---|---|---|
| Standard | Metric conversion | | |
| No. 2 | No. 6 | 0.250 (6.4) | 0.05 (31.6) |
| No. 3 | No. 10 | 0.375 (9.5) | 0.11 (71) |
| No. 4 | No. 13 | 0.500 (12.7) | 0.20 (129) |
| No. 5 | No. 16 | 0.625 (15.9) | 0.31 (199) |
| No. 6 | No. 19 | 0.750 (19.1) | 0.44 (284) |
| No. 7 | No. 22 | 0.875 (22.2) | 0.60 (387) |
| No. 8 | No. 25 | 1.000 (25.4) | 0.79 (510) |
| No. 9 | No. 29 | 1.128 (28.7) | 1.00 (645) |
| No. 10 | No. 32 | 1.270 (32.3) | 1.27 (819) |
| No. 11 | No. 36 | 1.410 (35.8) | 1.56 (1006) |

- In the case of an unconventional bar (a bar with a cross section that is not uniformly circular or solid), the outside diameter or the maximum outside dimension.

A bond grade will be added when a classification is available. An example of identification symbols is

XXX - G#4 - F100 - E6.0

where

XXX = manufacturer’s symbol or name;
G#4 = glass FRP bar No. 4 (nominal diameter of 1/2 in. [12 mm]);
F100 = strength grade of at least 100 ksi ($f_{fu}^{*} \geq 100$ ksi [689 MPa]); and
E6.0 = modulus grade of at least 6,000,000 psi (41 GPa).

In the case of a hollow or unconventionally shaped bar, an extra identification should be added to the identification symbol, shown as follows. This number, appended to the end of the label, refers to the maximum outside dimension of the bar and is intended for quality control and assurance only, as the engineer would specify the special shape in the design

XXX - G#4 - F100 - E6.0 - 0.63

where

0.63 = maximum outside dimension of the bar is 5/8 in. (16 mm).

Markings should be used at the construction site to verify that the specified type, grades, and bar sizes and shapes are being used.

### 5.5—Straight bars

Straight bars are cut to a specified length from longer stock lengths in a fabricator’s shop or at the manufacturing plant.

### 5.6—Bent bars

Bending FRP bars made of thermoset resin should be carried out before the resin is fully cured. After the bars have cured, bending or alteration is not possible due to the inflexibility or rigid nature of a cured FRP bar. Because thermoset polymers are highly cross-linked, heating the bar is not allowed as it would lead to a decomposition of the resin, thus creating a loss of strength in the FRP.

The strength of bent bars varies greatly for the same type of fiber, depending on the bending technique and type of resin used. Therefore, the strength of the bent portion should generally be determined based on suitable tests performed in accordance with the recommended test method cited in ACI 440.3R. Bars in which the resin has not yet fully cured can be bent, but only according to the manufacturer's specifications and with a gradual transition, avoiding sharp angles that damage the fibers.

## CHAPTER 6—CONSTRUCTION PRACTICES

FRP reinforcing bars are ordered for specific parts of a structure and are delivered to a job site storage area. Construction operations should be performed in a manner designed to minimize damage to the bars. Similarly to epoxy-coated steel bars, FRP bars should be handled, stored, and placed more carefully than uncoated steel reinforcing bars.

### 6.1—Handling and storage of materials

FRP reinforcing bars are susceptible to surface damage. Puncturing their surface can significantly reduce the strength of the FRP bars. In the case of GFRP bars, the surface damage can cause a loss of durability due to infiltration of alkalis. The following handling guidelines are recommended to minimize damage to the bars and injury to the bar handlers:

- FRP reinforcing bars should be handled with work gloves to avoid personal injuries from either exposed fibers or sharp edges;
- FRP bars should not be stored on the ground. Pallets should be placed under the bars to keep them clean and to provide easy handling;
- High temperatures, ultraviolet rays, and chemical substances (for example, solvents and gasoline) should be avoided because they can damage FRP bars;
- Occasionally, bars become contaminated with form-releasing agents or other substances. Substances that decrease bond should be removed by wiping the bars with solvents before placing FRP bars in concrete form. Caution on solvent selection and advice from the manufacturer are needed, as there are commercially available solvents known to damage FRP such as MEK, carbondisulfide, carbontetrachloride, gasoline (for some polymers), and even distilled water;
- It may be necessary to use a spreader bar so that the FRP bars can be hoisted without excessive bending; and
- When necessary, cutting should be performed with a high-speed grinding cutter (minimum no-load speed of 600 rpm) or a fine-blade saw. FRP bars should never be sheared. Dust masks, gloves, and glasses for eye protection are recommended when cutting. There is insufficient research available to make any recommendation on treatment of saw-cut bar ends.

### 6.2—Placement and assembly of materials

In general, placing FRP bars is similar to placing steel bars, and common practices and tolerances for construction and materials (refer to ACI 117) should apply with some exceptions for the specifications prepared by the engineer as noted:

- FRP reinforcement should be placed and supported using chairs that are consistent with the intended use of the reinforcement (for example, non-corrosive and non-magnetic properties) unless specific project conditions justify the use of conventional bar supports. The requirements for support chairs should be included in the project specifications;
- FRP reinforcement should be secured against displacement while the concrete is being placed. Coated tie wire, plastic or nylon ties, and plastic snap ties can be used in tying the bars. The requirement for ties should be included in the project specifications;
- Bending of cured thermoset FRP bars on site should not be permitted. For other FRP systems, manufacturer's specifications should be followed; and
- Whenever reinforcement continuity is required, lapped splices should be used. The length of lap splices varies with concrete strength, type of concrete, bar grades, size, surface geometry, spacing, and concrete cover. Details of lapped splices should be in accordance with Chapter 11 of this guide. Mechanical connections are not yet available.

### 6.3—Quality control and inspection

Quality control should be carried out by lot testing of FRP bars. The manufacturer should supply lot or production run traceability. Tests conducted by the manufacturer or a third-party independent testing agency can be used.

All tests should be performed using the recommended test methods cited in ACI 440.3R. Material characterization tests that provide the following properties should be performed at least once before and after any change in manufacturing process, procedure, or materials:

- Tensile strength, tensile modulus of elasticity, and ultimate strain;
- Fatigue strength;
- Bond strength;
- Coefficient of thermal expansion; and
- Durability in alkaline environment.

To assess quality control of an individual lot of FRP bars, it is recommended to determine tensile strength, tensile modulus of elasticity, and ultimate strain. The manufacturer should furnish, upon request, a certificate of conformance for any given lot of FRP bars with a description of the test protocol.

## CHAPTER 7—GENERAL DESIGN CONSIDERATIONS

The general design recommendations for flexural concrete elements reinforced with FRP bars are presented in this chapter. The recommendations presented are based on

principles of equilibrium and compatibility and the constitutive laws of the materials. Furthermore, the brittle behavior of both FRP reinforcement and concrete allows consideration to be given to either FRP rupture or concrete crushing as the mechanisms that control failure. Detrimental effects of high temperature and fire on FRP-reinforced structures are discussed in Section 3.4.

## 7.1—Design philosophy

Both strength and working stress design approaches were considered by this committee. The committee opted for the strength design approach of reinforced concrete members reinforced with FRP bars to ensure consistency with other ACI documents. In particular, this guide makes reference to provisions of ACI 318-05, "Building Code Requirements for Structural Concrete and Commentary." These design recommendations are based on limit state design principles in that an FRP-reinforced concrete member is designed based on its required strength and then checked for fatigue endurance, creep rupture endurance, and serviceability criteria. In many instances, serviceability criteria or fatigue and creep rupture endurance limits may control the design of concrete members reinforced for flexure with FRP bars (especially AFRP and GFRP that exhibit low stiffness).

The load factors given in ACI 318-05 are used to determine the required strength of a concrete member reinforced with FRP.

## 7.2—Design material properties

The material properties provided by the manufacturer, such as the guaranteed tensile strength, should be considered as initial properties that do not include the effects of long-term exposure to the environment. Because long-term exposure to various types of environments can reduce the tensile strength and creep rupture and fatigue endurance of FRP bars, the material properties used in design equations should be reduced based on the type and level of environmental exposure.

Equation (7-1) through (7-3) give the tensile properties that should be used in all design equations. The design tensile strength should be determined by

$$f_{fu} = C_E f_{fu}^* \tag{7-1}$$

where

$f_{fu}$ = design tensile strength of FRP, considering reductions for service environment, psi (MPa);

$C_E$ = environmental reduction factor, given in Table 7.1 for various fiber type and exposure conditions; and

$f_{fu}^*$ = guaranteed tensile strength of an FRP bar defined as the mean tensile strength of a sample of test specimens minus three times the standard deviation ($f_{fu}^* = f_{u,ave} - 3\sigma$), psi (MPa).

The design rupture strain should be determined as

$$\varepsilon_{fu} = C_E \varepsilon_{fu}^* \tag{7-2}$$

where

**Table 7.1—Environmental reduction factor for various fibers and exposure conditions**

| Exposure condition | Fiber type | Environmental reduction factor $C_E$ |
|---|---|---|
| Concrete not exposed to earth and weather | Carbon | 1.0 |
| | Glass | 0.8 |
| | Aramid | 0.9 |
| Concrete exposed to earth and weather | Carbon | 0.9 |
| | Glass | 0.7 |
| | Aramid | 0.8 |

$\varepsilon_{fu}$ = design rupture strain of FRP reinforcement; and

$\varepsilon_{fu}^*$ = guaranteed rupture strain of FRP reinforcement defined as the mean tensile strain at failure of a sample of test specimens minus three times the standard deviation ($\varepsilon_{fu}^* = \varepsilon_{u,ave} - 3\sigma$).

The design modulus of elasticity will be the same as the value reported by the manufacturer as the mean elastic modulus (guaranteed value) of a sample of test specimens ($E_f = E_{f,ave}$).

The environmental reduction factors given in Table 7.1 are conservative estimates, depending on the durability of each fiber type, and are based on the consensus of ACI Committee 440. Temperature effects are included in the $C_E$ values. FRP bars, however, should not be used in environments with a service temperature higher than the $T_g$ of the resin used for their manufacturing. It is expected that with continued research, these values will become more reflective of actual effects of environment. The methodology regarding the use of these factors, however, is not expected to change.

**7.2.1** *Tensile strength of FRP bars at bends*—The design tensile strength of FRP bars at a bend can be determined as

$$f_{fb} = \left(0.05 \cdot \frac{r_b}{d_b} + 0.3\right) f_{fu} \le f_{fu} \tag{7-3}$$

where

$f_{fb}$ = design tensile strength of the bend of FRP bar, psi (MPa);

$r_b$ = radius of the bend, in. (mm);

$d_b$ = diameter of reinforcing bar, in. (mm); and

$f_{fu}$ = design tensile strength of FRP, considering reductions for service environment, psi (MPa).

Equation (7-3) is adapted from design recommendations by the Japan Society of Civil Engineers (1997b). Limited research on FRP hooks (Ehsani et al. 1995) indicates that the tensile force developed by the bent portion of a GFRP bar is mainly influenced by the ratio of the bend radius to the bar diameter $r_b/d_b$, the tail length, and, to a lesser extent, the concrete strength.

For an alternative determination of the reduction in tensile strength due to bending, manufacturers of bent bars may provide test results based on test methodologies cited in ACI 440.3R.

## CHAPTER 8—FLEXURE

The design of FRP-reinforced concrete members for flexure is analogous to the design of steel-reinforced concrete members. Experimental data on concrete members reinforced with FRP bars show that flexural capacity can be calculated based on assumptions similar to those made for members reinforced with steel bars (Faza and GangaRao 1993a; Nanni 1993b; GangaRao and Vijay 1997a). The design of members reinforced with FRP bars should take into account the uniaxial stress-strain relationship of FRP materials.

### 8.1—General considerations

This chapter specifically references rectangular sections with a single layer of one type of tensile FRP reinforcement, as the experimental work has almost exclusively considered members with this cross-sectional shape and reinforcement layout. The concepts described herein, however, can also be applied to the analysis and design of members with different geometry and multiple types, multiple layers, or both, of FRP reinforcement. Although there is no evidence that the flexural theory, as developed herein, does not apply equally well to nonrectangular sections, the behavior of nonrectangular sections has yet to be confirmed by experimental results.

**8.1.1** *Flexural design philosophy*—Steel-reinforced concrete sections are commonly under-reinforced to ensure yielding of steel before the crushing of concrete. The yielding of the steel provides ductility and a warning of failure of the member. The nonductile behavior of FRP reinforcement necessitates a reconsideration of this approach.

If FRP reinforcement ruptures, failure of the member is sudden and catastrophic (Nanni 1993b; Jaeger et al. 1997; GangaRao and Vijay 1997a; Theriault and Benmokrane 1998); however, there would be limited warning of impending failure in the form of extensive cracking and large deflection due to the significant elongation that FRP reinforcement experiences before rupture. In any case, the member would not exhibit ductility as is commonly observed for under-reinforced concrete beams reinforced with steel reinforcing bars.

The concrete crushing failure mode is marginally more desirable for flexural members reinforced with FRP bars (Nanni 1993b). By experiencing concrete crushing, a flexural member does exhibit some plastic behavior before failure.

In conclusion, both failure modes (FRP rupture and concrete crushing) are acceptable in governing the design of flexural members reinforced with FRP bars provided that strength and serviceability criteria are satisfied. To compensate for the lack of ductility, the member should possess a higher reserve of strength. The margin of safety suggested by this guide against failure is therefore higher than that used in traditional steel-reinforced concrete design.

The use of high-strength concrete allows for better use of the high-strength properties of FRP bars and can increase the stiffness of the cracked section, but the brittleness of high-strength concrete, as compared with normal-strength concrete, can reduce the overall deformability of the flexural member (GangaRao and Vijay 1997a).

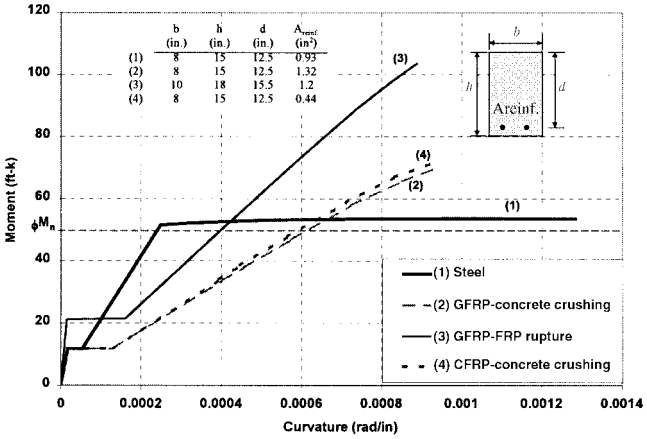


*Fig. 8.1—Theoretical moment-curvature relationships for reinforced concrete sections using steel and FRP bars ($\phi$ factors of 0.9, 0.65, 0.55, and 0.65, respectively).*

Figure 8.1 shows a comparison of the theoretical moment-curvature behavior of beam cross sections designed for the same strength $\phi M_n$ following the principles of ultimate strength design described in this chapter (including the recommended strength reduction factors according to ACI 318-05). Three cases are presented in addition to the steel-reinforced cross section: two sections reinforced with GFRP bars, and one reinforced with CFRP bars. For the section experiencing GFRP bars' rupture, the concrete dimensions are larger than for the other beams to attain the same design capacity.

**8.1.2** *Assumptions*—Computations of the strength of cross sections should be performed based on the following assumptions:

- Strain in the concrete and the FRP reinforcement is proportional to the distance from the neutral axis (that is, a plane section before loading remains plane after loading);
- The maximum usable compressive strain in the concrete is assumed to be 0.003;
- The tensile strength of concrete is ignored;
- The tensile behavior of the FRP reinforcement is linearly elastic until failure; and
- Perfect bond exists between concrete and FRP reinforcement.

### 8.2—Flexural strength

The strength design philosophy states that the design flexural strength at a section of a member must exceed the factored moment (Eq. (8-1)). Design flexural strength refers to the nominal flexural strength of the member multiplied by a strength reduction factor ($\phi$, discussed in Section 8.2.3). The factored moment refers to the moments calculated by the use of factored loads as prescribed in ACI 318-05 (for example, 1.2D + 1.6L + ...)

$$\phi M_n \geq M_u \tag{8-1}$$

The nominal flexural strength of an FRP-reinforced concrete member can be determined based on strain compatibility,

**Table 8.1—Typical values for balanced reinforcement ratio for a rectangular section with $f_c'$ = 5000 psi (34.5 MPa)**

| Bar type | Yield strength $f_y$ or tensile strength $f_{fu}$, ksi (MPa) | Modulus of elasticity, ksi (GPa) | $\rho_b$ or $\rho_{fb}$ |
|---|---|---|---|
| Steel | 60 (414) | 29,000 (200) | 0.0335 |
| GFRP | 80 (552) | 6000 (41.4) | 0.0078 |
| AFRP | 170 (1172) | 12,000 (82.7) | 0.0035 |
| CFRP | 300 (2070) | 22,000 (152) | 0.0020 |

internal force equilibrium, and the controlling mode of failure. Figure 8.2 illustrates the stress, strain, and internal forces for the three possible cases of a rectangular section reinforced with FRP bars.

**8.2.1** *Failure mode*—The flexural capacity of an FRP-reinforced flexural member is dependent on whether the failure is governed by concrete crushing or FRP rupture. The failure mode can be determined by comparing the FRP reinforcement ratio to the balanced reinforcement ratio (that is, a ratio where concrete crushing and FRP rupture occur simultaneously). Because FRP does not yield, the balanced ratio of FRP reinforcement is computed using its design tensile strength. The FRP reinforcement ratio can be computed from Eq. (8-2), and the balanced FRP reinforcement ratio can be computed from Eq. (8-3)

$$\rho_f = \frac{A_f}{bd} \tag{8-2}$$

$$\rho_{fb} = 0.85\beta_1 \frac{f_c'}{f_{fu}} \frac{E_f \varepsilon_{cu}}{E_f \varepsilon_{cu} + f_{fu}} \tag{8-3}$$

If the reinforcement ratio is less than the balanced ratio ($\rho_f < \rho_{fb}$), FRP rupture failure mode governs. Otherwise, ($\rho_f > \rho_{fb}$) concrete crushing governs.

Table 8.1 reports some typical values for the balanced reinforcement ratio, showing that the balanced ratio for FRP reinforcement $\rho_{fb}$ is much lower than the balanced ratio for steel reinforcement $\rho_b$. In fact, the balanced ratio for FRP reinforcement can be even lower than the minimum reinforcement ratio for steel ($\rho_{min}$ = 0.0035 for Grade 60 steel and $f_c'$ = 5000 psi [35 MPa]).

**8.2.2** *Nominal flexural strength*—When $\rho_f > \rho_{fb}$, the failure of the member is initiated by crushing of the concrete, and the stress distribution in the concrete can be approximated with the ACI rectangular stress block. Based on the equilibrium of forces and strain compatibility (shown in Fig. 8.2), the following can be derived

$$M_n = A_f f_f \left(d - \frac{a}{2}\right) \tag{8-4a}$$

$$a = \frac{A_f f_f}{0.85 f_c' b} \tag{8-4b}$$

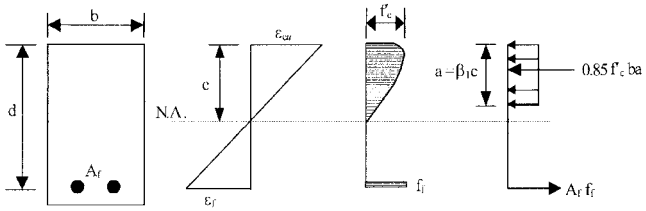


*(a) Failure governed by concrete crushing*

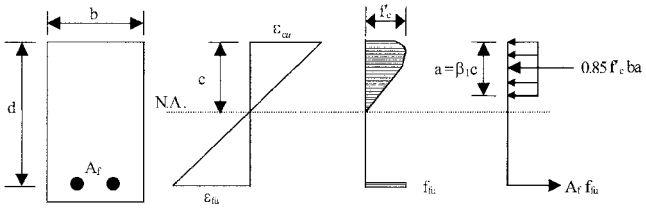


*(b) Balanced failure condition*

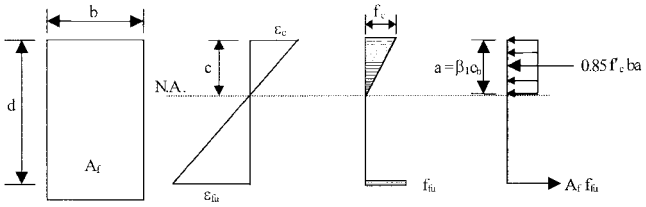


*(c) Failure governed by FRP rupture (concrete stress may be nonlinear)*

*Fig. 8.2—Strain and stress distribution at ultimate conditions.*

$$f_f = E_f \varepsilon_{cu} \frac{\beta_1 d - a}{a} \tag{8-4c}$$

Substituting $a$ from Eq. (8-4b) into Eq. (8-4c) and solving for $f_f$ gives

$$f_f = \left( \sqrt{\frac{(E_f \varepsilon_{cu})^2}{4} + \frac{0.85\beta_1 f_c'}{\rho_f} E_f \varepsilon_{cu}} - 0.5 E_f \varepsilon_{cu} \right) \le f_{fu} \tag{8-4d}$$

The nominal flexural strength can be determined from Eq. (8-4a), (8-4b), and (8-4d). FRP reinforcement is linearly elastic at concrete crushing failure mode, so the stress level in the FRP can be found from Eq. (8-4c) because it is less than $f_{fu}$.

Alternatively, the nominal flexural strength at a section can be expressed in terms of the FRP reinforcement ratio as given in Eq. (8-5) to replace Eq. (8-4a).

$$M_n = \rho_f f_f \left(1 - 0.59 \frac{\rho_f f_f}{f_c'}\right) b d^2 \tag{8-5}$$

When $\rho_f < \rho_{fb}$, the failure of the member is initiated by rupture of FRP bar, and the ACI stress block is not applicable because the maximum concrete strain (0.003) may not be

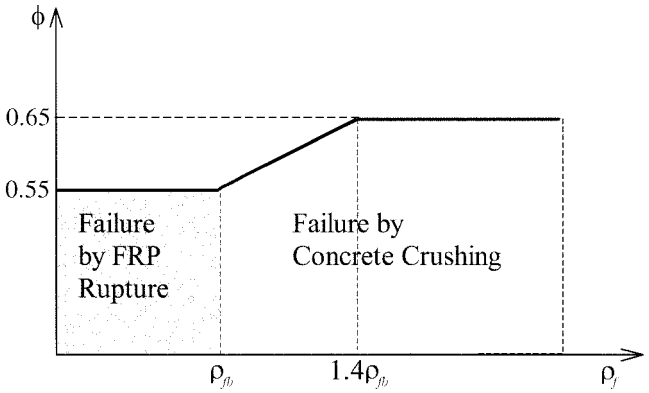


*Fig. 8.3—Strength reduction factor as a function of the reinforcement ratio.*

attained. In this case, an equivalent stress block would need to be used that approximates the stress distribution in the concrete at the particular strain level reached.

The analysis incorporates two unknowns: the concrete compressive strain at failure $\varepsilon_c$ and the depth to the neutral axis $c$. In addition, the rectangular stress block factors, $\alpha_1$ and $\beta_1$, are unknown. The factor $\alpha_1$ is the ratio of the average concrete stress to the concrete strength. Factor $\beta_1$ is the ratio of the depth of the equivalent rectangular stress block to the depth of the neutral axis. The analysis involving all these unknowns becomes complex. Nominal flexural strength at a section can be computed as shown in Eq. (8-6a)

$$M_n = A_f f_{fu}\left(d - \frac{\beta_1 c}{2}\right) \tag{8-6a}$$

For a given section, the product of $\beta_1 c$ in Eq. (8-6a) varies depending on material properties and FRP reinforcement ratio. The maximum value for this product is equal to $\beta_1 c_b$ and is achieved when the maximum concrete strain (0.003) is attained. A simplified and conservative calculation of the nominal flexural strength of the member can be based on Eq. (8-6b) and (8-6c) as follows

$$M_n = A_f f_{fu}\left(d - \frac{\beta_1 c_b}{2}\right) \tag{8-6b}$$

$$c_b = \left(\frac{\varepsilon_{cu}}{\varepsilon_{cu} + \varepsilon_{fu}}\right) d \tag{8-6c}$$

**8.2.3** *Strength reduction factor for flexure*—Because FRP members do not exhibit ductile behavior, a conservative strength reduction factor should be adopted to provide a higher reserve of strength in the member. The Japanese recommendations for design of flexural members using FRP suggest a strength reduction factor equal to 0.77 (JSCE 1997b). Other researchers (Benmokrane et al. 1996a) suggest a value of 0.75 determined based on probabilistic concepts.

Based on ACI 318-05, the $\phi$ factor for compression-controlled failure is 0.65, with a target reliability index between 3.5 to 4.0 (Szerszen and Nowak 2003). A reliability analysis on FRP-reinforced beams in flexure using Load Combination 2 from ACI 318-05 for live to dead load ratios between 1 and 3 indicated reliability indexes between 3.5 and 4.0 when the $\phi$ factor was set to 0.65 for concrete crushing failure, and 0.55 for FRP reinforcing bar rupture failure using Eq. (8-6b) (Gulbrandsen 2005). A nonlinear sectional analysis of curvatures at failure showed that the curvatures of typical FRP-reinforced beams at failure varied between 0.0138/$d$ and 0.0176/$d$ for tension-controlled failures, and between 0.0089/$d$ and 0.012/$d$ for compression-controlled failures (Gulbrandsen 2005).

ACI 318-05 considers a failure tension-controlled whenever the curvature is greater than 0.008/$d$ (corresponding to a strain in the steel of 0.005). This indicates that due to the low modulus of elasticity of the reinforcement, FRP-reinforced beams will have large deflections at ultimate, and that FRP-reinforced beams that fail by FRP reinforcing bar rupture will have larger deflections at ultimate than those that fail by concrete crushing. Even though the curvature values of FRP-reinforced beams are larger than those of equivalent steel-reinforced beams, the committee recommends a $\phi$ factor of 0.55 for tension-controlled failure to maintain a minimum reliability index of 3.5.

While a concrete crushing failure mode can be predicted based on calculations, the member as constructed may not fail accordingly. For example, if the concrete strength is higher than specified, the member can fail due to FRP rupture. For this reason and to establish a transition between the two values of $\phi$, a section controlled by concrete crushing is defined as a section in which $\rho_f \geq 1.4\rho_{fb}$, and a section controlled by FRP rupture is defined as one in which $\rho_f < \rho_{fb}$.

The strength reduction factor for flexure can be computed by Eq. (8-7). This equation is represented graphically by Fig. 8.3, and gives a factor of 0.65 for sections controlled by concrete crushing, 0.55 for sections controlled by FRP rupture, and provides a linear transition between the two.

$$\phi = \begin{cases} 0.55 \text{ for } \rho_f \leq \rho_{fb} \\ 0.3 + 0.25\dfrac{\rho_f}{\rho_{fb}} \text{ for } \rho_{fb} < \rho_f < 1.4\rho_{fb} \\ 0.65 \text{ for } \rho_f \geq 1.4\rho_{fb} \end{cases} \tag{8-7}$$

**8.2.4** *Minimum FRP reinforcement*—If a member is designed to fail by FRP rupture $\rho_f < \rho_{fb}$, a minimum amount of reinforcement should be provided to prevent failure upon concrete cracking (that is, $\phi M_n \geq M_{cr}$, where $M_{cr}$ is the cracking moment). The provisions in ACI 318-05 for minimum reinforcement are based on this concept and, with modifications, are applicable to FRP-reinforced members. The modifications result from a different strength reduction factor (that is, 0.55 for tension-controlled sections, instead of 0.9). The minimum reinforcement area for FRP-reinforced members is obtained by multiplying the existing ACI 318-05 equation for steel reinforcement by 1.64 (1.64 = 0.90/0.55). This results in Eq. (8-8)

$$A_{f,\,min} = \frac{4.9\sqrt{f'_c}}{f_{fu}} b_w d \geq \frac{330}{f_{fu}} b_w d \qquad (8\text{-}8)$$

If failure of a member is not controlled by FRP rupture $\rho_f > \rho_{fb}$, the minimum amount of reinforcement to prevent failure upon cracking is automatically achieved. Therefore, Eq. (8-8) is required as a check only if $\rho_f < \rho_{fb}$.

**8.2.5** *Special considerations*

**8.2.5.1** *Multiple layers of reinforcement and combinations of different FRP types*—In a tension-controlled section, all steel tension reinforcement is assumed to yield at ultimate when using the strength design method to calculate the nominal flexural strength of members with steel reinforcement arranged in multiple layers. Therefore, the tension force is assumed to act at the centroid of the reinforcement with a magnitude equal to the area of tension reinforcement times the yield strength of steel. Because FRP materials have no plastic region, the stress in each reinforcement layer will vary depending on its distance from the neutral axis. Similarly, if different types of FRP bars are used to reinforce the same member, the variation in the stress level in each bar type should be considered when calculating the flexural capacity. In these cases, failure of the outermost layer controls overall reinforcement failure, and the analysis of the flexural capacity should be based on a strain-compatibility approach.

**8.2.5.2** *Moment redistribution*—The failure mechanism of FRP-reinforced flexural members should not be based on the formation of plastic hinges, because FRP materials demonstrate a linear-elastic behavior up to failure. Moment redistribution in continuous beams or other statically indeterminate structures should not be considered for FRP-reinforced concrete.

**8.2.5.3** *Compression reinforcement*—FRP reinforcement has a significantly lower compressive strength than tensile strength, and is subject to significant variation (Kobayashi and Fujisaki 1995; JSCE 1997b). Therefore, the strength of any FRP bar in compression should be ignored in design calculations (Almusallam et al. 1997).

This guide does not recommend using FRP bars as longitudinal reinforcement in columns or as compression reinforcement in flexural members. Placing FRP bars in the compression zone of flexural members, however, cannot be avoided in some cases. Examples include the supports of continuous beams or where bars secure the stirrups in place. In these cases, confinement should be considered for the FRP bars in compression regions to prevent their instability and to minimize the effect of the relatively high transverse expansion of some types of FRP bars. The transverse FRP reinforcement in the form of ties should have a spacing smaller than the member width or 16 longitudinal bar diameters or 48 tie bar diameters.

## 8.3—Serviceability

FRP-reinforced concrete members have a relatively small stiffness after cracking. Consequently, permissible deflections under service loads can control the design. In general, designing FRP-reinforced cross sections for concrete crushing failure satisfies serviceability criteria for deflection and crack width (Nanni 1993a; GangaRao and Vijay 1997a; Theriault and Benmokrane 1998).

Serviceability can be defined as satisfactory performance under service load conditions. This, in turn, can be described in terms of two parameters:

- Cracking—Excessive crack width is undesirable for aesthetic and other reasons (for example, to prevent water leakage) that can damage or deteriorate the structural concrete; and
- Deflection—Deflections should be within acceptable limits imposed by the use of the structure (for example, supporting attached nonstructural elements without damage).

The serviceability provisions given in ACI 318-05 need to be modified for FRP-reinforced members due to differences in properties of steel and FRP, such as lower stiffness, bond strength, and corrosion resistance. The substitution of FRP for steel on an equal-area basis, for example, would typically result in larger deflections and wider crack widths (Gao et al. 1998a; Tighiouart et al. 1998).

**8.3.1** *Cracking*—FRP bars are corrosion resistant; therefore, the maximum crack width limitation can be relaxed when corrosion of reinforcement is the primary reason for crack width limitations. Other considerations with regard to acceptable crack width limits include aesthetics and shear effects.

The Japan Society of Civil Engineers (1997b) only considers aesthetics in setting a maximum allowable crack width of 0.020 in. (0.5 mm). CAN/CSA S806-02, "Design and Construction of Building Components with Fibre-Reinforced Polymers," (Canadian Standards Association 2002) implicitly allows crack widths of 0.020 in. (0.5 mm) for exterior exposure and 0.028 in. (0.7 mm) for interior exposure when FRP reinforcement is used. The ACI 318-05 provisions do not address FRP reinforcement. For comparison purposes, however, the crack control provisions for steel reinforcement correspond to a maximum crack width of approximately 0.016 in. (0.4 mm). The committee recommends that the Canadian Standards Association (2002) limits be used for most cases. These limitations may not be sufficiently restrictive for structures exposed to aggressive environments or designed to be watertight. Therefore, additional caution is recommended for such cases. Conversely, for structures with short life-cycle requirements or those for which aesthetics is not a concern, crack width requirements can be disregarded unless steel reinforcement is also present.

The maximum reinforcement spacing provisions of ACI 318-05 for the control of cracking are derived from a crack width formulation based on a physical model, rather than being empirically derived (Frosch 1999). This formula is independent of the type of reinforcement (steel or FRP) except that it should be modified by a bond quality coefficient $k_b$. Therefore, the maximum probable crack width for FRP-reinforced members may be calculated from Eq. (8-9)

$$w = 2\frac{f_f}{E_f}\beta k_b \sqrt{d_c^2 + \left(\frac{s}{2}\right)^2} \qquad (8\text{-}9)$$

**Table 8.2—Recommended minimum thickness of nonprestressed beams or one-way slabs**

| | Minimum thickness $h$ | | | |
|---|---|---|---|---|
| | Simply supported | One end continuous | Both ends continuous | Cantilever |
| Solid one-way slabs | $\ell$/13 | $\ell$/17 | $\ell$/22 | $\ell$/5.5 |
| Beams | $\ell$/10 | $\ell$/12 | $\ell$/16 | $\ell$/4 |

in which $w$ = maximum crack width, in. or mm; $f_f$ = reinforcement stress, psi or MPa; $E_f$ = reinforcement modulus of elasticity, psi or MPa; β = ratio of distance between neutral axis and tension face to distance between neutral axis and centroid of reinforcement; $d_c$ = thickness of cover from tension face to center of closest bar, in. or mm; and $s$ = bar spacing, in. or mm.

The $k_b$ term is a coefficient that accounts for the degree of bond between FRP bar and surrounding concrete. For FRP bars having bond behavior similar to uncoated steel bars, the bond coefficient $k_b$ is assumed equal to 1. For FRP bars having bond behavior inferior to steel, $k_b$ is larger than 1.0, and for FRP bars having bond behavior superior to steel, $k_b$ is smaller than 1.0. Gao et al. (1998a) introduced a similar formula based on test results that indicated that bond characteristics of GFRP bars can vary from those of steel bars. Bakis and Boothby (2004) found that crack widths in GFRP-reinforced concrete beams under sustained loads increased beyond initial values by approximately 40% in an indoor environment and by approximately 60% in an outdoor environment over a period of 3 years. Further research is needed to verify the effect of surface characteristics of FRP bars on the bond behavior and on crack widths. Data should be obtained for commercially available FRP bars. For an analysis of crack width data performed by members of this committee on a variety of concrete cross sections and FRP bar manufacturers, fiber types, resin formulations, and surface treatments, average $k_b$ values ranged from 0.60 to 1.72, with a mean of 1.10. Data for rough sand-coated FRP bar surface treatments trended toward the lower end of this range. The consensus of the committee, for the case where $k_b$ is not known from experimental data, is that a conservative value of 1.4 should be assumed. Smooth bars and grids are specifically excluded from this recommendation. Data should be obtained for commercially available FRP smooth bars and grids. Further analysis is needed before a committee consensus can be reached on $k_b$ for such reinforcement.

**8.3.2** *Deflections*—In general, ACI 318-05 provisions for deflection control are concerned with deflections that occur at service levels under immediate and sustained static loads, and do not apply to dynamic loads such as earthquakes, transient winds, or vibration of machinery. Two methods are presently given in ACI 318-05 for control of deflections of one-way flexural members:

- The indirect method of mandating the minimum thickness of the member (Table 9.5(a) in ACI 318-05); and
- The direct method of limiting computed deflections (Table 9.5(b) in ACI 318-05).

Because of the variable stiffness, brittle-elastic nature, and particular bond features of FRP reinforcement, deflections of FRP-reinforced concrete members are more sensitive to the variables affecting deflection than steel-reinforced members of identical size and reinforcement layout. Deflections in members with FRP reinforcement also tend to be greater in magnitude because of the lower stiffness associated with commercially available FRP reinforcement. This guide therefore requires the use of a direct method of deflection control, as outlined in Sections 8.3.2.2 and 8.3.2.3. Recommended minimum thicknesses for FRP-reinforced members are provided in Section 8.3.2.1 for convenience in establishing member proportions for design only.

**8.3.2.1** *Recommended minimum thicknesses for design*—Recommended minimum thicknesses for design of one-way slabs and beams are provided in Table 8.2. The table is intended to only provide guidance for initial design, and use of these recommended minimum thicknesses does not guarantee that all deflection considerations will be satisfied for a particular project.

Values in Table 8.2 are based on a generic maximum span-depth ratio limitation (Ospina et al. 2001) corresponding to the limiting curvature associated with a target deflection-span ratio (Eq. (8-10)). The procedure can be applied to any type of reinforcement

$$\frac{\ell}{h} = \frac{48\eta}{5K_1}\left(\frac{1-k}{\varepsilon_f}\right)\left(\frac{\Delta}{\ell}\right)_{max} \quad (8\text{-}10)$$

In Eq. (8-10), η = $d/h$; $k$ is as defined in Eq. (8-12); and $(\Delta/\ell)_{max}$ is the limiting service load deflection-span ratio. $K_1$ is a parameter that accounts for boundary conditions. It may be taken as 1.0, 0.8, 0.6, and 2.4 for uniformly loaded simply-supported, one end continuous, both ends continuous, and cantilevered spans, respectively. The term $\varepsilon_f$ is the strain in the FRP reinforcement under service loads, evaluated at midspan except for cantilevered spans. For cantilevers, $\varepsilon_f$ shall be evaluated at the support.

Equation (8-10) assumes no tensile contribution from concrete between cracks, also referred to as tension stiffening. To consider the effects of tension stiffening in developing Table 8.2, the values resulting from Eq. (8-10) were modified by the ratio of effective and fully cracked moments of inertia computed using Eq. (8-13a) and (8-11), respectively. Tabulated values are based on an assumed service deflection limit of $\ell$/240 under total service load, and assumed reinforcement ratios of $2.0\rho_{fb}$ and $3.0\rho_{fb}$ for slabs and beams, respectively.

**8.3.2.2** *Effective moment of inertia*—When a section is uncracked, its moment of inertia is equal to the gross moment of inertia $I_g$. When the applied moment $M_a$ exceeds the cracking moment $M_{cr}$, cracking occurs, which causes a reduction in the stiffness; the moment of inertia is based on the cracked section $I_{cr}$. For a rectangular section, the gross moment of inertia is calculated as $I_g = bh^3/12$, while $I_{cr}$ can be calculated using an elastic analysis. The elastic analysis for FRP-reinforced concrete is similar to the analysis used for steel-reinforced concrete (that is, concrete in tension is neglected) and is given by Eq. (8-11) and (8-12) with $n_f$ as the modular ratio between the FRP reinforcement and the concrete

$$I_{cr} = \frac{bd^3}{3}k^3 + n_f A_f d^2(1-k)^2 \quad (8\text{-}11)$$

$$k = \sqrt{2\rho_f n_f + (\rho_f n_f)^2} - \rho_f n_f \quad (8\text{-}12)$$

The overall flexural stiffness $E_cI$ of a flexural member that has experienced cracking at service varies between $E_cI_g$ and $E_cI_{cr}$, depending on the magnitude of the applied moment. Branson (1977) derived an equation to express the transition from $I_g$ to $I_{cr}$. Branson's equation was adopted by ACI 318-05 as the following expression for the effective moment of inertia $I_e$

$$I_e = \left(\frac{M_{cr}}{M_a}\right)^3 I_g + \left[1 - \left(\frac{M_{cr}}{M_a}\right)^3\right] I_{cr} \le I_g$$

Branson's equation reflects two different phenomena: the variation of $EI$ stiffness along the member and the effect of concrete tension stiffening.

This equation was based on the behavior of steel-reinforced beams at service load levels. Research on deflection of FRP-reinforced beams (Benmokrane et al. 1996a; Brown and Bartholomew 1996; Zhao et al. 1997; Yost et al. 2003; Rasheed et al. 2004) indicates that on a plot of load-versus-deflection of simply supported beams, the experimental curves are roughly parallel to those predicted by Branson's equation. Branson's equation, however, has been found to overestimate the effective moment of inertia of FRP-reinforced beams, especially for lightly reinforced beams, implying a lesser degree of tension stiffening than in comparable steel-reinforced beams (Nawy and Neuwerth 1977; Benmokrane et al. 1996a; Toutanji and Saafi 2000). This reduced tension stiffening may be attributed to the lower modulus of elasticity and different bond stress levels for the FRP reinforcement as compared with those of steel.

Gao et al. (1998a) concluded that to account for reduced tension stiffening in FRP-reinforced members, a modified expression for the effective moment of inertia is required. This expression is recommended and is given by Eq. (8-13a)

$$I_e = \left(\frac{M_{cr}}{M_a}\right)^3 \beta_d I_g + \left[1 - \left(\frac{M_{cr}}{M_a}\right)^3\right] I_{cr} \le I_g \quad (8\text{-}13a)$$

The factor $\beta_d$ is a reduction coefficient related to the reduced tension stiffening exhibited by FRP-reinforced members. Research has demonstrated that the degree of tension stiffening is affected by the amount and stiffness of the flexural reinforcement and by the relative reinforcement ratio (ratio of $\rho_f$ to $\rho_{fb}$) (Toutanji and Saafi 2000; Yost et al. 2003). Based on an evaluation of experimental results from several studies, the committee recommends the following simple relationship for $\beta_d$

$$\beta_d = \frac{1}{5} \cdot \left(\frac{\rho_f}{\rho_{fb}}\right) \le 1.0 \quad (8\text{-}13b)$$

Equation (8-13a) is only valid if the maximum unfactored moment in the member is equal to or greater than the cracking moment ($M_a \ge M_{cr}$). Recommended minimum thickness values in Table 8.2 assume this condition. If during the design process the designer finds the maximum unfactored moment in the member to be significantly lower than the cracking moment, then the deflection calculated according to Sections 8.3.2.2 and 8.3.2.3 should be based on $I_g$. In cases where the calculated maximum unfactored moment is only slightly less than the cracking moment, the designer is advised to assume a cracked section because factors such as shrinkage and temperature may cause the section to crack even if $M_a < M_{cr}$. This can be achieved by using Eq. (8-13a) with $M_a = M_{cr}$.

Other methods of computing the effective moment of inertia that are not based on Branson's approach have also been proposed (Bischoff 2005).

**8.3.2.3** *Calculation of deflection (direct method)*—When deflections are estimated by computation according to the provisions of this section, the designer should compare computed deflections to acceptable limits set as part of the design criteria for the project. In many cases, these deflection criteria are set by local building codes.

The short-term deflections (instantaneous deflection under service loads) of an FRP one-way flexural member can be calculated using the effective moment of inertia of the FRP-reinforced beam and the usual structural analysis techniques.

The magnitude of long-term deflection can be several times the short-term deflection, and both short-term and long-term deflections under service loads should be considered in the design. The long-term increase in deflection is a function of member geometry (reinforcement area and member size), load characteristics (age of concrete at the time of loading, and magnitude and duration of sustained load), and material characteristics (elastic moduli of the concrete and FRP reinforcement, creep and shrinkage of concrete, formation of new cracks, and widening of existing cracks).

Data on time-dependent deflections of FRP-reinforced members due to creep and shrinkage indicates that the time-versus-deflection curves of FRP-reinforced and steel-reinforced members have the same basic shape, indicating that the same fundamental approach for estimating the long-term deflection can be used (Brown 1997).

According to ACI 318-05, the long-term deflection due to creep and shrinkage $\Delta_{(cp+sh)}$ can be computed according to the following equations

$$\Delta_{(cp+sh)} = \lambda(\Delta_i)_{sus} \quad (8\text{-}14a)$$

$$\lambda = \frac{\xi}{1 + 50\rho'} \quad (8\text{-}14b)$$

The parameter $\lambda$ in Eq. (8-14b) reduces to $\xi$ because compression reinforcement is not considered for FRP-reinforced members ($\rho_f' = 0$). Values of $\xi$ are reported in ACI 318-05.

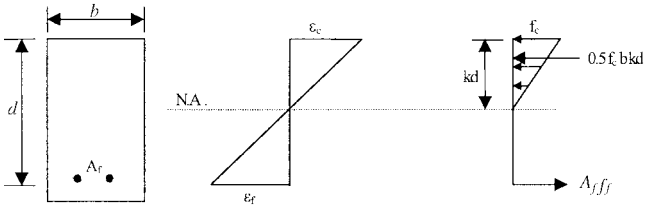


*Fig. 8.4—Elastic stress and strain distribution.*

These equations can be used for FRP reinforcement with modifications to account for the differences in the axial stiffness of the reinforcement for FRP-reinforced concrete members as compared with steel-reinforced concrete members. With either FRP or steel reinforcement, concrete creep leads to an effective reduction in the flexural stiffness $E_cI$. For simplicity, this reduction can be considered as the superposition of two contradictory effects. The first effect is the decrease in effective elastic modulus as a direct result of the concrete creep. The second effect, which can be approximated using an elastic cross-section analysis with the reduced elastic modulus for concrete, is an increase in neutral axis depth. This increased neutral axis depth leads to an effective increase in the moment of inertia of the cracked section. The increase in neutral axis depth can be shown to be proportionally more significant for FRP-reinforced members than for steel-reinforced members because of the lower axial stiffness of the reinforcement in typical FRP-reinforced concrete members. As a result, the time-dependent deflection increase for FRP reinforced concrete can be expected to be proportionally less than for steel-reinforced concrete.

Brown (1997) observed that the time-dependent deflection of FRP-reinforced beams with no compression reinforcement over a sustained loading period of 6 months was 60 to 90% of the initial deflection. The measured additional time-dependent deflection was only 50 to 75% of the deflection suggested by Eq. (8-14a) and (8-14b). Similar results have been reported in other studies (Vijay et al. 1998; Arockiasamy et al. 1998) for both GFRP and CFRP.

Based on the aforementioned results, a modification factor of 0.6 is recommended to be applied to Eq. (8-14a). For typical applications, the long-term deflection of FRP-reinforced members can therefore be determined from Eq. (8-15)

$$\Delta_{(cp+sh)} = 0.6\xi(\Delta_i)_{sus} \tag{8-15}$$

Gross et al. (2003) found that for beams that are not cracked prior to application of the sustained load, Eq. (8-15) may significantly underestimate the time-dependent deflection multiplier. This situation may be found in members where most or all of the service load is sustained load. They attributed this underestimation to the fact that additional flexural cracks were observed to form in the beams over time under the sustained loading. Further experimental work is necessary to validate Eq. (8-15) for applications with high levels of sustained load.

**Table 8.3—Creep rupture stress limits in FRP reinforcement**

| Fiber type | GFRP | AFRP | CFRP |
|---|---|---|---|
| Creep rupture stress limit $f_{f,s}$ | $0.20f_{fu}$ | $0.30f_{fu}$ | $0.55f_{fu}$ |

## 8.4—Creep rupture and fatigue

To avoid creep rupture of the FRP reinforcement under sustained stresses or failure due to cyclic stresses and fatigue of the FRP reinforcement, the stress levels in the FRP reinforcement under these stress conditions should be limited. Because these stress levels will be within the elastic range of the member, the stresses can be computed through an elastic analysis as depicted in Fig. 8.4.

**8.4.1** *Creep rupture stress limits*—To avoid failure of an FRP-reinforced member due to creep rupture of the FRP, stress limits should be imposed on the FRP reinforcement. The stress level in the FRP reinforcement can be computed using Eq. (8-16), with $M_s$ equal to the unfactored moment due to all sustained loads (dead loads and the sustained portion of the live load)

$$f_{f,s} = M_s \frac{n_f d(1-k)}{I_{cr}} \tag{8-16}$$

The cracked moment of inertia $I_{cr}$ and the ratio of the effective depth to the depth of the elastic neutral axis $k$ are computed using Eq. (8-11) and (8-12).

Values for safe sustained stress levels are given in Table 8.3. These values are based on the creep rupture stress limits previously stated in Section 3.3.1, with an imposed safety factor of 1/0.60.

**8.4.2** *Fatigue stress limits*—If the structure is subjected to fatigue regimes, the FRP stress should be limited to the values stated in Table 8.3. The FRP stress can be calculated using Eq. (8-16), with $M_s$ equal to the moment due to all sustained loads plus the maximum moment induced in a fatigue loading cycle.

# CHAPTER 9—SHEAR

The design of FRP-reinforced concrete is similar to that of steel-reinforced concrete members. The different mechanical properties of FRP bars, however, affect shear strength and must be considered. This chapter addresses the shear resistance of FRP-reinforced beams and one-way slabs, the use of FRP stirrups, and the punching shear capacity of FRP-reinforced two-way slabs.

## 9.1—General considerations

Several issues need to be considered for the shear design of FRP reinforced members:

- FRP has a relatively low modulus of elasticity;
- FRP has low transverse shear resistance;
- FRP has a high tensile strength and no yield point; and
- The tensile strength of the bent of an FRP bar is significantly lower than that of the straight portion.

**9.1.1** *Shear design philosophy*—The design of FRP shear reinforcement is based on the strength design method. The

strength reduction factor of 0.75 given by ACI 318-05 for reducing nominal shear capacity of steel-reinforced concrete members should also be used for FRP reinforcement. The factored shear strength $\Phi V_n$ must be larger than the factored shear force $V_u$ at the section considered. Computation of the maximum shear force $V_u$ at beam supports can be attained following ACI 318-05 provisions.

## 9.2—Shear strength of FRP-reinforced members

According to ACI 318-05, the nominal shear strength of a reinforced concrete cross section $V_n$ is the sum of the shear resistance provided by concrete $V_c$ and the steel shear reinforcement $V_s$.

Compared with a steel-reinforced section with equal areas of longitudinal reinforcement, a cross section using FRP flexural reinforcement after cracking has a smaller depth to the neutral axis because of the lower axial stiffness (that is, product of reinforcement area and modulus of elasticity). The compression region of the cross section is reduced, and the crack widths are wider. As a result, the shear resistance provided by both aggregate interlock and compressed concrete is smaller. Research on the shear capacity of flexural members without shear reinforcement has indicated that the concrete shear strength is influenced by the stiffness of the tensile (flexural) reinforcement (Nagasaka et al. 1993; Zhao et al. 1995; JSCE 1997b; Sonobe et al. 1997; Michaluk et al. 1998; Tureyen and Frosch 2002, 2003).

The contribution of longitudinal FRP reinforcement in terms of dowel action has not been determined. Because of the lower strength and stiffness of FRP bars in the transverse direction, however, it is assumed that their dowel action contribution is less than that of an equivalent steel area. Further research is needed to quantify this effect.

The concrete shear capacity $V_c$ of flexural members using FRP as main reinforcement can be evaluated according to Eq. (9-1)

$$V_c = 5\sqrt{f_c'}\, b_w c \tag{9-1}$$

For SI units

$$V_c = \frac{2}{5}\sqrt{f_c'}\, b_w c$$

where $b_w$ = width of the web, in. (mm for SI); and $c$ = cracked transformed section neutral axis depth, in. (mm for SI).

For singly reinforced, rectangular cross sections, the neutral axis depth $c$ may be computed as

$$c = kd$$

$$k = \sqrt{2\rho_f n_f + (\rho_f n_f)^2} - \rho_f n_f$$

$\rho_f$ = FRP reinforcement ratio = $A_f / b_w d$

Equation (9-1) accounts for the axial stiffness of the FRP reinforcement through the neutral axis depth $c$, which is a function of the reinforcement ratio $\rho_f$ and the modular ratio $n_f$. This equation has been shown to provide a reasonable factor of safety for FRP-reinforced specimens across the range of reinforcement ratios and concrete strengths tested to date (Tureyen and Frosch 2003).

Equation (9-1) may be rewritten as Eq. (9-1a). This form of the equation indicates that Eq. (9-1) is simply the ACI 318-05 shear equation for steel reinforcement $V_c$ modified by the factor ([5/2]$k$), which accounts for the axial stiffness of the FRP reinforcement.

$$V_c = \left(\frac{5}{2}k\right) 2\sqrt{f_c'}\, b_w d \tag{9-1a}$$

The ACI 318-05 method used to calculate the shear contribution of steel stirrups is applicable when using FRP as shear reinforcement. The shear resistance provided by FRP stirrups perpendicular to the axis of the member $V_f$ can be written as

$$V_f = \frac{A_{fv} f_{fv} d}{s} \tag{9-2}$$

The stress level in the FRP shear reinforcement should be limited to control shear crack widths and maintain shear integrity of the concrete and to avoid failure at the bent portion of the FRP stirrup (Eq. (7-3)). Equation (9-3) gives the stress level in the FRP shear reinforcement at ultimate for use in design

$$f_{fv} = 0.004 E_f \le f_{fb} \tag{9-3}$$

When using shear reinforcement perpendicular to the axis of the member, the required spacing and area of shear reinforcement can be computed from Eq. (9-4)

$$\frac{A_{fv}}{s} = \frac{(V_u - \phi V_c)}{\phi f_{fv} d} \tag{9-4}$$

When inclined FRP stirrups are used as shear reinforcement, Eq. (9-5) is used to calculate the contribution of the FRP stirrups

$$V_f = \frac{A_{fv} f_{fv} d}{s}(\sin\alpha + \cos\alpha) \tag{9-5}$$

When continuous FRP rectangular spirals are used as shear reinforcement (in this case, $s$ is the pitch, and $\alpha$ is the angle of inclination of the spiral), Eq. (9-6) gives the contribution of the FRP spirals

$$V_f = \frac{A_{fv} f_{fv} d}{s}(\sin\alpha) \tag{9-6}$$

Shear failure modes of members with FRP as shear reinforcement can be classified into two types (Nagasaka et

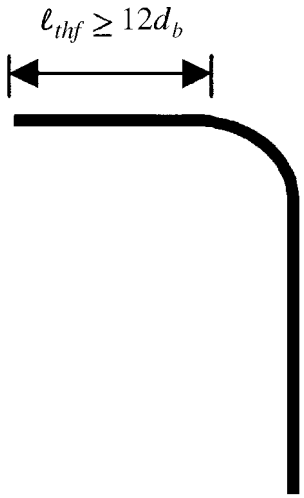


*Fig. 9.1—Required tail length for FRP stirrups.*

al. 1993): shear-tension failure mode (controlled by the rupture of FRP shear reinforcement) and shear-compression failure mode (controlled by the crushing of the concrete web). The first mode is more brittle, and the latter results in larger deflections. Experimental results have shown that the modes of failure depend on the shear reinforcement index $\rho_{fv}E_f$, where $\rho_{fv}$ is the ratio of FRP shear reinforcement $A_{fv}/b_w s$. As the value of $\rho_{fv}E_f$ increases, the shear capacity in shear tension increases, and the mode of failure changes from shear tension to shear compression.

**9.2.1** *Limits on tensile strain of shear reinforcement*—The design assumption that concrete and reinforcement capacities are added is accurate when shear cracks are adequately controlled. Therefore, the tensile strain in FRP shear reinforcement should be limited to ensure that the ACI design approach is applicable.

The Canadian Highway Bridge Design Code (Canadian Standards Association 2000) limits the tensile strain in FRP shear reinforcement to 0.002 in./in. It is recognized that this strain value (corresponding to the yield strain of Grade 60 steel) may be very conservative. Experimental evidence shows the attainment of higher strain values (Wang 1998; Zhao et al. 1995; Okamoto et al. 1994). The Eurocrete Project provisions limit the value of the shear strain in FRP reinforcement to 0.0025 in./in. (Dowden and Dolan 1997). Given the high strain to failure of FRP, the engineer could consider using 0.00275 as implicitly allowed by previous editions of ACI 318. In no case should effective strain in FRP shear reinforcement exceed 0.004, nor should the design strength exceed the strength of the bent portion of the stirrup $f_{fb}$. The value of 0.004 is justified as the strain that prevents degradation of aggregate interlock and corresponding concrete shear (Priestley et al. 1996).

**9.2.2** *Minimum amount of shear reinforcement*—ACI 318-05 requires a minimum amount of shear reinforcement when $V_u$ exceeds $\phi V_c/2$. This requirement is to prevent or restrain shear failure in members where the sudden formation of cracks can lead to excessive distress (Joint ACI-ASCE Committee 426 1974). To prevent brittle shear failure, adequate reserve strength should be provided to ensure a factor of safety similar to ACI 318-05 provisions for steel reinforcement. Equation (9-7) gives the recommended minimum amount of FRP shear reinforcement

$$A_{fv,\,min} = \frac{50 b_w s}{f_{fv}} \quad (9\text{-}7)$$

For SI units

$$A_{fv,\,min} = 0.35\frac{b_w s}{f_{fv}} \quad (9\text{-}7)$$

with $b_w$ and $s$ in mm, and $f_{fv}$ in MPa.

The minimum amount of reinforcement given by Eq. (9-7) is independent of the strength of concrete. If steel stirrups are used, the minimum amount of reinforcement provides a shear strength that varies from $1.50V_c$ when $f_c'$ is 2500 psi (17 MPa) to $1.25V_c$ when $f_c'$ is 10,000 psi (69 MPa). Equation (9-7), which was derived for steel-reinforced members, is more conservative when used with FRP-reinforced members. For example, when applied to a flexural member having GFRP as longitudinal reinforcement, the shear strength provided by Eq. (9-7) could exceed $3V_c$. The ratio of the shear strength provided by Eq. (9-7) to $V_c$ will decrease as the stiffness of longitudinal reinforcement increases or as the strength of concrete increases.

**9.2.3** *Shear failure due to crushing of the web*—Studies by Nagasaka et al. (1993) indicate that for FRP-reinforced sections, the transition from rupture to crushing failure mode occurs at an average value of $0.3f_c' b_w d$ for $V_c$, but can be as low as $0.18f_c' b_w d$. When $V_c$ is smaller than $0.18f_c' b_w d$, shear-tension can be expected, whereas when $V_c$ exceeds $0.3f_c' b_w d$, crushing failure is expected. The correlation between rupture and the crushing failure is not fully understood, and it is more conservative and recommended to use the ACI 318-05 limit of $8\sqrt{f_c'}\, b_w d$ rather than $0.3f_c' b_w d$. In fact, the ACI limitation is aimed at controlling excess shear crack widths and is thus below values corresponding to crushing of the web.

## 9.3—Detailing of shear stirrups

The maximum spacing of vertical steel stirrups given in ACI 318-05 as the smaller of $d/2$ or 24 in. is used for vertical FRP shear reinforcement. This limit ensures that each shear crack is intercepted by at least one stirrup.

Tests by Ehsani et al. (1995) indicated that for specimens with $r_b/d_b$ of zero, the reinforcing bars failed in shear at very low load levels at the bends. Therefore, although manufacturing of FRP bars with sharp bends is possible, such details should be avoided. A minimum $r_b/d_b$ ratio of 3 is recommended. In addition, FRP stirrups should be closed with 90-degree hooks.

ACI 318-05 provisions for bond of hooked steel bars cannot be applied directly to FRP reinforcing bars because of their different mechanical properties. The tensile force in a vertical stirrup leg is transferred to the concrete through the

tail beyond the hook, as shown in Fig. 9.1. Ehsani et al. (1995) found that for a tail length $\ell_{thf}$ beyond $12d_b$, there is no significant slippage and no influence on the tensile strength of the stirrup leg. Therefore, it is recommended that a minimum tail length of $12d_b$ be used.

## 9.4—Shear strength of FRP-reinforced two-way concrete slabs

Experimental evidence (Ahmad et al. 1993; Bank and Xi 1995; Banthia et al. 1995; Matthys and Taerwe 2000; El-Ghandour et al. 2003; Ospina et al. 2003) shows that the axial stiffness of the FRP reinforcement, as well as the concrete strength $f_c'$, significantly affect the transverse shear response of interior FRP-reinforced two-way slab-column connections. Test results of isolated FRP-reinforced two-way slab specimens subjected to uniform gravity loading indicate that an increase in the top FRP mat stiffness increases punching shear capacity and decreases the ultimate slab deflection. Punching shear failure in slabs reinforced with FRP bars is sudden and brittle. Conversely, punching test results (Bank and Xi 1995; Ospina et al. 2003) show that two-way slabs reinforced with FRP grids rather than bars do not exhibit a sharp load drop at punching failure. Instead, they continue to absorb energy in a stable fashion following initial failure.

A statistical evaluation of test results reveal that the one-way shear design model proposed by Tureyen and Frosch (2003), which accounts for reinforcement stiffness, can be modified (Ospina 2005) to account for the shear transfer in two-way concrete slabs. The modification leads to Eq. (9-8), which can be used to calculate the concentric punching shear capacity of FRP-reinforced two-way concrete slabs that are either supported by interior columns or subjected to concentrated loads that are either square or circular in shape

$$V_c = 10\sqrt{f_c'}\, b_o c \qquad (9\text{-}8)$$

For SI units

$$V_c = \frac{4}{5}\sqrt{f_c'}\, b_o c$$

where $b_o$ = perimeter of critical section for slabs and footings, in. (mm for SI); and $c$ = cracked transformed section neutral axis depth, in. (mm for SI).

For slabs, the neutral axis depth $c$ may computed as follows

$$c = kd$$

$$k = \sqrt{2\rho_f n_f + (\rho_f n_f)^2} - \rho_f n_f$$

$\rho_f$ = FRP reinforcement ratio

In the evaluation of Eq. (9-8), $b_o$ should be computed at $d/2$ away from the column face. In addition, the shape of the critical surface should be the same as that of the column.

Equation (9-8) can be rewritten as Eq. (9-8a). This equation is simply the basic ACI 318-05 concentric punching shear equation for steel-reinforced slabs $V_c$ modified by the factor ([5/2]$k$) that accounts for the axial stiffness of the FRP reinforcement.

$$V_c = \left(\frac{5}{2}k\right) 4\sqrt{f_c'}\, b_o c \qquad (9\text{-}8a)$$

Equation (9-8) provides a reasonable factor of safety for FRP-reinforced two-way slabs across the range of reinforcement ratios and concrete strengths tested to date. Further research is needed to examine the punching capacity of FRP-reinforced two-way slabs supported by edge and corner columns as well as the effects of column rectangularity and unbalanced moment transfer on the punching capacity of FRP-reinforced two-way slabs supported on interior columns.

# CHAPTER 10—TEMPERATURE AND SHRINKAGE REINFORCEMENT

Shrinkage and temperature reinforcement is intended to limit crack width. The stiffness and strength of reinforcing bars control this behavior. Shrinkage cracks perpendicular to the member span are restricted by flexural reinforcement; thus, shrinkage and temperature reinforcement are only required in the direction perpendicular to the span. ACI 318-05 requires a minimum steel reinforcement ratio of 0.0020 when using Grade 40 or 50 deformed steel bars, and 0.0018 when using Grade 60 deformed bars or welded reinforcement (deformed or smooth). ACI 318-05 also requires that the spacing of shrinkage and temperature reinforcement not exceed five times the member thickness or 18 in. (500 mm).

No experimental data are available for the minimum FRP reinforcement ratio for shrinkage and temperature. ACI 318-05, Section 7.12.2, states that for slabs with steel reinforcement having a yield stress exceeding 60 ksi (414 MPa) measured at a yield strain of 0.0035, the ratio of reinforcement to gross area of concrete should be at least $0.0018 \times 60/f_y$, where $f_y$ is in ksi, but not less than 0.0014. The stiffness and the strength of shrinkage and temperature for FRP reinforcement can be incorporated in this formula. Therefore, when deformed FRP shrinkage and temperature reinforcement is used, the amount of reinforcement should be determined by using Eq. (10-1)

$$\rho_{f,ts} = 0.0018 \times \frac{60{,}000}{f_{fu}} \frac{E_s}{E_f} \text{ (U.S.)} \qquad (10\text{-}1)$$

$$\rho_{f,ts} = 0.0018 \times \frac{414}{f_{fu}} \frac{E_s}{E_f} \text{ (SI)}$$

Due to limited experience, it is recommended that the ratio of temperature and shrinkage reinforcement given by Eq. (10-1) be taken not less than 0.0014, the minimum value specified by ACI 318-05 for steel shrinkage and temperature reinforcement.

The engineer may consider an upper limit for the ratio of temperature and shrinkage reinforcement equal to 0.0036, or compute the ratio based on calculated strain levels corresponding to the nominal flexural capacity rather than the strains calculated using Eq. (10-1). Spacing of shrinkage and temperature of FRP reinforcement should not exceed three times the slab thickness or 12 in. (300 mm), whichever is less. The use of FRP for temperature and shrinkage reinforcement for slabs-on-ground is presented in Appendix A.

## CHAPTER 11—DEVELOPMENT AND SPLICES OF REINFORCEMENT

In a reinforced concrete flexural member, the tension force carried by the reinforcement balances the compression force in the concrete. The tension force is transferred to the reinforcement through the bond between the reinforcement and the surrounding concrete. Bond stresses exist whenever the force in the tensile reinforcement changes. Bond between FRP reinforcement and concrete is developed through a mechanism similar to that of steel reinforcement and depends on FRP type, elastic modulus, surface deformation, and the shape of the FRP bar (Al-Zahrani et al. 1996; Uppuluri et al. 1996; Gao et al. 1998b).

### 11.1—Development of stress in straight bar

Figure 11.1 shows the equilibrium condition of an FRP bar of length $\ell_e$ embedded in concrete. The force in the bar is resisted by an average bond stress $u$ acting on the surface of the bar. Equilibrium of forces can be written as follows

$$\ell_e \pi d_b u = A_{f,bar} f_f \tag{11-1}$$

in which $A_{f,bar}$ is the area of one bar, $d_b$ is the bar diameter, and $f_f$ is the stress developed in the bar at the end of the embedment length. In contrast to steel bars, the full strength of an FRP bar need not be developed, especially when flexural capacity is controlled by concrete crushing and the required stress in the bar at failure is less than its guaranteed ultimate strength. Additionally, changing a failure mode from bar fracture or concrete crushing to bond failure does not significantly change the ductility associated with the failure.

The development length equation for steel reinforcing bars found in ACI 318-05 is based on the work done by Orangun et al. (1977). The development length equation was based on 62 unconfined splice tests and 54 confined splice tests that failed by splitting of the concrete. In their work, Orangun et al. developed an equation relating the average bond stress normalized by the square root of the concrete compressive strength to the normalized cover to the center of the bar $C/d_b$ and the normalized splice length $d_b/\ell_e$ using linear regression. This equation served as the foundation for the development length equation for steel reinforcing bars found in ACI 318-05.

A similar methodology was followed by Wambeke and Shield (2006) in which a consolidated database of 269 beam bond tests was created. The database was limited to beam-end tests, notch-beam tests, and splice tests. The majority of the bars represented in the database were composed of GFRP. In Wambeke and Shield's database (2006), there

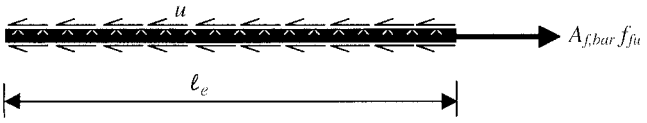


*Fig. 11.1—Transfer of force through bond.*

were 82 beam tests that resulted in splitting failures based on the work of Ehsani et al. (1996a), Daniali (1992), Shield et al. (1997, 1999), and Tighiouart et al. (1999). The tests included both spiral wrap and helical lug patterned bars with and without confining reinforcement. A linear regression of the normalized average bond stress versus the normalized cover and embedment (splice) length resulted in the following relationship after rounding the coefficients

$$\frac{u}{\sqrt{f'_c}} = 4.0 + 0.3\frac{C}{d_b} + 100\frac{d_b}{\ell_e} \tag{11-2}$$

For SI units

$$\frac{u}{0.083\sqrt{f'_c}} = 4.0 + 0.3\frac{C}{d_b} + 100\frac{d_b}{\ell_e}$$

where $C$ is the lesser of the cover to the center of the bar or one-half of the center-on-center spacing of the bars being developed. The bar surface (spiral wrap versus helical lug) did not appear to affect the results, nor surprisingly did the presence of confining reinforcement (Wambeke and Shield 2006). Darwin et al. (1996) found that confining steel used in beams that had steel reinforcing bars with a high relative rib area had more of a beneficial increase in the bond force over the same-size steel bars with moderate rib area. The counterargument is proposed herein. The GFRP bars have a very low relative rib area and, therefore, the presence of confinement may not increase the average bond stress. Additional research into the effect of confining reinforcement on bond of GFRP bars, however, is warranted.

Equation (11-1) and (11-2) can be solved for the achievable bar stress given the existing embedment length and cover. A subset of the full database developed by Wambeke and Shield (2006) was used to determine a factor of safety for use with these equations so that the probability of a test-predicted ratio less than 1.0 was 22%. This database included both splitting and pullout failures with embedment lengths of at least $19d_b$. Additionally, a limit of 3.5 was put on the $C/d_b$ term so that the same equation could be used to predict developable bar stresses for either bond failure mode (splitting or pullout). When the normalized cover was over 3.5 and the embedment length was greater than $19d_b$, the failure mode was always pullout. The resulting expression for developable bar stress is

$$f_{fe} = \sqrt{f'_c}\left(\frac{\ell_e}{0.1} + 1300\frac{\ell_e}{d_b} + \frac{C}{d_b}\frac{\ell_e}{d_b} + 340\right) \le f_{fu} \tag{11-3}$$

For SI units

$$f_{fe} = \frac{0.083\sqrt{f'_c}}{\alpha}\left(13.6\frac{\ell_e}{d_b} + \frac{C}{d_b}\frac{\ell_e}{d_b} + 340\right) \le f_{fu}$$

in which the term $C/d_b$ should not be taken larger than 3.5, and $\alpha$ is a factor to account for bar location (discussed in Section 11.1.1) The mean of the test-predicted ratio of bar stresses using this equation was 1.14, with a coefficient of variation of 15.8%. The appropriateness of this equation for embedment lengths greater than $100d_b$ is questionable, as the dataset used to develop it did not include any bond failures with embedment lengths greater than $100d_b$. Embedment lengths shorter than $20d_b$ are not recommended. Additional work needs to be performed to determine the effect of the chosen factor of safety for bond on the flexural reliability of the section.

When applying Eq. (11-3) for design purposes, it should be assumed that the maximum achievable bar stress varies linearly from 0 to the value produced by Eq. (11-3) along the first $20d_b$ of the bar embedment. After this point, Eq. (11-3) can be used to determine the achievable bar stress along the bar. A check should be made to determine if adequate moment capacity can be achieved at the end of the available embedment length. If not, then the embedment length must be increased, the number of bars increased so that a lower stress in each bar is required at ultimate, or the nominal moment capacity must be recalculated to include the possibility of bond failure as described in Section 11.1.3. It should be noted that increasing the number of bars may decrease the stress developed in any one bar, as the term $C/d_b$ may decrease as the bar spacing decreases.

**11.1.1** *Bar location modification factor*—The default bar location modification factor is 1.0.

While placing concrete, air, water, and fine particles migrate upward through the concrete. This can cause a significant drop in bond strength under the horizontal reinforcement. The term "top reinforcement" usually refers to horizontal reinforcement with more than 12 in. (305 mm) of concrete below it at the time of embedment. The database assembled by Wambeke and Shield (2006) included 15 tests using top bars with embedment lengths greater than $16d_b$ that resulted in bond failure (Ehsani et al. 1996a; Mosley 2002). Based on these data, for bars with more than 12 in. (300 mm) of concrete cast below, $\alpha$ in Eq. (11-3) should be taken as 1.5.

**11.1.2** *Material modification factor*—A limited amount of bond data exists in the Wambeke and Shield (2006) database for AFRP bars (Mosley 2002). Based on these few tests, however, the development length of AFRP bars appears to be similar to that of GFRP bars. Therefore, the development length equations provided are also reasonable for AFRP bars without the addition of a material modification factor. No data exists in the database for CFRP bars; it is anticipated that the much larger stiffness of the CFRP bars will likely decrease the required development lengths and, correspondingly, its material modification factor. At this time, a material factor equal to 1.0 is recommended for CFRP bars.

**11.1.3** *Nominal moment strength of bond critical sections*—Bond critical sections are defined as sections where the maximum achievable stress in the FRP bar is limited by Eq. (11-3). For this case, the nominal moment capacity should be recalculated using a modification of the method described in Section 8.2. When bond limits the stress that can be developed in the bar, the two possible failure modes are concrete crushing and bond failure. The capacity for a concrete crushing failure can be calculated using Eq. (8-5). This equation is applicable if the bar stress that can be developed ($f_{fe}$ as determined from Eq. (11-3)) is greater than or equal to the bar stress determined by Eq. (8-4d). When $\rho < \rho_{fb}$ or $\rho > \rho_{fb}$ and the bar stress required in Eq. (8-4d) cannot be developed, the capacity for failure controlled by bond can be determined using Eq. (8-6b) with $f_{fe}$ from Eq. (11-3) substituted for $f_{fu}$, and $f_{fe}/E_f$ substituted for $\varepsilon_{fu}$ in Eq. (8-6c). A strength reduction factor of 0.55 is recommended for flexure when the mode of failure is bond.

## 11.2—Development length of bent bar

Limited experimental data are available on the bond behavior of hooked FRP reinforcing bars. ACI 318-05 provisions for development length of hooked steel bars are not applicable to FRP bars due to the differences in material characteristics.

Ehsani et al. (1996b) tested 36 specimens with hooked GFRP bars. Based on the results of the study, the expression for the development length of a 90-degree hooked bar $\ell_{bhf}$ was proposed as follows

$$\ell_{bhf} = K_4\frac{d_b}{\sqrt{f'_c}} \qquad (11\text{-}4)$$

The $K_4$ factor for the calculation of the development length in this equation is 1820 (150 for SI units) for bars with $f_{fu}$ less than 75,000 psi (517 MPa). This factor should be multiplied by $f_{fu}/75{,}000$ ($f_{fu}/517$ for SI units) for bars having a tensile strength between 75,000 psi (517 MPa) and 150,000 psi (1034 MPa).

When the side cover (normal to the plane of hook) is more than 2-1/2 in. (64 mm) and the cover extension beyond hook is not less than 2 in. (50 mm), another multiplier of 0.7 can be applied (Ehsani et al. 1996b). These modification factors are similar to those in ACI 318-05, Section 12.5.3, for steel hooked bars. To account for the lack of experimental data, the use of Eq. (11-5) in calculating the development length of hooked bars is recommended by the committee

$$\ell_{bhf} = \begin{cases} 2000\dfrac{d_b}{\sqrt{f'_c}} & \text{for } f_{fu} \le 75{,}000 \text{ psi} \\ \dfrac{f_{fu}}{37.5}\dfrac{d_b}{\sqrt{f'_c}} & \text{for } 75{,}000 < f_{fu} < 150{,}000 \text{ psi} \\ 4000\dfrac{d_b}{\sqrt{f'_c}} & \text{for } f_{fu} \ge 150{,}000 \text{ psi} \end{cases} \qquad (11\text{-}5)$$

For SI units,

$$\ell_{bhf} = \begin{cases} 165\dfrac{d_b}{\sqrt{f'_c}} & \text{for } f_{fu} \le 520 \text{ MPa} \\ \dfrac{f_{fu}}{3.1}\dfrac{d_b}{\sqrt{f'_c}} & \text{for } 520 < f_{fu} < 1040 \text{ MPa} \\ 330\dfrac{d_b}{\sqrt{f'_c}} & \text{for } f_{fu} \ge 1040 \text{ MPa} \end{cases}$$

with $\ell_{bhf}$ in mm, $f_{fu}$ and $f'_c$ in MPa, and $d_b$ in mm.

The value calculated using Eq. (11-5) should not be less than $12d_b$ or 9 in. (230 mm). These values are based on test results reported by Ehsani et al. (1995), in which the tensile force and slippage of a hooked bar stabilized in the neighborhood of $12d_b$. The tail length of a hooked bar, $\ell_{thf}$ (Fig. 9.1), should not be less than $12d_b$. Longer tail lengths were found to have an insignificant influence on the ultimate tensile force and slippage of the hook. To avoid shear failure at the bend, the radius of the bend should not be less than $3d_b$ (Ehsani et al. 1995).

### 11.3—Development of positive moment reinforcement

In general, the requirements of Sections 12.10 and 12.11 of ACI 318-05 should be met when using FRP reinforcement with the following changes: for straight bars, the stress to be developed $f_{fr}$ should be the minimum of $f_{fu}$, the stress given by Eq. (8-4d), and the stress given by Eq. (11-3). The development length for straight bars is defined as the bond length required to develop $f_{fr}$ and is given by

$$\ell_d = \frac{\alpha\dfrac{f_{fr}}{\sqrt{f'_c}} - 340}{13.6 + \dfrac{C}{d_b}} d_b \qquad (11\text{-}6)$$

For SI units

$$\ell_d = \frac{\alpha\dfrac{f_{fr}}{0.083\sqrt{f'_c}} - 340}{13.6 + \dfrac{C}{d_b}} d_b$$

Because of the reduced resistance factor compared with steel, the provision for development of positive reinforcement at points of inflection and simple supports given in ACI 318-05 (Section 12.11.3) should be altered to

$$\ell_d \le \frac{\phi M_n}{V_u} + \ell_a \qquad (11\text{-}7)$$

where $M_n$ is the nominal moment strength assuming all reinforcement at the section to be stressed to the required bar stress $f_{fr}$; $V_u$ is the factored shear force at the section; and $\ell_a$, at a support, is the embedment length beyond center of the support, or $\ell_a$, at a point of inflection, is the larger of the effective depth of the member or $12d_b$. The value of $\phi M_n/V_u$ may be increased by 30% when the ends of the reinforcement are confined by a compressive reaction. This restriction on the development length need not be met if it can be shown by refined analysis that the design moment capacity is greater than the factored moment everywhere along the development length.

### 11.4—Tension lap splice

ACI 318-05, Section 12.15, distinguishes between two types of tension lap splices depending on the fraction of the bars spliced in a given length and on the reinforcement stress in the splice. For steel reinforcement, the splice length for a Class A splice is $1.0\ell_d$, and for a Class B splice is $1.3\ell_d$. This classification for FRP applications is inappropriate, as often the full tensile strength of the bar need not be developed; hence, it is conservative to assume that all splices are Class B splices. Limited data are available for the minimum development length of FRP tension lap splices. (Benmokrane 1997; Mosley 2002). Consequently, a value of $1.3\ell_d$ is recommended for all splices.

## CHAPTER 12—REFERENCES

### 12.1—Referenced standards and reports

The standards and reports listed below were the latest editions at the time this document was prepared. Because these documents are revised frequently, the reader is advised to contact the proper sponsoring organization for the latest edition.

*American Concrete Institute (ACI)*

| | |
|---|---|
| 117 | Standard Specifications for Tolerances for Concrete Construction and Materials |
| 216R | Guide for Determining the Fire Endurance of Concrete Elements |
| 360R | Design of Slabs on Grade |
| 440R | State-of-the-Art Report on FRP Reinforcement for Concrete Structures |
| 440.3R | Guide Test Methods for Fiber-Reinforced Polymers (FRPs) for Reinforcing or Strengthening Concrete Structures |
| 440.4R | Prestressing Concrete Structures with FRP Tendons |

These publications may be obtained from:

American Concrete Institute
P. O. Box 9094
Farmington Hills, Mich. 48333-9094
www.concrete.org

### 12.2—Cited references

ACI Committee 318, 2005, "Building Code Requirements for Structural Concrete (ACI 318-05) and Commentary (318R-05)," American Concrete Institute, Farmington Hills, Mich., 430 pp.

Adimi, R.; Rahman, H.; Benmokrane, B.; and Kobayashi, K., 1998, "Effect of Temperature and Loading Frequency on

the Fatigue Life of a CFRP Bar in Concrete," *Proceedings of the Second International Conference on Composites in Infrastructure (ICCI-98)*, Tucson, Ariz., V. 2, pp. 203-210.

Ahmad, S. H.; Zia, P.; Yu, T.; and Xie, Y., 1993, "Punching Shear Tests of Slabs Reinforced with 3-D Carbon Fiber Fabric," *Concrete International*, V. 16, No. 6, June, pp. 36-41.

Al-Dulaijan, S. U.; Nanni, A.; Al-Zahrani, M. M.; and Bakis, C. E., 1996, "Bond Evaluation of Environmentally Conditioned GFRP/Concrete System," *Proceedings of the Second International Conference on Advanced Composite Materials in Bridges and Structures (ACMBS-2)*, M. M. El-Badry, ed., Canadian Society for Civil Engineering, Montreal, Quebec, pp. 845-852.

Almusallam, T. H.; Al-Salloum, Y.; Alsayed, S.; and Amjad, M., 1997, "Behavior of Concrete Beams Doubly Reinforced by FRP Bars," *Proceedings of the Third International Symposium on Non-Metallic (FRP) Reinforcement for Concrete Structures (FRPRCS-3)*, Japan Concrete Institute, Tokyo, Japan, V. 2, pp. 471-478.

Al-Zahrani, M. M.; Nanni, A.; Al-Dulaijan, S. U.; and Bakis, C. E., 1996, "Bond of FRP to Concrete for Rods with Axisymmetric Deformations," *Proceedings of the Second International Conference on Advanced Composite Materials in Bridges and Structures (ACMBS-II)*, Montreal, Canada, pp. 853-860.

Ando, N.; Matsukawa, H.; Hattori, A.; and Mashima, A., 1997, "Experimental Studies on the Long-Term Tensile Properties of FRP Tendons," *Proceedings of the Third International Symposium on Non-Metallic (FRP) Reinforcement for Concrete Structures (FRPRCS-3)*, V. 2, Japan Concrete Institute, Tokyo, Japan, pp. 203-210.

Arockiasamy, M.; Amer, A.; and Shahawy, M., 1998, "Environmental and Long-Term Studies on CFRP Cables and CFRP Reinforced Concrete Beams," *Proceedings of the First International Conference on Durability of Composites for Construction*, B. Benmokrane and H. Rahman, eds., Sherbrooke, Quebec, pp. 599-610.

Bakis, C. E., 1993, "FRP Composites: Materials and Manufacturing," *Fiber-Reinforced-Plastic for Concrete Structures: Properties and Applications*, A. Nanni, ed., Elsevier, Amsterdam, pp. 13-58.

Bakis, C. E.; Al-Dulaijan, S. U.; Nanni, A.; Boothby, T. E.; and Al-Zahrani, M. M., 1998a, "Effect of Cyclic Loading on Bond Behavior of GFRP Rods Embedded in Concrete Beams," *Journal of Composites Technology and Research*, V. 20, No. 1, pp. 29-37.

Bakis, C. E., and Boothby, T. E., 2004, "Evaluation of Crack Width and Bond Strength in GFRP Reinforced Beams Subjected to Sustained Loads," *Proceedings of the 4th International Conference on Advanced Composite Materials in Bridges and Structures—ACMBS-IV*, M. El-Badry and L. Dunaszegi, eds. (CD-ROM)

Bakis, C. E.; Freimanis, A. J.; Gremel, D.; and Nanni, A., 1998b, "Effect of Resin Material on Bond and Tensile Properties of Unconditioned and Conditioned FRP Reinforcement Rods," *Proceedings of the First International Conference on Durability of Composites for Construction*, B. Benmokrane and H. Rahman, eds., Sherbrooke, Quebec, pp. 525-535.

Bank, L. C., 1993, "Properties of FRP Reinforcement for Concrete," *Fiber-Reinforced-Plastic (FRP) Reinforcement for Concrete Structures: Properties and Applications, Developments in Civil Engineering*, V. 42, A. Nanni, ed., Elsevier, Amsterdam, pp. 59-86.

Bank, L. C., and Puterman, M., 1997, "Microscopic Study of Surface Degradation of Glass Fiber-Reinforced Polymer Rods Embedded in Concrete Castings Subjected to Environmental Conditioning," *High Temperature and Environmental Effects on Polymeric Composites*, V. 2, ASTM STP 1302, T. S. Gates and A.-H. Zureick, eds., ASTM International, West Conshohocken, Pa., pp. 191-205.

Bank, L. C.; Puterman, M.; and Katz, A., 1998, "The Effect of Material Degradation on Bond Properties of FRP Reinforcing Bars in Concrete," *ACI Materials Journal*, V. 95, No. 3, May-June, pp. 232-243.

Bank, L. C., and Xi, Z., 1995 "Punching Shear Behavior of Pultruded FRP Grating Reinforced Concrete Slabs," *Proceedings*, 2nd International Symposium on Non-Metallic (FRP) Reinforcement for Concrete Structures, Ghent, Belgium, pp. 360-367.

Banthia, N.; Al-Asaly, M.; and Ma, S., 1995, "Behavior of Concrete Slabs Reinforced with Fiber-Reinforced Plastic Grid," *Journal of Materials in Civil Engineering*, ASCE, V. 7, No. 4, pp. 643-652.

Benmokrane, B., 1997, "Bond Strength of FRP Rebar Splices," *Proceedings of the Third International Symposium on Non-Metallic (FRP) Reinforcement for Concrete Structures (FRPRCS-3)*, V. 2, Japan Concrete Institute, Tokyo, Japan, pp. 405-412.

Benmokrane, B.; Chaallal, O.; and Masmoudi, R., 1996, "Flexural Response of Concrete Beams Reinforced with FRP Reinforcing Bars," *ACI Structural Journal*, V. 93, No. 1, Jan.-Feb., pp. 46-55.

Benmokrane, B.; El-Salakawy, E.; El-Ragaby, A.; Desgagne, G.; and Lackey, T., 2004, "Design, Construction and Monitoring of Four Innovative Concrete Bridge Decks Using Non-Corrosive FRP Composite Bars," *2004 Annual Conference of the Transportation Association of Canada*, Québec City, Québec, Canada.

Benmokrane, B., and Rahman, H., eds., 1998, "Durability of Fiber Reinforced Polymer (FRP) Composites for Construction," *Proceedings of the First International Conference (CDCC '98)*, Québec, Canada, 692 pp.

Bischoff, P., 2005, "Reevaluation of Deflection Prediction for Concrete Beams Reinforced with Steel and Fiber-Reinforced Polymer Bars," *Journal of Structural Engineering*, ASCE, V. 131, No. 5, May, pp. 752-767.

Bootle, J.; Burzesi, F.; and Fiorini, L., 2001, "Design Guidelines," *ASM Handbook*, V. 21, Composites, ASM International, Material Park, Ohio, pp. 388-395.

Boyle, H. C., and Karbhari, V. M., 1994, "Investigation of Bond Behavior Between Glass Fiber Composite Reinforcements and Concrete," *Journal of Polymer-Plastic Technology Engineering*, V. 33, No. 6, pp. 733-753.

Branson, D. E., 1977, *Deformation of Concrete Structures*, McGraw-Hill Book Co., New York, 546 pp.

Brown, V., 1997, "Sustained Load Deflections in GFRP-Reinforced Concrete Beams," *Proceedings of the Third International Symposium on Non-Metallic (FRP) Reinforcement for Concrete Structures (FRPRCS-3)*, V. 2, Japan Concrete Institute, Tokyo, Japan, pp. 495-502.

Brown, V., and Bartholomew, C., 1996, "Long-Term Deflections of GFRP-Reinforced Concrete Beams," *Proceedings of the First International Conference on Composites in Infrastructure (ICCI-96)*, H. Saadatmanesh and M. R. Ehsani, eds., Tucson, Ariz., pp. 389-400.

Burgoyne, C., ed., 2001, "Non-Metallic Reinforcement for Concrete Structures—FRPRCS-5," *Proceedings*, International Conference, Cambridge, UK.

CAN/CSA-S6-00, 2000, "Canadian High Bridge Design Code," Clause 16.8.6, Canadian Standard Association (CSA) International, Toronto, Ontario, Canada, 734 pp.

CAN/CSA-S6-02, 2002, "Design and Construction of Building Components with Fibre-Reinforced Polymers," CAN/CSA S806-02, Canadian Standards Association, Rexdale, Ontario, Canada, 177 pp.

Chang, K. K., 2001, "Aramid Fibers," *ASM Handbook*, V. 21, Composites, ASM International, Material Park, Ohio, pp. 41-45.

Clarke, J., and Sheard, P., 1998, "Designing Durable FRP Reinforced Concrete Structures," *Proceedings of the First International Conference on Durability of Composites for Construction*, B. Benmokrane and H. Rahman, eds., Sherbrooke, Québec, Canada, pp. 13-24.

Conrad, J. O.; Bakis, C. E.; Boothby, T. E.; and Nanni, A., 1998, "Durability of Bond of Various FRP Rods in Concrete," *Proceedings of the First International Conference on Durability of Composites for Construction*, B. Benmokrane and H. Rahman, eds., Sherbrooke, Quebec, Canada, pp. 299-310.

Coomarasamy, A., and Goodman, S., 1997, "Investigation of the Durability Characteristics of Fiber Reinforced Polymer (FRP) Materials in Concrete Environment," *American Society for Composites—Twelfth Technical Conference*, Dearborn, Mich.

Cosenza, E.; Manfredi, G.; and Nanni, A., eds., 2001, "Composites in Construction: A Reality," *Proceedings, International Workshop*, Capri, Italy, ASCE, Reston, Va., 277 pp.

Curtis, P. T., 1989, "The Fatigue Behavior of Fibrous Composite Materials," *Journal of Strain Analysis*, V. 24, No. 4, pp. 235-244.

Dally, J. W., and Riley, W. F., 1991, *Experimental Stress Analysis*, 3rd Edition, McGraw Hill, New York, 672 pp.

Daniali, S., 1992 "Development Length for Fiber-Reinforced Plastic Bars," *Advanced Composite Materials in Bridges and Structures*, K. W. Neale and P. Labossiere, eds., pp. 179-188.

Darwin, D.; Zuo, J.; Tholen, M.; and Idun, E., 1996, "Development Length Criteria for Conventional and High Relative Rib Area Reinforcing Bars," *ACI Structural Journal*, V. 93, No. 3, May-June, pp. 347-359.

Devalapura, R. K.; Greenwood, M. E.; Gauchel, J. V.; and Humphrey, T. J., 1996, *Advanced Composite Materials in Bridges and Structures*, M. M. El-Badry, ed., Canadian Society for Civil Engineering, Montreal, Québec, Canada, pp. 107-116.

Dolan, C. W.; Rizkalla, S.; and Nanni, A., eds., 1999, *Fourth International Symposium on Fiber Reinforced Polymer Reinforcement for Reinforced Concrete Structures*, SP-188, C. W. Dolan, S. H. Rizkalla, and A. Nanni, eds., American Concrete Institute, Farmington Hills, Mich., 1182 pp.

Dowden, D. M., and Dolan, C. W., 1997, "Comparison of Experimental Shear Data with Code Predictions for FRP Prestressed Beams," *Proceedings of the Third International Symposium on Non-Metallic (FRP) Reinforcement for Concrete Structures (FRPRCS-3)*, V. 2, Japan Concrete Institute, Tokyo, Japan, pp. 687-694.

Ehsani, M. R., 1993, "Glass-Fiber Reinforcing Bars," *Alternative Materials for the Reinforcement and Prestressing of Concrete*, J. L. Clarke, Blackie Academic & Professional, London, pp. 35-54.

Ehsani, M. R.; Saadatmanesh, H.; and Tao, S., 1995, "Bond of Hooked Glass Fiber Reinforced Plastic (GFRP) Reinforcing Bars to Concrete," *ACI Materials Journal*, V. 92, No. 4, July-Aug., pp. 391-400.

Ehsani, M. R.; Saadatmanesh, H.; and Tao, S., 1996a, "Design Recommendation for Bond of GFRP Rebars to Concrete," *Journal of Structural Engineering*, V. 122, No. 3, pp. 247-257.

Ehsani, M. R.; Saadatmanesh, H.; and Tao, S., 1996b, "Bond Behavior and Design Recommendations for Fiber-Glass Reinforcing Bars," *Proceedings of the First International Conference on Composites in Infrastructure (ICCI-96)*, H. Saadatmanesh and M. R. Ehsani, eds., Tucson, Ariz., pp. 466-476.

El-Badry, M., ed., 1996, "Advanced Composite Materials in Bridges and Structures (ACMBS-II)," *Proceedings of the Second International Conference*, Montreal, Canada, 1027 pp.

El-Ghandour, A. W.; Pilakoutas, K.; and Waldron, P., 2003, "Punching Shear Behavior of Fiber Reinforced Polymers Reinforced Concrete Flat Slabs: Experimental Study," *Journal of Composites for Construction*, ASCE, V. 7, No. 3, pp. 258-265.

Faza, S. S., and GangaRao, H. V. S., 1990, "Bending and Bond Behavior of Concrete Beams Reinforced with Plastic Rebars," *Transportation Research Record* 1290, pp. 185-193.

Faza, S. S., and GangaRao, H. V. S., 1993a, "Theoretical and Experimental Correlation of Behavior of Concrete Beams Reinforced with Fiber Reinforced Plastic Rebars," *Fiber-Reinforced-Plastic Reinforcement for Concrete Structures—International Symposium*, SP-138, A. Nanni and C. W. Dolan, eds., American Concrete Institute, Farmington Hills, Mich., pp. 599-614.

Faza, S. S., and GangaRao, H. V. S., 1993b, "Glass FRP Reinforcing Bars for Concrete," *Fiber-Reinforced-Plastic (FRP) Reinforcement for Concrete Structures: Properties and Applications, Developments in Civil Engineering*, V. 42, A. Nanni, ed., Elsevier, Amsterdam, pp. 167-188.

Figueiras, J.; Juvandes, L.; and Furia, R., eds., 2001, "Composites in Construction," *Proceedings*, CCC 2001, Porto, Portugal.

Freimanis, A. J.; Bakis, C. E.; Nanni, A.; and Gremel, D., 1998, "A Comparison of Pullout and Tensile Behaviors of FRP Reinforcement for Concrete," *Proceedings of the Second International Conference on Composites in Infrastructure (ICCI-98)*, V. 2, Tucson, Ariz., pp. 52-65.

Frosch, R. J., 1999, "Another Look at Cracking and Crack Control in Reinforced Concrete," *ACI Structural Journal*, V. 96, No. 3, May-June, pp. 437-442.

GangaRao, H. V. S., and Vijay, P. V., 1997a, "Design of Concrete Members Reinforced with GFRP Bars," *Proceedings of the Third International Symposium on Non-Metallic (FRP) Reinforcement for Concrete Structures (FRPRCS-3)*, V. 1, Japan Concrete Institute, Tokyo, Japan, pp. 143-150.

GangaRao, H. V. S., and Vijay, P. V., 1997b, "Aging of Structural Composites under Varying Environmental Conditions," *Proceedings of the Third International Symposium on Non-Metallic (FRP) Reinforcement for Concrete Structures (FRPRCS-3)*, V. 2, Japan Concrete Institute, Tokyo, Japan, pp. 91-98.

Gao, D.; Benmokrane, B.; and Masmoudi, R., 1998a, "A Calculating Method of Flexural Properties of FRP-Reinforced Concrete Beam: Part 1: Crack Width and Deflection," *Technical Report*, Department of Civil Engineering, University of Sherbrooke, Sherbrooke, Québec, Canada, 24 pp.

Gao, D.; Benmokrane, B.; and Tighiouart, B., 1998b, "Bond Properties of FRP Rebars to Concrete," *Technical Report*, Department of Civil Engineering, University of Sherbrooke, Sherbrooke, Quebec, Canada, 27 pp.

Gentry, T. R.; Bank, L. C.; Barkatt, A.; and Prian, L., 1998, "Accelerated Test Methods to Determine the Long-Term Behavior of Composite Highway Structures Subject to Environmental Loading," *Journal of Composites Technology & Research*, V. 20, No. 1, pp. 38-50.

Gerritse, A., 1992, "Durability Criteria for Non-Metallic Tendons in an Alkaline Environment," *Proceedings of the First International Conference on Advance Composite Materials in Bridges and Structures (ACMBS-I)*, Canadian Society of Civil Engineers, Sherbrooke, Canada, pp. 129-137.

Gross, S.; Yost, J.; and Kevgas, G., 2003, "Time-Dependent Behavior of Normal and High Strength Concrete Beams Reinforced With GFRP Bars Under Sustained Loads," *High Performance Materials in Bridges*, American Society of Civil Engineers, pp. 451-462.

Gulbrandsen, P., 2005, "Reliability Analysis of the Flexural Capacity of Fiber Reinforced Polymer Bars in Concrete Beams," Masters thesis, University of Minnesota, 80 pp.

Hayes, M. D.; Garcia, K.; Verghese, N.; and Lesko, J., 1998, "The Effect of Moisture on the Fatigue Behavior of a Glass/Vinyl Ester Composite," *Proceedings of the Second International Conference on Composites in Infrastructure (ICCI-98)*, V. 1, Tucson, Ariz., pp. 1-12.

Hughes, B. W., and Porter, M. L., 1996, "Experimental Evaluation of Non-Metallic Dowel Bars in Highway Pavements," *Proceedings of the First International Conference on Composites in Infrastructure (ICCI-96)*, H. Saadatmanesh and M. R. Ehsani, eds., Tucson, Ariz., pp. 440-450.

Humar, J., and Razaqpur, A. G., eds., 2000, "Advanced Composite Materials in Bridges and Structures," *Proceedings*, 3rd International Conference, Ottawa, Canada.

Iyer, S. L., and Sen, R., eds., 1991, "Advanced Composite Materials in Civil Engineering Structures," *Proceedings of the Specialty Conference*, American Society of Civil Engineers, New York, 443 pp.

Jaeger, L. G.; Mufti, A.; and Tadros, G., 1997, "The Concept of the Overall Performance Factor in Rectangular-Section Reinforced Concrete Beams," *Proceedings of the Third International Symposium on Non-Metallic (FRP) Reinforcement for Concrete Structures (FRPRCS-3)*, V. 2, Japan Concrete Institute, Tokyo, Japan, pp. 551-558.

Japan Society of Civil Engineers (JSCE) Subcommittee on Continuous Fiber Reinforcement, 1992, *Proceedings of the Utilization of FRP-Rods for Concrete Reinforcement*, Japan Society of Civil Engineers, Tokyo, Japan, 314 pp.

Japan Society of Civil Engineers (JSCE), 1997a, *Proceedings of the Third International Symposium on Non-Metallic (FRP) Reinforcement for Concrete Structures (FRPRCS-3)*, V. 2, Japan Concrete Institute, Tokyo, Japan, pp. 511-518.

Japan Society of Civil Engineers (JSCE), 1997b, "Recommendation for Design and Construction of Concrete Structures Using Continuous Fiber Reinforcing Materials," *Concrete Engineering Series* No. 23, 325 pp.

Joint ACI-ASCE Committee 426, 1974, "The Shear Strength of Reinforced Concrete Members," American Concrete Institute, Farmington Hills, Mich., 111 pp.

Katz, A., 1998, "Effect of Helical Wrapping on Fatigue Resistance of GFRP," *Journal of Composites for Construction*, V. 2, No. 3, pp. 121-125.

Katz, A., 2000, "Bond to Concrete of FRP Rebars after Cyclic Loading," *Journal of Composites for Construction*, V. 4, No. 3, pp. 137-144.

Katz, A.; Berman, N.; and Bank, L. C., 1998, "Effect of Cyclic Loading and Elevated Temperature on the Bond Properties of FRP Rebars," *International Conference on the Durability of Fiber Reinforced Polymer (FRP) Composites for Construction*, Sherbrooke, Canada, pp. 403-413.

Katz, A.; Berman, N.; and Bank, L. C., 1999, "Effect of High Temperature on the Bond Strength of FRP Rebars," *Journal of Composites for Construction*, V. 3, No. 2, pp. 73-81.

Keesler, R. J., and Powers, R. G., 1988, "Corrosion of Epoxy Coated Rebars—Keys Segmental Bridge—Monroe County," *Report* No. 88-8A, Florida Dept. of Transportation, Materials Office, Corrosion Research Laboratories, Gainesville, Fla.

Kobayashi, K., and Fujisaki, T., 1995, "Compressive Behavior of FRP Reinforcement in Non-prestressed Concrete Members," *Proceedings of the Second International RILEM Symposium on Non-Metallic (FRP) Reinforcement for Concrete Structures (FRPRCS-2)*, Ghent, Belgium, pp. 267-274.

Kocaoz, S.; Samaranayake, V. A.; and Nanni, A., 2005, "Tensile Characterization of Glass FRP Bars," *Composites*, Part B, V. 36, No. 1, Jan., pp. 127-134.

Kollár, L. P., and Springer, G. S., 2003, *Mechanics of Composite Structures*, Cambridge University Press, New York, 498 pp.

Kumahara, S.; Masuda, Y.; and Tanano, Y., 1993, "Tensile Strength of Continuous Fiber Bar Under High Temperature," *Fiber-Reinforced-Plastic Reinforcement for Concrete Structures—International Symposium*, SP-138, A. Nanni and C. W. Dolan, eds., American Concrete Institute, Farmington Hills, Mich., pp. 731-742.

Lamouroux, F.; Bertrand, S.; Pailler, R.; Naslain, R.; and Cataldi, M., 1999, "Oxidation-Resistant Carbon-Fiber-Reinforced Ceramic-Matrix Composites," *Composites Science and Technology*, V. 59, No. 7, May, pp. 1073-1085.

Litherland, K. L.; Oakley, D. R.; and Proctor, B. A., 1981, "The Use of Accelerated Aging Procedures to Predict the Long Term Strength of GRC Composites," *Cement and Concrete Research*, V. 11, No. 3, pp. 455-466.

Mallick, P. K., 1988, *Fiber Reinforced Composites, Materials, Manufacturing, and Design*, Marcell Dekker, Inc., New York, 469 pp.

Mandell, J. F., 1982, "Fatigue Behavior of Fiber-Resin Composites," *Developments in Reinforced Plastics*, V. 2, Applied Science Publishers, London, pp. 67-107.

Mandell, J. F., and Meier, U., 1983, "Effects of Stress Ratio Frequency and Loading Time on the Tensile Fatigue of Glass-Reinforced Epoxy," *Long Term Behavior of Composites*, ASTM STP 813, ASTM International, West Conshohocken, Pa., pp. 55-77.

Matthys, S., and Taerwe, L., 2000, "Concrete Slabs Reinforced with FRP Grids. II: Punching Resistance," *Journal of Composites for Construction*, ASCE, V. 4, No. 3, pp. 154-161.

Meier, U., 1992, "Carbon Fiber Reinforced Polymers: Modern Materials in Bridge Engineering," *Structural Engineering International*, Journal of the International Association for Bridge and Structural Engineering, V. 2, No. 1, pp. 7-12.

Michaluk, C. R.; Rizkalla, S.; Tadros, G.; and Benmokrane, B., 1998, "Flexural Behavior of One-Way Concrete Slabs Reinforced by Fiber Reinforced Plastic Reinforcement," *ACI Structural Journal*, V. 95, No. 3, May-June, pp. 353-364.

MIL-17, 1999, "Guidelines for Characterization of Structural Materials, Composite Materials Handbook," V. 1, Rev. E, June 1999.

Mindess, S.; Young, J. F.; and Darwin, D., 2003, *Concrete*, 2nd Edition, Prentice-Hall, Upper Saddle River, N.J., 644 pp.

Mosley, C. P., 2002, "Bond Performance of Fiber Reinforced Plastic (FRP) Reinforcement in Concrete," MS thesis, Purdue University, West Lafayette, Ind.

Mutsuyoshi, H.; Uehara, K.; and Machida, A., 1990, "Mechanical Properties and Design Method of Concrete Beams Reinforced with Carbon Fiber Reinforced Plastics," *Transaction of the Japan Concrete Institute*, V. 12, Japan Concrete Institute, Tokyo, Japan, pp. 231-238.

Nagasaka, T.; Fukuyama, H.; and Tanigaki, M.; 1993, "Shear Performance of Concrete Beams Reinforced with FRP Stirrups," *Fiber-Reinforced-Plastic Reinforcement for Concrete Structures—International Symposium*, SP-138, A. Nanni and C. W. Dolan, eds., American Concrete Institute, Farmington Hills, Mich., pp. 789-811.

Nanni, A., ed., 1993a, "Fiber-Reinforced-Plastic (FRP) Reinforcement for Concrete Structures: Properties and Applications," *Developments in Civil Engineering*, Elsevier, V. 42, 450 pp.

Nanni, A., 1993b, "Flexural Behavior and Design of Reinforced Concrete Using FRP Rods," *Journal of Structural Engineering*, V. 119, No. 11, pp. 3344-3359.

Nanni, A., 2001, "Relevant Field Applications of FRP Composites in Concrete Structures," *Proceedings of the International Conference Composites in Construction—CCC2001*, J. Figueiras, L. Juvandes, and R. Faria, eds., Portugal, pp. 661-670.

Nanni, A.; Bakis, C. E.; and Boothby, T. E., 1995, "Test Methods for FRP-Concrete Systems Subjected to Mechanical Loads: State of the Art Review," *Journal of Reinforced Plastics and Composites*, V. 14, pp. 524-588.

Nanni, A., and Dolan, C. W., eds., 1993, *Fiber-Reinforced-Plastic Reinforcement for Concrete Structures—International Symposium*, SP-138, American Concrete Institute, Farmington Hills, Mich., 977 pp.

Nanni, A.; Nenninger, J.; Ash, K.; and Liu, J., 1997, "Experimental Bond Behavior of Hybrid Rods for Concrete Reinforcement," *Structural Engineering and Mechanics*, V. 5, No. 4, pp. 339-354.

Nanni, A.; Rizkalla, S.; Bakis, C. E.; Conrad, J. O.; and Abdelrahman, A. A., 1998, "Characterization of GFRP Ribbed Rod Used for Reinforced Concrete Construction," *Proceedings of the International Composites Exhibition (ICE-98)*, Nashville, Tenn., pp. 16A/1-6.

National Research Council, 1991, "Life Prediction Methodologies for Composite Materials," *Committee on Life Prediction Methodologies for Composites*, NMAB-460, National Materials Advisory Board, Washington, D.C., 66 pp.

Nawy, E., and Neuwerth, G., 1977, "Fiberglass Reinforced Concrete Slabs and Beams," *Journal of the Structural Division*, ASCE, V. 103, No. ST2, pp. 421-440.

Neale, K.W., and Labossiere, P., eds., 1992, "Advanced Composite Materials in Bridges and Structures," *Proceedings of the First International Conference (ACMBS-I)*, Sherbrooke, Canada, 705 pp.

Noritake, K.; Kakihara, R.; Kumagai, S.; and Mizutani, J., 1993, "Technora, an Aramid FRP Rod," *Fiber-Reinforced-Plastic (FRP) Reinforcement for Concrete Structures: Properties and Applications, Developments in Civil Engineering*, V. 42, A. Nanni, ed., Elsevier, Amsterdam, pp. 267-290.

Odagiri, T.; Matsumoto, K.; and Nakai H., 1997, "Fatigue and Relaxation Characteristics of Continuous Aramid Fiber Reinforced Plastic Rods," *Proceedings of the Third International Symposium on Non-Metallic (FRP) Reinforcement for*

*Concrete Structures (FRPRCS-3)*, V. 2, Japan Concrete Institute, Tokyo, Japan, pp. 227-234.

Okamoto, T.; Matsubara, S.; Tanigaki, M.; and Jasuo, K., 1993, "Practical Application and Performance of PPC Beams Reinforced with Braided FRP Bars," *Fiber-Reinforced-Plastic Reinforcement for Concrete Structures—International Symposium*, SP-138, A. Nanni and C. W. Dolan, eds., American Concrete Institute, Farmington Hills, Mich., pp. 875-894.

Okamoto, T.; Nagasaka, T.; and Tanigaki, M., 1994, "Shear Capacity of Concrete Beams Using FRP Reinforcement," *Journal of Structural Construction Engineering*, No. 455, pp. 127-136.

Orangun, C.; Jirsa, J. O.; and Breen, J. E., 1977, "A Reevaluation of Test Data on Development Length and Splices," ACI JOURNAL, *Proceedings* V. 74, No. 3, Mar., pp. 114-122.

Ospina, C. E., 2005, "Alternative Model for Concentric Punching Capacity Evaluation of Reinforced Concrete Two-Way Slabs, *Concrete International*, V. 27, No. 9, Sept., pp. 53-57.

Ospina, C. E.; Alexander, S.; and Cheng, J. J., 2001, "Behaviour of Concrete Slabs with Fibre-Reinforced Polymer Reinforcement," *Structural Engineering Report* No. 242, Department of Civil and Environmental Engineering, University of Alberta, Alberta, Canada, 355 pp.

Ospina, C. E.; Alexander, S. D. B.; and Cheng, J. J. R., 2003, "Punching of Two-way Concrete Slabs with Fiber-Reinforced Polymer Reinforcing Bars or Grids," *ACI Structural Journal*, V. 100, No. 5, Sept.-Oct., pp. 589-598.

Plecnik, J., and Ahmad, S. H., 1988, "Transfer of Composite Technology to Design and Construction of Bridges," *Final Report* to USDOT, Contract No. DTRS 5683-C000043.

Porter, M. L., and Barnes, B. A., 1998, "Accelerated Aging Degradation of Glass Fiber Composites," *Second International Conference on Composites in Infrastructure*, V. II, H. Saadatmanesh and M. R. Eshani, eds., University of Arizona, Tucson, Ariz., pp. 446-459.

Porter, M. L.; Hughes, B. W.; Barnes, B. A.; and Viswanath, K. P., 1993, "Non-Corrosive Tie Reinforcing and Dowel Bars for Highway Pavement Slabs," *Report* No. HR-343, Iowa Highway Research Board and Iowa Department of Transportation, Ames, Iowa.

Porter, M. L.; Mehus, J.; Young, K. A.; O'Neil, E. F.; and Barnes, B. A., 1997, "Aging for Fiber Reinforcement in Concrete," *Proceedings of the Third International Symposium on Non-Metallic (FRP) Reinforcement for Concrete Structures (FRPRCS-3)*, V. 2, Japan Concrete Institute, Tokyo, Japan, pp. 59-66.

Portland Cement Association (PCA), 1990, "Concrete Floors on Ground," Skokie, Ill., 36 pp. (revised)

Priestley, M. N.; Seible, F.; and Calvi, G. M., 1996, *Seismic Design and Retrofit of Bridges*, John Wiley and Sons, New York, 704 pp.

Rahman, A. H.; Kingsley, C. Y.; and Crimi, J., 1996, "Durability of FRP Grid Reinforcement," *Advanced Composite Materials in Bridges and Structures*, M. M. El-Badry, ed., Canadian Society for Civil Engineering, Montreal, Québec, Canada, pp. 681-690.

Rahman, A. H., and Kingsley, C. Y., 1996, "Fatigue Behavior of a Fiber-Reinforced-Plastic Grid as Reinforcement for Concrete," *Proceedings of the First International Conference on Composites in Infrastructure (ICCI-96)*, H. Saadatmanesh and M. R. Ehsani, eds., Tucson, Ariz., pp. 427-439.

Rahman, H.; Adimi, R.; and Crimi, J., 1997, "Fatigue Behavior of a Carbon FRP Grid Encased in Concrete," *Proceedings of the Third International Symposium on Non-Metallic (FRP) Reinforcement for Concrete Structures (FRPRCS-3)*, V. 2, Japan Concrete Institute, Tokyo, Japan, pp. 219-226.

Rasheed, H. A.; Nayal, R.; and Melhem, H. G., 2004, "Response Prediction of Concrete Beams Reinforced with FRP Bars," *Composite Structures*, V. 65, pp. 193-204.

Rizkalla, S. H., 1997, "A New Generation of Civil Engineering Structures and Bridges," *Proceedings of the Third International Symposium on Non-Metallic (FRP) Reinforcement for Concrete Structures (FRPRCS-3)*, V. 1, Japan Concrete Institute, Tokyo, Japan, pp. 113-128.

Rostasy, F. S., 1997, "On Durability of FRP in Aggressive Environments," *Proceedings of the Third International Symposium on Non-Metallic (FRP) Reinforcement for Concrete Structures (FRPRCS-3)*, V. 2, Japan Concrete Institute, Tokyo, Japan, pp. 107-114.

Roylance, M.; and Roylance, O., 1981, "Effect of Moisture on the Fatigue Resistance of an Aramid-Epoxy Composite," *Organic Coatings and Plastics Chemistry*, American Chemical Society, Washington, D.C., V. 45, pp. 784-788.

Saadatmanesh, H., and Ehsani, M. R., eds., 1998, "Fiber Composites in Infrastructure," *Proceedings of the Second International Conference on Composites in Infrastructure (ICCI-98)*, Tucson, Ariz.

Saadatmanesh, H., and Tannous, F. E., 1999a, "Relaxation, Creep, and Fatigue Behavior of Carbon Fiber-Reinforced Plastic Tendons," *ACI Materials Journal*, V. 96, No. 2, Mar.-Apr., pp. 143-153.

Saadatmanesh, H., and Tannous, F. E., 1999b, "Long-Term Behavior of Aramid Fiber-Reinforced Plastic Tendons," *ACI Materials Journal*, V. 96, No. 3, May-June, pp. 297-305.

Sakashita, M.; Masuda, Y.; Nakamura, K.; Tanano, H.; Nishida, I.; and Hashimoto, T., 1997, "Deflection of Continuous Fiber Reinforced Concrete Beams Subjected to Loaded Heating," *Proceedings of the Third International Symposium on Non-Metallic (FRP) Reinforcement for Concrete Structures (FRPRCS-3)*, V. 2, Japan Concrete Institute, Tokyo, Japan, pp. 51-58.

Santoh, N., 1993, "CFCC (Carbon Fiber Composite Cable)," *Fiber-Reinforced-Plastic (FRP) Reinforcement for Concrete Structures: Properties and Applications, Developments in Civil Engineering*, V. 42, A. Nanni, ed., Elsevier, Amsterdam, pp. 223-247.

Sasaki, I.; Nishizaki, I.; Sakamoto, H.; Katawaki, K.; and Kawamoto, Y., 1997, "Durability Evaluation of FRP Cables by Exposure Tests," *Proceedings of the Third International Symposium on Non-Metallic (FRP) Reinforcement for*

*Concrete Structures (FRPRCS-3)*, V. 2, Japan Concrete Institute, Tokyo, Japan, pp. 131-137.

Scheibe, M., and Rostasy, F. S., 1998, "Stress-Rupture Behavior of AFRP Bars in Concrete and Under Natural Environment," *Second International Conference on Composites in Infrastructure*, V. II, H. Saadatmanesh and M. R. Eshani, eds., University of Arizona, Tucson, Ariz., pp. 138-151.

Seki, H.; Sekijima, K.; and Konno, T., 1997, "Test Method on Creep of Continuous Fiber Reinforcing Materials," *Proceedings of the Third International Symposium on Non-Metallic (FRP) Reinforcement for Concrete Structures (FRPRCS-3)*, V. 2, Japan Concrete Institute, Tokyo, Japan, pp. 195-202.

Sen, R.; Shahawy, M.; Sukumar, S.; and Rosas, J., 1998a, "Effect of Tidal Exposure on Bond of CFRP Rods," *Second International Conference on Composites in Infrastructure*, V. II, H. Saadatmanesh and M. R. Eshani, eds., University of Arizona, Tucson, Ariz., pp. 512-523.

Sen, R.; Shahawy, M.; Rosas, J.; and Sukumar, S., 1998b, "Durability of Aramid Pretensioned Elements in a Marine Environment," *ACI Structural Journal*, V. 95, No. 5, Sept.-Oct., pp. 578-587.

Shield, C.; French, C.; and Hanus, J., 1999, "Bond of GFRP Rebar for Consideration in Bridge Decks," *Fourth International Symposium on Fiber Reinforced Polymer Reinforcement for Reinforced Concrete Structures*, SP-188, C. W. Dolan, S. H. Rizkalla, and A. Nanni, eds., American Concrete Institute, Farmington Hills, Mich., pp. 393-406.

Shield, C.; French, C.; and Retika, A., 1997, "Thermal and Mechanical Fatigue Effects on GFRP Rebar-Concrete Bond," *Proceedings of the Third International Symposium on Non-Metallic (FRP) Reinforcement for Concrete Structures (FRPRCS-3)*, V. 2, Japan Concrete Institute, Tokyo, Japan, pp. 381-388.

Sippel, T. M., and Mayer, U., 1996, "Bond Behavior of FRP Strands under Short-Term, Reversed and Cyclic Loading," *Proceedings of the Second International Conference on Advanced Composite Materials in Bridges and Structures (ACMBS-2)*, M. M. El-Badry, ed., Canadian Society for Civil Engineering, Montreal, Québec, Canada, pp. 837-844.

Sonobe, Y.; Fukuyama, H.; Okamoto, T.; Kani, N.; Kobayashi, K.; Masuda, Y.; Matsuzaki, Y.; Mochizuki, S.; Nagasaka, T.; Shimizu, A.; Tanano, H.; Tanigaki, M.; and Tenshigawara, M., 1997, "Design Guidelines of FRP Reinforced Concrete Building Structures," *Journal of Composites for Construction*, V. 1, No. 3, pp. 90-113.

Szerszen, M., and Nowak, A., 2003, "Calibration of Design Code for Buildings (ACI 318): Part 2—Reliability Analysis and Resistance Factors," *ACI Structural Journal*, V. 100, No. 3, May-June, pp. 383-391.

Tadros, G.; Tromposch, E.; and Mufti, A., 1998, "University Drive/Crowchild Trail Bridge Superstructure Replacement," *Proceedings of the Second International Conference on Composites in Infrastructure (ICCI-98)*, V. 1, Tucson, Ariz., pp. 693-704.

Taerwe, L., ed., 1995, "Non-Metallic (FRP) Reinforcement for Concrete Structures," *Proceedings of the Second International RILEM Symposium on Non-Metallic (FRP) Reinforcement for Concrete Structures (FRPRCS-2)*, Ghent, Belgium, 714 pp.

Taerwe, L., 1997, "FRP Activities in Europe: Survey of Research and Applications," *Proceedings of the Third International Symposium on Non-Metallic (FRP) Reinforcement for Concrete Structures (FRPRCS-3)*, V. 1, Japan Concrete Institute, Tokyo, Japan, pp. 59-74.

Takewaka, K., and Khin, M., 1996, "Deterioration of Stress-Rupture of FRP Rods in Alkaline Solution Simulating as Concrete Environment," *Advanced Composite Materials in Bridges and Structures*, M. M. El-Badry, ed., Canadian Society for Civil Engineering, Montreal, Québec, Canada, pp. 649-664.

Tamura, T., 1993, "FiBRA," *Fiber-Reinforced-Plastic (FRP) Reinforcement for Concrete Structures: Properties and Applications, Developments in Civil Engineering*, V. 42, A. Nanni, ed., Elsevier, Amsterdam, pp. 291-303.

Tannous, F. E.; and Saadatmanesh, H., 1999, "Durability of AR-Glass Fiber Reinforced Plastic Bars," *Journal of Composites for Construction*, V. 3, No. 1, pp. 12-19.

Teng, J.-G., ed., 2001, "FRP Composites in Civil Engineering," *Proceedings CICE 2001*, Hong Kong, China, V. 1 and 2.

Tepfers R., 2002, "Test System for Evaluation of Bond Properties of FRP Reinforcement in Concrete," *Proceedings of the Third International Symposium on Bond in Concrete—from Research to Standards*, Budapest, Hungary, Nov. 20-22, 2002, pp. 657-666.

Theriault, M., and Benmokrane, B., 1998, "Effects of FRP Reinforcement Ratio and Concrete Strength on Flexural Behavior of Concrete Beams," *Journal of Composites for Construction*, V. 2, No. 1, pp. 7-16.

Tighiouart, B.; Benmokrane, B.; and Gao, D., 1998, "Investigation of Bond in Concrete Member with Fiber Reinforced Polymer (FRP) Bars," *Construction and Building Materials Journal*, Dec. 1998, p. 10.

Tighiouart, B.; Benmokrane, B.; and Mukhopadhyaya, P., 1999, "Bond Strength of Glass FRP Rebar Splices in Beams Under Static Loading," *Construction and Building Materials*, V. 13, No. 7, pp. 383-392.

Tokyo Rope, 2000, "CFCC, Carbon Fiber Composite Cable," *Product Circular* No. 991-2T-SA, Tokyo Rope Manufacturing Co., Tokyo. (http://www.tokyorope.co.jp/).

Tomosawa, F., and Nakatsuji, T., 1996, "Evaluation of the ACM Reinforcement Durability by Exposure Test," *Advanced Composite Materials in Bridges and Structures*, M. M. El-Badry, ed., Canadian Society for Civil Engineering, Montreal, Québec, Canada, pp. 699-706.

Tomosawa, F., and Nakatsuji, T., 1997, "Evaluation of the ACM Reinforcement Durability by Exposure Test," *Proceedings of the Third International Symposium on Non-Metallic (FRP) Reinforcement for Concrete Structures (FRPRCS-3)*, V. 2, Japan Concrete Institute, Tokyo, Japan, pp. 139-146.

Toutanji, H., and Saafi, M., 2000, "Flexural Behavior of Concrete Beams Reinforced with Glass Fiber-Reinforced Polymer (GFRP) Bars," *ACI Structural Journal*, V. 97, No. 5, Sept.-Oct., pp. 712-719.

Tureyen, A. K., and Frosch, R. J., 2002, "Shear Tests of FRP Reinforced Concrete Beams without Stirrups," *ACI Structural Journal*, V. 99, No. 4, July-Aug. 2002, pp. 427-434.

Tureyen, A. K., and Frosch, R. J., 2003, "Concrete Shear Strength: Another Perspective," *ACI Structural Journal*, V. 100, No. 5, Sept.-Oct. 2003, pp. 609-615.

Uomoto, T., 2000, "Durability of FRP as Reinforcement for Concrete Structures," *Proceedings of the 3rd International Conference on Advanced Composite Materials in Bridges and Structures, ACMBS-3*, J. L. Humar and A. G. Razaqpur, eds., Canadian Society for Civil Engineering, Montreal, Québec, Canada, pp. 3-17.

Uppuluri, V. S.; Bakis, C. E.; Nanni, A.; and Boothby, T. E., 1996, "Analysis of the Bond Mechanism in FRP Reinforcement Rods: The Effect of Rod Design and Properties," *Proceedings of the Second International Conference on Advanced Composite Materials in Bridges and Structures (ACMBS-II)*, Montreal, Québec, Canada, pp. 893-900.

Vijay, P. V., and GangaRao, H. V. S., 1999, "Accelerated and Natural Weathering of Glass Fiber Reinforced Plastic Bars," *Fourth International Symposium on Fiber Reinforced Polymer Reinforcement for Reinforced Concrete Structures*, SP-188, C. W. Dolan, S. H. Rizkalla, and A. Nanni, eds., American Concrete Institute, Farmington Hills, Mich., pp. 605-614.

Vijay, P. V.; GangaRao, H. V. S.; and Kalluri, R., 1998, "Hygrothermal Response of GFRP Bars under Different Conditioning Schemes," *Proceedings of the First International Conference (CDCC 1998)*, Sherbrooke, Canada, pp. 243-252.

Wallenberger, F. T.; Watson, J. C.; and Hong, L., 2001, "Glass Fibers," *ASM Handbook*, V. 21, Composites, ASM International, Material Park, Ohio, pp. 27-34.

Walsh, P. J., 2001, "Carbon Fibers," *ASM Handbook*, V. 21, Composites, ASM International, Material Park, Ohio, pp. 35-40.

Wambeke, B., and Shield, C., 2006, "Development Length of Glass Fiber Reinforced Polymer Bars in Concrete," *ACI Structural Journal*, V. 103, No. 1, Jan.-Feb., pp. 11-17.

Wang, J., 1998, "Determination of the Shear Resistance of Concrete Beams and Slabs Reinforced with Fibre Reinforced Plastics," MS thesis, Carleton University, Ottawa, Canada.

Wang, N., and Evans, J. T., 1995, "Collapse of Continuous Fiber Composite Beam at Elevated Temperatures," *Composites*, V. 26, No. 1, pp. 56-61.

White, T. D., ed., 1992, "Composite Materials and Structural Plastics in Civil Engineering Construction," *Proceedings of the Materials Engineering Congress*, American Society of Civil Engineers, New York, pp. 532-718.

Wu, W. P., 1990, "Thermomechanical Properties of Fiber Reinforced Plastic (FRP) Bars," PhD dissertation, West Virginia University, Morgantown, W.Va., 292 pp.

Yamaguchi, T.; Kato, Y.; Nishimura, T.; and Uomoto, T., 1997, "Creep Rupture of FRP Rods Made of Aramid, Carbon and Glass Fibers," *Proceedings of the Third International Symposium on Non-Metallic (FRP) Reinforcement for Concrete Structures (FRPRCS-3)*, V. 2., Japan Concrete Institute, Tokyo, Japan, pp. 179-186.

Ye, L. P.; Feng, P.; Zhang, K.; Lin, L.; Hong, W. H.; Yue, Q. R.; Zhang, N.; and Yang, T., 2003, "FRP in Civil Engineering in China: Research and Applications," *Proceedings of the Sixth International Symposium on FRP Reinforcement for Concrete Structures (FRPRCS-6)*, K. H. Tan, ed., Singapore, p. 1401.

Yost, J.; Gross, S.; and Dinehart, D., 2003, "Effective Moment of Inertia for GFRP Reinforced Concrete Beams," *ACI Structural Journal*, V. 100, No. 6, Nov.-Dec., pp. 732-739.

Zhao, W.; Maruyama, K.; and Suzuki, H., 1995, "Shear Behavior of Concrete Beams Reinforced by FRP Rods as Longitudinal and Shear Reinforcement," *Proceedings of the Second International RILEM Symposium on Non-Metallic (FRP) Reinforcement for Concrete Structures (FRPRCS-2)*, Ghent, Belgium, pp. 352-359.

Zhao, W.; Pilakoutas, K.; and Waldron, P., 1997, "FRP Reinforced Concrete Beams: Calculations for Deflection," *Proceedings of the Third International Symposium on Non-Metallic (FRP) Reinforcement for Concrete Structures (FRPCS-3)*, V. 2, Japan Concrete Institute, Tokyo, Japan, pp. 511-518.

## CHAPTER 13—BEAM DESIGN EXAMPLE

This example of beam design follows the ultimate strength approach described in this document and includes the load factors according to ACI 318-05.

A simply supported, normalweight concrete beam with $f'_c$ = 4000 psi (27.6 MPa) is needed in a medical facility to support an MRI unit. The beam is an interior beam. The beam is to be designed to carry a service live load of $w_{LL}$ = 400 lb/ft (5.8 kN/m) (20% sustained) and a superimposed service dead load of $w_{SDL}$ = 208 lb/ft (3.0 kN/m) over a span of $\ell$ = 11 ft (3.35 m). The beam deflection should not exceed $\ell$/240, which is the limitation for long-term deflection. Due to construction restriction, the depth of the member should not exceed 14 in. (356 mm). GFRP reinforcing bars are selected to reinforce the beam; material properties of the bars (as reported by the bar manufacturer) are shown in Table 13.1.

**Table 13.1—Manufacturer's reported GFRP bar properties**

| | | |
|---|---|---|
| Tensile strength $f^*_{fu}$ | 90,000 psi | 620.6 MPa |
| Rupture strain $\varepsilon^*_{fu}$ | 0.014 | 0.014 |
| Modulus of elasticity $E_f$ | 6,500,000 psi | 44,800 MPa |

The design procedure presented hereafter is equally applicable to CFRP and AFRP bars, with use of appropriate manufacturer's reported material properties similar to Table 13.1.

| Procedure | Calculation in U.S. units | Calculation in SI units |
|---|---|---|
| **Step 1—Estimate the appropriate cross-sectional dimensions of the beam.** An initial value for the depth of a simply supported reinforced concrete beam can be estimated from Table 8.2. | | |
| $h = \frac{\ell}{10}$ | $h = \frac{(11\text{ ft})\left(12\frac{\text{in.}}{\text{ft}}\right)}{10} = 13.2\text{ in.}$ | $h = \frac{3.35\text{ m}}{10} = 0.335\text{ m}$ |
| Recognizing that the values suggested in the table are meant only to be a starting point for design, try $h$ = 12 in. | Try $h$ = 12 in. < 13.2 in. | Try $h$ = 305 mm < 335 mm |
| | Assuming No. 5 bars for main = 5/8 in. = 0.625 in.<br>Assuming No. 3 bars for shear = 3/8 in. = 0.375 in.<br>Cover = 1.5 in. | Assuming ϕ16 mm bars for main<br>Assuming ϕ9.5 mm bars for shear<br>Cover = 38 mm |
| An effective depth of the section is estimated using 1-1/2 in. clear cover | A minimum width of approximately 7 in. is required when using two No. 5 or two No. 6 bars with No. 3 stirrups<br>Try $b$ = 7 in. | A minimum width of approximately 178 mm is required when using two ϕ16 or two ϕ19 bars with ϕ9.5 stirrups<br>Try $b$ = 0.178 m |
| Estimated $d = h - \text{cover} - d_{b,shear} - \frac{d_b}{2}$ | Estimated $d = 12 - 1.5 - 0.375 - \frac{0.625}{2} = 9.81\text{ in.}$ | Estimated $d = 305\text{ mm} - 38\text{ mm} - 9.5\text{ mm} - \frac{16\text{ mm}}{2}$<br>$= 250\text{ mm}$ |
| **Step 2—Compute the factored load.** The uniformly distributed dead load can be computed including the self-weight of the beam. | | |
| $w_{DL} = w_{SDL} + w_{SW}$ | $w_{DL} = 208\frac{\text{lb}}{\text{ft}} + \frac{(7\text{ in.})(12\text{ in.})}{\left(12\frac{\text{in.}}{\text{ft}}\right)^2}\left(150\frac{\text{lb}}{\text{ft}^2}\right) = 295.5\frac{\text{lb}}{\text{ft}}$ | $w_{DL} = (3.0\text{ kN/m}) + (0.178\text{ m})(0.305\text{ m})(24\text{ kN/m}^3) = 4.3\text{ kN/m}$ |
| Compute the factored uniform load and ultimate moment | $w_u = 1.2\left(295.5\frac{\text{lb}}{\text{ft}}\right) + 1.6\left(400\frac{\text{lb}}{\text{ft}}\right) = 995\frac{\text{lb}}{\text{ft}}$ | $w_u = 1.2(4.3\text{ kN/m}) + 1.7(5.8\text{ kN/m})$<br>$w_u = 14.4\text{ kN/m}$ |
| $w_u = 1.4w_{DL} + 1.6w_{LL}$<br>$M_u = \frac{w_u\ell^2}{8}$ | $M_u = \frac{\left(995\frac{\text{lb}}{\text{ft}}\right)(11\text{ ft}^2)}{8} \cdot \frac{1\text{ kip}}{1000\text{ lb}} = 15.04\text{ kip·ft}$ | $M_u = \frac{(14.4\text{ kN/m})(3.35\text{ m})^2}{8} = 20.2\text{ kN·m}$ |
| **Step 3—Compute the design rupture stress of the FRP bars.** The beam will be located in an interior conditioned space. Therefore, for glass FRP bars, an environmental reduction factor $C_E$ of 0.80 is as per Table 7.1. | | |
| $f_{fu} = C_E f^*_{fu}$ | $f_{fu}$ = (0.80)(90 ksi) = 72 ksi | $f_{fu}$ = (0.80)(620.6 MPa) = 496 MPa |
| **Step 4—Determine the area of GFRP bars required for flexural strength.** Find the reinforcement ratio required for flexural strength by trial and error using Eq. (8-1), (8-4d), and (8-5). | | |
| Assume an initial amount of FRP reinforcement | Try two No. 5 bars | Try two ϕ16 bars |

| Procedure | Calculation in U.S. units | Calculation in SI units |
|---|---|---|
| Computed the balanced FRP reinforcement ratio<br>$\rho_{fb} = 0.85\frac{f'_c}{f_{fu}}\beta_1\frac{E_f\varepsilon_{cu}}{E_f\varepsilon_{cu}+f_{fu}}$ | $\rho_{fb} = 0.85\frac{4}{72}0.85\frac{(6500)(0.003)}{(6500)(0.003)+72} = 0.0086$ | $\rho_{fb} = 0.85\frac{27.6\text{ MPa}}{496\text{ MPa}}0.85\frac{(44{,}800\text{ MPa})(0.003)}{(44{,}800\text{ MPa})(0.003)+(496\text{ MPa})}$<br>$\rho_{fb} = 0.0086$ |
| $\rho_f = \frac{A_f}{bd}$ | $\rho_f = \frac{(0.62\text{ in.}^2)}{(7\text{ in.})(9.81\text{ in.})} = 0.009$ | $\rho_f = \frac{(400\text{ mm}^2)}{(178\text{ mm})(250\text{ mm})} = 0.009$ |
| $f_f = \left[\sqrt{\frac{(E_f\varepsilon_{cu})^2}{4}+\frac{0.85\beta_1 f'_c}{\rho_f}E_f\varepsilon_{cu}}-0.5E_f\varepsilon_{cu}\right]$ | | |
| Setting<br>$A = \frac{(E_f\varepsilon_{cu})^2}{4}$ | $A = \frac{(6500(0.003))^2}{4} = 95.06$ | $A = \frac{((44{,}800\text{ MPa})(0.003))^2}{4} = 4516$ |
| $B = \frac{0.85\beta_1 f'_c}{\rho_f}E_f\varepsilon_{cu}$ | $B = \frac{0.85(0.85)(4)}{(0.009)}(6500)(0.003) = 6262$ | $B = \frac{0.85(0.85)(27.6\text{ MPa})}{(0.009)}(44{,}800\text{ MPa})(0.003) = 297{,}800$ |
| $C = 0.5E_f\varepsilon_{cu}$ | $C = 0.5(6500)(0.003) = 9.75$ | $C = 0.5(44{,}800\text{ MPa})(0.003) = 67.2$ |
| Then<br>$f_f = [\sqrt{A+B}-C]$ | $f_f = \sqrt{95.06+6262}-9.75 = 70$ ksi | $f_f = \sqrt{4516+297{,}800}-67.2 = 483$ MPa |
| $M_n = \rho_f f_f\left(1-0.59\frac{\rho_f f_f}{f'_c}\right)bd^2$ | $M_n = (0.009)(70)\left(1-0.59\frac{(0.009)(70)}{(4)}\right)$<br>$(7)(9.81)^2/12 = 32.08$ kip·ft | $M_n = (0.009)(483\text{ MPa})\left(1-0.59\frac{(0.009)(483\text{ MPa})}{(27.6\text{ MPa})}\right)$<br>$(178\text{ mm})(250\text{ mm})^2 = 43.9$ kN·m |
| Compute the strength reduction factor<br>$\phi = 0.30\frac{\rho_f}{4\rho_{fb}}$ for $\rho_{fb} < \rho_f \le 1.4\rho_{fb}$ | $\phi = 0.30+\frac{0.009}{4(0.0086)} = 0.562$ | $\phi = 0.30+\frac{0.009}{4(0.0086)} = 0.562$ |
| Check $\phi M_n \ge M_u$ | $\phi M_n = (0.562)(32\text{ kip·ft})$<br>$\phi M_n = 17.98\text{ kip·ft} \ge M_u = 15.04\text{ kip·ft}$ | $\phi M_n = (0.562)(43.9\text{ kN·m})$<br>$\phi M_n = 24.7\text{ kN·m} \ge M_u = 20.2\text{ kN·m}$ |
| **Step 5—Check the crack width.**<br>Compute the stress level in the FRP bars under dead load plus live load. | | |
| $M_{DL} = \frac{\omega_{DL}\ell^2}{8}$ | $M_{DL} = \frac{\left(295.5\frac{\text{lb}}{\text{ft}}\right)(11\text{ ft}^2)}{8}\cdot\frac{1\text{ kip}}{1000\text{ lb}} = 4.47$ kip·ft | $M_{DL} = \frac{4.3(3.35)^2}{8} = 6.03$ kN·m |
| $M_{LL} = \frac{\omega_{LL}\ell^2}{8}$ | $M_{LL} = \frac{\left(400\frac{\text{lb}}{\text{ft}}\right)(11\text{ ft}^2)}{8}\cdot\frac{1\text{ kip}}{1000\text{ lb}} = 6.05$ kip·ft | $M_{LL} = \frac{5.8(3.35)^2}{8} = 8.14$ kN·m |
| $M_{DL+LL} = M_{DL}+M_{LL}$ | $M_{DL+LL} = 4.47+6.05 = 10.5$ kip·ft | $M_{DL+LL} = 6.03+8.14 = 14.17$ kN·m |
| $n_f = \frac{E_f}{E_c} = \frac{E_f}{57{,}000\sqrt{f'_c}}$ (U.S.) | $n_f = \frac{6{,}500{,}000\text{ psi}}{57{,}000\sqrt{4000\text{ psi}}} = 1.8$ | |
| $n_f = \frac{E_f}{E_c} = \frac{E_f}{4750\sqrt{f'_c}}$ (SI) | | $n_f = \frac{44{,}800\text{ MPa}}{4750\sqrt{27.6\text{ MPa}}} = 1.8$ |
| $k = \sqrt{2\rho_f n_f+(\rho_f n_f)^2}-\rho_f n_f$ | $k = \sqrt{2(0.009)(1.8)+[(0.009)(1.8)]^2}$<br>$-(0.009)(1.8) = 0.165$ | $k = \sqrt{2(0.009)(1.8)+[(0.009)(1.8)]^2}$<br>$-(0.009)(1.8) = 0.165$ |
| $f_f = \frac{M_{DL+LL}}{A_f d(1-k/3)}$ | $f_f = \frac{(10.5\text{ kip·ft})(12\text{ in./ft})}{(0.62\text{ in.}^2)(9.81\text{ in.})(1-0.165/3)} = 21.9$ ksi | $f_f = \frac{14.17\times10^6\text{ N·m}}{(400\text{ mm}^2)(250\text{ mm})(1-0.165/3)} = 149.9$ MPa |

| Procedure | Calculation in U.S. units | Calculation in SI units |
|---|---|---|
| Determine the strain gradient used to transform reinforcement level strains to the near surface of the beam where cracking is expected. $\beta = \frac{h-kd}{d(1-k)}$ | $\beta = \frac{12\text{ in.} - (0.165)(9.81\text{ in.})}{(9.81\text{ in.})(1-0.165)} = 1.267$ | $\beta = \frac{305\text{ mm} - (0.165)(250\text{ mm})}{(250\text{ mm})(1-0.165)} = 1.263$ |
| Calculate the distance from the extreme tension fiber of the concrete to the centerline of the flexural reinforcement. $d_c = h - d$ | $d_c = (12\text{ in.}) - (9.81\text{ in.}) = 2.19\text{ in.}$ | $d_c = 305\text{ mm} - 250\text{ mm} = 55\text{ mm}$ |
| Calculate bar spacing $s$. $s = b - 2d_c$ | $s = 7\text{ in.} - 2(2.19\text{ in.}) = 2.62\text{ in.}$ | $s = 178\text{ mm} - 2(55\text{ mm}) = 68\text{ mm}$ |
| Compare the crack width from Eq. (8-9) using the recommended value of $k_b = 1.4$ for deformed FRP bars. $w = 2\frac{f_f}{E_f}\beta k_b\sqrt{d_c^2 + \left(\frac{s}{2}\right)^2}$ | $w = 2\frac{(21.9\text{ ksi})}{(6500\text{ ksi})}(1.267)(1.4)$ $\sqrt{(2.19\text{ in.})^2 + \left(\frac{2.62\text{ in.}}{2}\right)^2} = 37\text{ mils} > 28\text{ mils}\ \therefore$ **n.g.** | $w = 2\frac{(149.9\text{ MPa})}{(44{,}800\text{ MPa})}(1.263)(1.4)$ $\sqrt{(55\text{ mm})^2 + \left(\frac{68\text{ mm}}{2}\right)^2} = 0.77\text{ mm} > 0.7\text{ mm}\ \therefore$ **n.g.** |
| Crack width limitation controls the design. Try larger amount of FRP reinforcement. | Note that it is preferable to use bars with smaller diameters to mitigate cracking. For example, using three No. 4 bars will result in approximately the same area of FRP and nearly the same effective depth; however, the width of the member would need to be increased. To maintain $b = 7.0$ in. Try two No. 6 $\rightarrow A_f = 0.88\text{ in.}^2$ | Note that it is preferable to use bars with smaller diameters to mitigate cracking. For example, using three $\phi$12.7 bars will result in approximately the same area of FRP and nearly the same effective depth; however, the width of the member would need to be increased. To maintain $b = 0.178$ mm Try $2\phi19 \rightarrow A_f = 567\text{ mm}^2$ |
| Estimated $d = h - \text{cover} - d_{b,shear} - \frac{d_b}{2}$ | Estimated $d = 12 - 1.5 - 0.375 - \frac{0.75}{2} = 9.75$ in. | Estimated $d = 305 - 38 - 9.5 - \frac{19}{2} = 248$ mm |
| $\rho_f = \frac{A_f}{bd}$ | $\rho_f = \frac{(0.88\text{ in.}^2)}{(0.7\text{ in.})(9.75\text{ in.})} = 0.0129$ | $\rho_f = \frac{(567\text{mm}^2)}{(178\text{ mm})(248\text{ mm})} = 0.0128$ |
| Calculate the new capacity. $f_f = \left[\sqrt{\frac{(E_f\varepsilon_{cu})^2}{4} + \frac{0.85\beta_1 f_c'}{\rho_f}E_f\varepsilon_{cu}} - 0.5E_f\varepsilon_{cu}\right]$ | | |
| Setting $A = \frac{(E_f\varepsilon_{cu})^2}{4}$ | $A = \frac{(6500(0.003))^2}{4} = 95.06$ | $A = \frac{((44{,}800\text{ MPa})(0.003))^2}{4} = 4516$ |
| $B = \frac{0.85\beta_1 f_c'}{\rho_f}E_f\varepsilon_{cu}$ | $B = \frac{0.85(0.85)(4)}{(0.0129)}(6500)(0.003) = 4369$ | $B = \frac{0.85(0.85)(27.6\text{ MPa})}{(0.0128)}(44{,}800\text{ MPa})(0.003) = 209{,}400$ |
| $C = 0.5E_f\varepsilon_{cu}$ | $C = 0.5(6500)(0.003) = 9.75$ | $C = 0.5(44{,}800\text{ MPa})(0.003) = 67.2$ |
| Then $f_f = [\sqrt{A+B} - C]$ | $f_f = \sqrt{95.06 + 4369} - 9.75 = 57.1$ ksi | $f_f = \sqrt{4516 + 209{,}400} - 67.2 = 395.3$ MPa |
| $M_n = \rho_f f_f\left(1 - 0.59\frac{\rho_f f_f}{f_c'}\right)bd^2$ | $M_n = (0.0129)(57.1)\left(1 - 0.59\frac{(0.0129)(57.1)}{(4)}\right)$ $(7)(9.75)^2 = 36.4$ kip·ft | $M_n = (0.0128)(395.3)\left(1 - 0.59\frac{(0.0128)(395.3)}{(27.6)}\right)$ $(178)(248)^2 = 49.4$ kN·m |
| $\phi = 0.65$ for $\rho_f \geq 1.4\rho_{fb}$ | $\rho_f = 0.0129 > 1.4\rho_{fb} = 0.012 \rightarrow \phi = 0.65$ | $\rho_f = 0.0128 > 1.4\rho_{fb} = 0.012 \rightarrow \phi = 0.65$ |
| Check $\phi M_n \geq M_u$ | $\phi M_n = (0.65)(36.4\text{ kip·ft})$ $\phi M_n = 23.7\text{ kip·ft} \geq M_u = 16.5\text{ kip·ft}$ | $\phi M_n = (0.65)(49.4\text{ kN·m})$ $\phi M_n = 32.1\text{ kN·m} \geq M_u = 22.3\text{ kN·m}$ |
| $k = \sqrt{2\rho_f n_f + (\rho_f n_f)^2} - \rho_f n_f$ | $k = \sqrt{2(0.0129)(1.8) + [(0.0129)(1.8)]^2}$ $- (0.0129)(1.8) = 0.194$ | $k = \sqrt{2(0.0128)(1.8) + [(0.0128)(1.8)]^2}$ $- (0.0128)(1.8) = 0.193$ |
| $f_f = \frac{M_{DL+LL}}{A_f d(1-k/3)}$ | $f_f = \frac{(10.5\text{ kip·ft})(12\text{in./ft})}{(0.88\text{in.}^2)(9.75\text{in.})(1-0.194/3)} = 15.7$ ksi | $f_f = \frac{14.17\times10^{-6}\text{ N·mm}}{(567\text{mm}^2)(248\text{mm})(1-0.193/3)}$ $= 107.7$ MPa |
| $\beta = \frac{h-kd}{d(1-k)}$ | $\beta = \frac{12\text{ in.} - (0.194)(9.75\text{ in.})}{(9.75\text{ in.})(1-0.194)} = 1.286$ | $\beta = \frac{305\text{ mm} - (0.193)(248\text{ mm})}{(248\text{ mm})(1-0.193)} = 1.285$ |
| $d_c = h - d$ | $d_c = (12\text{ in.}) - (9.75\text{ in.}) = 2.25\text{ in.}$ | $d_c = (305\text{ mm}) - (248\text{ mm}) = 57\text{ mm}$ |

| Procedure | Calculation in U.S. units | Calculation in SI units |
|---|---|---|
| Calculate bar spacing $s$. $s = b - 2d_c$ | $s = 7$ in. $- 2(2.25$ in.$) = 2.5$ in. | $s = 178$ mm $- 2(57$ mm$) = 64$ mm |
| Compare the crack width from Eq. (8-9) to the design limit using the default value of $k_b = 1.4$ for deformed FRP bars. $w = 2\frac{f_f}{E_f}\beta k_b\sqrt{d_c^2 + \left(\frac{s}{2}\right)^2}$ | $w = 2\frac{(15.7\text{ ksi})}{(6500\text{ ksi})}(1.286)(1.4)\sqrt{(2.25\text{ in.})^2 + \left(\frac{2.5\text{ in.}}{2}\right)^2} = 22$ mils $< 28$ mils $\therefore$ **OK** | $w = 2\frac{(107.7\text{ MPa})}{(44{,}800\text{ MPa})}(1.285)(1.4)\sqrt{(57\text{ mm})^2 + \left(\frac{64\text{ mm}}{2}\right)^2} = 0.57$ mm $< 0.7$ mm $\therefore$ **OK** |
| **Step 6—Check the long-term deflection of the beam** Compute the gross moment of inertia for the section. $I_g = \frac{bh^3}{12}$ | $I_g = \frac{(7\text{ in.})(12\text{ in.})^3}{12} = 1008\text{ in.}^4$ | $I_g = \frac{(178\text{ mm})(305\text{ mm})^3}{12} = 4.209 \times 10^8\text{ mm}^4$ |
| Calculate the cracked section properties and cracking moment. $f_r = 7.5\sqrt{f'_c}$ (U.S.) $f_r = 0.62\sqrt{f'_c}$ (SI) | $f_r = 7.5\sqrt{4000\text{ psi}} = 474$ psi | $f_r = 0.62\sqrt{27.6}\text{ MPa} = 3.26$ MPa |
| $M_{cr} = \frac{2f_r I_g}{h}$ | $M_{cr} = \frac{2(474.34\text{ psi})(1008\text{ in.}^4)}{12\text{ in.}}\frac{1}{12{,}000\text{ in.-lb}} = 6.6$ kip·ft | $M_{cr} = \frac{2(3.26)(4.209 \times 10^8)}{305} = 9.00$ kN·m |
| $I_{cr} = \frac{bd^3}{3}k^3 + n_f A_f d^2(1-k)^2$ | $I_{cr} = \frac{(7\text{ in.})(9.75\text{ in.})^3}{3}(0.194)^3 + 1.8(0.88\text{ in.}^2)(9.75\text{ in.}^2)^2(1-0.194)^2 = 114\text{ in.}^4$ | $I_{cr} = \frac{(178)(248)^3}{3}(0.193)^3 + 1.8(567)(248)^2(1-0.193)^2 = 4.74 \times 10^7\text{ mm}^4$ |
| Compute the modification factor $\beta_d$. $\beta_d = \frac{1}{5}\left[\frac{\rho_f}{\rho_{fb}}\right]$ | $\beta_d = \frac{1}{5}\left[\frac{0.0129}{0.0086}\right] = 0.30$ | $\beta_d = \frac{1}{5}\left[\frac{0.0128}{0.0086}\right] = 0.30$ |
| Compute the deflection due to dead load plus live load. $(I_e)_{DL+LL} = \left(\frac{M_{cr}}{M_a}\right)^3\beta_d I_g + \left[1 - \left(\frac{M_{cr}}{M_a}\right)^3\right]I_{cr}$ | $(I_e)_{DL+LL} = \left(\frac{6.6}{10.5}\right)^3(0.30)(1008) + \left[1 - \left(\frac{6.6}{10.5}\right)^3\right](114) = 160.8\text{ in.}^4$ | $(I_e)_{DL+LL} = \left(\frac{9.00}{14.17}\right)^3(0.30)(4.209 \times 10^8) + \left[1 - \left(\frac{9.00}{14.17}\right)^3\right](4.74 \times 10^7) = 6.76 \times 10^7\text{ mm}^4$ |
| $(\Delta_i)_{DL+LL} = \frac{5M_{DL+LL}\ell^2}{48E_c(I_e)_{DL+LL}}$ | $(\Delta_i)_{DL+LL} = \frac{5(10.5\text{ kip·in.})(11\text{ ft})^2\left(12\frac{\text{in.}}{\text{ft}}\right)^3}{48(3605\text{ ksi})(160.8\text{ in.}^4)} = 0.39$ in. | $(\Delta_i)_{DL} = \frac{5(14.17 \times 10^6\text{ N·mm})(3350\text{ mm})^2}{48(2.49 \times 10^4\text{ mm})(6.67 \times 10^7\text{ mm}^4)} = 10$ mm |
| Compute the deflection due to dead load alone and live load alone. $(\Delta_i)_{DL} = \frac{w_{DL}}{w_{DL+LL}}(\Delta_i)_{DL+LL}$ | $(\Delta_i)_{DL} = \frac{295.5\text{ lb/ft}}{295.5\text{ lb/ft} + 400\text{ lb/ft}}(0.39\text{ in.}) = 0.17$ in. | $(\Delta_i)_{DL} = \frac{4.3\text{ kN/m}}{4.3\text{ kN/m} + 5.8\text{ kN/m}}(10\text{ mm}) = 4.3$ mm |
| $(\Delta_i)_{LL} = \frac{w_{LL}}{w_{DL+LL}}(\Delta_i)_{DL+LL}$ | $(\Delta_i)_{LL} = \frac{400\text{ lb/ft}}{295.5\text{ lb/ft} + 400\text{ lb/ft}}(0.39\text{ in.}) = 0.22$ in. | $(\Delta_i)_{LL} = \frac{5.8\text{ kN/m}}{4.3\text{ kN/m} + 5.8\text{ kN/m}}(10\text{ mm}) = 5.7$ mm |
| Compute the multiplier for time-dependent deflection using a $\xi = 2.0$ (recommended by ACI 318 for a duration of more than 5 years). $\lambda = 0.60\xi$ | $\lambda = 0.60(2.0) = 1.2$ | $\lambda = 0.60(2.0) = 1.2$ |
| Compute the long-term deflection (initial deflection due to live load plus the time-dependent deflection due to sustained loads). $\Delta_{LT} = (\Delta_i)_{LL} + \lambda[(\Delta_i)_{DL} + 0.20(\Delta_i)_{LL}]$ | $\Delta_{LT} = (0.22\text{ in.}) + 1.2[(0.17\text{ in.}) + 0.2(0.22\text{ in.})] = 0.48$ in. | $\Delta_{LT} = (5.7\text{ mm}) + 1.2[(4.3\text{ mm}) + 0.2(5.7\text{ mm})] = 12.2$ mm |
| Check computed deflection against deflection limitations. $\Delta_{LT} \le \frac{\ell}{240}$ | $0.48\text{ in.} < \frac{(11\text{ ft})\left(12\frac{\text{in.}}{\text{ft}}\right)}{240} = 0.55\text{ in.}$ **OK** | $12.2\text{ mm} < \frac{3350\text{ mm}}{240} = 14$ mm **OK** |

| Procedure | Calculation in U.S. units | Calculation in SI units |
|---|---|---|
| **Step 7—Check the creep rupture stress limits.** Compute the moment due to all sustained loads (dead load plus 20% of the live load). | | |
| $M_s = \frac{w_{DL} + 0.20 w_{LL}}{w_{DL} + w_{LL}} M_{DL+LL}$ | $M_s = \frac{295.5 \text{ lb/ft} + 0.20 \cdot 400 \text{ lb/ft}}{295.5 \text{ lb/ft} + 400 \text{ lb/ft}} 10.5 \text{ kip·ft}$ = 5.67 kip·ft | $M_s = \frac{4.3 \text{kN/m} + 0.20 \cdot 5.8 \text{ kN/m}}{4.3 \text{kN/m} + 5.8 \text{ kN/m}} 14.17 \text{ kN·m}$ = 7.66 kN·m |
| Compute the sustained stress level in the FRP bars. | | |
| $f_{f,s} = \frac{M_s}{A_f d(1 - k/3)}$ | $f_{f,s} = \frac{(5.67 \text{ kip·ft})(12 \text{ in./ft})}{(0.88 \text{ in.}^2)(9.75 \text{ in.})(1 - 0.194/3)} = 8.47 \text{ ksi}$ | $f_{f,s} = \frac{7.66 \times 10^6 \text{ N·mm}}{(567 \text{mm}^2)(248 \text{ mm})(1 - 0.193/3)}$ = 58.2 MPa |
| Check the stress limits given in Table 8.2 for glass FRP bars. | | |
| $f_{f,s} \le 0.20 f_{fu}$ | 8.52 ksi ≤ 0.20(72 ksi) = 14.4 ksi | 58.2 MPa ≤ 0.20(496) = 99.2 MPa |
| **Step 8—Design for shear.** Determine the factored shear demand at a distance $d$ from the support. | | |
| $V_u = \frac{w_u \ell}{2} - w_u d$ | $V_u = \frac{(995 \text{lb/ft})(11 \text{ ft})}{2} - (995 \text{ lb/ft})\left(\frac{9.75 \text{ in.}}{12 \text{ in./ft}}\right)$ = 4664 lb = 4.66 kips | $V_u = \frac{(14.4 \text{ kN/m})(3.35 \text{ m})}{2}$ – (14.4 kN/m)(0.248 m) = 20.6 kN |
| Compute the shear contribution of the concrete for an FRP-reinforced member. | | |
| $V_c = 5\sqrt{f'_c}\, b_w c$ (U.S.) | $k = 1.94$<br>$d = 9.75$ in.<br>$c = (0.194)(9.75 \text{ in.}) = 1.89$ in. | $k = 1.93$<br>$d = 248$ mm<br>$c = (0.193)(248 \text{ mm}) = 47.9$ mm |
| $V_c = \frac{2}{5}\sqrt{f'_c}\, b_w c$ (SI) | $V_c = 5\frac{\sqrt{4000 \text{ psi}}}{1000 \text{ psi/ksi}} (7 \text{ in.})(1.89 \text{ in.}) = 4.18 \text{ kips}$ | $V_c = \frac{2}{5}\sqrt{27.6 \text{ MPa}} (178 \text{ mm})(47.9 \text{ mm}) = 17.9 \text{ kN}$ |
| FRP shear reinforcement will be required. The FRP shear reinforcement will be assumed to be No. 3 closed stirrups oriented vertically. To determine the amount of FRP shear reinforcement required, the effective stress level in the FRP shear reinforcement must be determined. This stress level may be governed by the allowable stress in the stirrup at the location of a bend, which is computed as follows: | | |
| $f_{fb} = \left(0.05\frac{r_b}{d_b} + 0.3\right) f_{fu}$ | $f_{fb} = \left(0.05\frac{3(0.375 \text{ in.})}{(0.375 \text{ in.})} + 0.3\right)(72 \text{ ksi}) = 32.4 \text{ ksi}$<br>Note that the minimum radius of the bend is three bar diameters. | $f_{fb} = \left(0.05\frac{3(9.5)}{9.5} + 0.3\right)(496 \text{ MPa}) = 223.2 \text{ MPa}$<br>Note that the minimum radius of the bend is three bar diameters. |
| The design stress of FRP stirrup is limited to: $f_{fv} = 0.004 E_f \le f_{fb}$ | $f_{fv} = 0.004(6500 \text{ ksi}) = 26 \text{ ksi} \le 32.4 \text{ ksi}$ | $f_{fv} = 0.004(44{,}800 \text{ MPa}) = 179.2 \text{ MPa} \le 223.2 \text{ MPa}$ |
| The required spacing of the FRP stirrups can be computed by rearranging Eq. (9-4). | | |
| $s = \frac{\phi A_{fv} f_{fv} d}{(V_u - \phi V_c)}$ | $s = \frac{0.75(2 \times 0.11 \text{ in.}^2)(26 \text{ ksi})(9.75 \text{ in.})}{(4.66 \text{ kips} - 0.75(4.18 \text{ kips}))} = 27.4 \text{ in.}$ | $s = \frac{0.75(2 \times 71 \text{ mm}^2)(179.2 \text{ MPa})(248 \text{ mm})}{(20{,}600 \text{ N} - 0.75(17{,}900 \text{ N}))}$ = 660 mm |
| Check maximum spacing limit = $d/2$ or 24 in. | $s \le (9.75 \text{ in.}/2) = 4.9$ in.<br>$s \le 24$ in. | $s \le (248 \text{ mm}/2) = 124$ mm<br>$s \le 600$ mm |
| Equation (9-7) for minimum amount of shear reinforcement can be rearranged as $s \le A_{fv} f_{fv}/50 b_w$ (U.S.) = $A_{fv} f_{fv}/0.35 b_w$ (SI). | $s \le \frac{(2)(0.11 \text{ in.}^2)(26{,}000 \text{ psi})}{50(7 \text{ in.})} = 16.3 \text{ in.}$<br>∴ Use No. 3 stirrups spaced at 4.5 in. on center. | $s \le \frac{(2)(71 \text{ mm}^2)(179.2 \text{ MPa})}{(0.3)(178 \text{ mm})} = 477 \text{ mm}$<br>∴ Use No. 10 stirrups spaced at 120 mm on center. |
| **Step 9—Check that the required bar stress can be developed, and that anchorage bond is sufficient.** | | |
| Find $C$ = min(cover to the center of the bar, 1/2 c-o-c spacing) | $C = \min(1.5 \text{ in.} + 0.375 \text{ in.} + \frac{0.75 \text{ in.}}{2}, \frac{2.5 \text{ in.}}{2})$<br>$C = 1.25$ in. | $C = \min(38 \text{ mm} + 9.5 \text{ mm} + \frac{19 \text{ mm}}{2}, \frac{64 \text{ mm}}{2})$<br>$C = 32$ mm |

| Procedure | Calculation in U.S. units | Calculation in SI units |
|---|---|---|
| Determine the bar stress that is developable at mid-span for the provided embedment length $\ell_e = \ell/2$.<br><br>$f_{fe} = \frac{\sqrt{f'_c}}{\alpha}\left(13.6\frac{\ell_e}{d_b} + \frac{C}{d_b}\frac{\ell_e}{d_b} + 340\right) \le f_{fu}$ (U.S.)<br><br>$f_{fe} = \frac{0.083\sqrt{f'_c}}{\alpha}\left(13.6\frac{\ell_e}{d_b} + \frac{C}{d_b}\frac{\ell_e}{d_b} + 340\right) \le f_{fu}$ (SI) | $f_{fe} = \frac{\sqrt{4000\text{ psi}}}{1}\frac{1\text{ ksi}}{1000\text{ psi}}$<br><br>$\left(13.6\frac{66\text{ in.}}{0.75\text{ in.}} + \frac{1.25\text{ in.}}{0.75\text{ in.}}\frac{66\text{ in.}}{0.75\text{ in.}} + 340\right) \le 72\text{ ksi}$<br><br>$= 72$ ksi | $f_{fe} = \frac{0.083\sqrt{27.6\text{ MPa}}}{1}$<br><br>$\left(13.6\frac{1675\text{ mm}}{19\text{ mm}} + \frac{32\text{ mm}}{19\text{ mm}}\frac{1675\text{ mm}}{19\text{ mm}} + 340\right)$<br><br>$\le 496\text{ MPa} = 496\text{ MPa}$ |
| Compare developable bar stress $f_{fe}$ with required bar stress for flexural strength $f_f$. | 72 ksi > 57.1 ksi, so flexural strength is not limited by bond. | 496 MPa > 395.3 MPa, so flexural strength is not limited by bond. |
| Check anchorage development in positive moment region.<br><br>$\ell_d = \frac{\alpha\frac{f_{fr}}{\sqrt{f'_c}} - 340}{13.6 + \frac{C}{d_b}} d_b$ (U.S.)<br><br>$\ell_d = \frac{\alpha\frac{f_{fr}}{0.0083\sqrt{f'_c}} - 340}{13.6 + \frac{C}{d_b}} d_b$ (SI) | $\ell_d = \frac{1\frac{57.1\text{ ksi}}{\sqrt{4000\text{ psi}}}\frac{1000\text{ psi}}{1\text{ ksi}} - 340}{13.6 + \frac{1.25\text{ in.}}{0.75\text{ in.}}} 0.75\text{ in.}$<br><br>$\ell_d = 27.6$ in. | $\ell_d = \frac{1\frac{395.3\text{ MPa}}{0.083\sqrt{27.6\text{ MPa}}} - 340}{13.6 + \frac{32\text{ mm}}{19\text{ mm}}} 19\text{ mm} \approx 700\text{ mm}$<br><br>$\ell_d \approx 700$ mm |
| Check the development of the positive reinforcement at the simply supported end.<br><br>$\ell_d \le 1.3\frac{\phi M_n}{V_u} = \ell_a$ | $27.6\text{ in.} \le 1.3\frac{23.7\text{ kip·ft} \times 12\text{ in./ft}}{4.66\text{ kip}} + 0\text{ in.} = 79.34\text{ in.}$<br><br>**OK** | $700\text{ mm} \le 1.3\frac{32{,}100\text{ kN·mm}}{20.6\text{ kN}} + 0 = 2025\text{ mm}$<br><br>**OK** |

## APPENDIX A—SLABS-ON-GROUND

Two of the most common types of construction for slabs-on-ground are discussed in this chapter: plain concrete slabs and slabs reinforced with temperature and shrinkage reinforcement.

### A.1—Design of plain concrete slabs

Plain concrete slabs-on-ground transmit loads to the subgrade with minimal distress and are designed to remain uncracked under service loads. To reduce shrinkage crack effects, the spacing of construction or contraction joints, or both, is usually limited. For details of design methods of plain concrete slabs-on-ground, refer to ACI 360R.

### A.2—Design of slabs with shrinkage and temperature reinforcement

When designing a slab with shrinkage and temperature reinforcement, it should be considered a plain concrete slab without reinforcement to determine its thickness. The slab is assumed to remain uncracked when loads are placed on its surface. Shrinkage crack width and spacing are limited by a nominal amount of distributed FRP reinforcement placed in the upper half of the slab. The primary purpose of shrinkage reinforcement is to control the width of any crack that forms between joints. Shrinkage reinforcement does not prevent cracking, nor does it significantly add to the flexural capacity of the slab. Increasing the thickness of the slab can increase the flexural capacity.

Even though the slab is intended to remain uncracked under service loading, the reinforcement is used to limit crack spacing and width, permit the use of wider joint spacing, increase the ability to transfer load at joints, and provide a reserve strength after shrinkage or temperature cracking has occurred.

The subgrade drag method is frequently used to determine the amount of nonprestressed shrinkage and temperature reinforcement that is needed, but does not apply when prestressing or randomly distributed fibers are used (Portland Cement Association 1990). When using steel reinforcement, the drag equation is as follows

$$A_s = \frac{\mu L w}{2 f_s} \quad \text{(A-1)}$$

where

$A_s$ = cross-sectional area of steel per linear foot, in.$^2$ (mm$^2$ per linear meter);

$f_s$ = allowable stress in steel reinforcement, psi (MPa), commonly taken as 2/3 to 3/4 of $f_y$;

$\mu$ = coefficient of subgrade friction; (1.5 is recommended for floors on ground [Portland Cement Association 1990])

$L$ = distance between joints, ft (m); and

$w$ = dead weight of the slab, lb/ft$^2$ (N/m$^2$), usually assumed to be 12.5 lb/ft$^2$ per in. of slab thickness (24 N/m$^2$ per mm).

Because of the lower modulus of the FRP reinforcement, the governing equation should be based on the strain rather than the stress level when designing shrinkage and temperature FRP reinforcement. At the allowable stress, the strain in steel reinforcement is approximately 0.0012; implementing the same strain for FRP will result in a stress of $0.0012E_f$, and Eq. (A-1) can be written

$$A_{f,sh} = \frac{\mu L w}{2(0.0012 E_f)} \quad \text{(A-2)}$$

where $A_{f,sh}$ is the cross-sectional area of FRP reinforcement (in.$^2$) per linear foot (mm$^2$ per linear meter).

Equation (A-2) can also be used to determine joint spacing $L$ for a set amount of reinforcement. No experimental data have been reported on FRP slab-on-ground applications; research is required to validate this approach.